TRIBHUVAN UNIVERSITY
INSTITUTE OF ENGINEERING
PULCHOWK CAMPUS

THESIS NO.: M-353-MSREE-2015-2023

Impact of Climate Change on Hydropower Generation: A Case Study of Devighat Hydropower Station

by

Bed Prakash Nepal

A THESIS
SUBMITTED TO THE DEPARTMENT OF MECHANICAL AND AEROSPACE ENGINEERING IN PARTIAL FULFILLMENT OF THE REQUIREMENTS FOR THE DEGREE OF MASTER OF SCIENCE IN RENEWABLE ENERGY ENGINEERING

DEPARTMENT OF MECHANICAL AND AEROSPACE ENGINEERING
LALITPUR, NEPAL

AUGUST, 2023

COPYRIGHT

TRIBHUVAN UNIVERSITY

INSTITUTE OF ENGINEERING

PULCHOWK CAMPUS

DEPARTMENT OF MECHANICAL AND AEROSPACE ENGINEERING

The undersigned certify that they have read, and recommended to the Institute of Engineering for acceptance, a thesis entitled "**Impact of Climate Change on Hydropower Generation: A Case Study of Devighat Hydropower Station**" submitted by Bed Prakash Nepal, in partial fulfillment of the requirements for the degree of Master of Science in Renewable Energy Engineering.

Supervisor, Prof. Dr. Laxman Poudel
Department of Mechanical and Aerospace Engineering,
Pulchowk Campus

Supervisor, Assist. Prof. Laxman Motra
Deputy Head
Department of Mechanical and Aerospace Engineering,
Pulchowk Campus

6th Aug 2023

External Examiner, Pashupati Raj Gautam
Deputy Manager, Nepal Electricity Authority

Tribhuvan University
Institute of Engineering
Department of Mechanical and Aerospace Engineering
Pulchowk Campus

Committee Chairperson, Dr. Sudip Bhattrai
Head
Department of Mechanical and Aerospace Engineering,
Pulchowk Campus

Date: August 06, 2023

ABSTRACT

The proper study of climatic parameters is the most important, yet somewhat neglected aspect during the design, construction, and operation of most of the hydropower plants in Nepal. This research aims to screen climate change's impact on hydrology and hydro energy production at Devighat Hydropower Station a cascade of the Trishuli Hydropower Plant in Nepal.

The study implements a simulation model developed on the Arc SWAT application using the spatial-meteorological data inputs of the basin. SUFI-2 algorithm is used for calibration and validation purposes. The temperature and precipitation time series data from 1997 to 2019 are used to create the baseline scenario. In order to evaluate future hydropower production, the future climatic dataset (2023-2100) was created using a group of five CMIP6 models from the most recent generations under two Shared Socio-Economic Pathways (SSP245 and SSP585).

Model calibration was performed from 2000-2010 for eleven years and validation from 2011-2019 for ten years. The Trishuli Basin has clearly seen the effects of climate change, with observable changes in climatic variables. Clear predictions point to a significant increase in the basin's temperature and precipitation. It is projected that the basin's average annual flow would significantly increase. The yearly flow is expected to go down by 1.4% in the near future under the SSP245 Scenario, but to go up by 4% and 7.4% in the mid-and far future, respectively. Similar to the SSP585 Scenario, the yearly flow is anticipated to climb by 14.5% and 26.5% in the mid- and long-term, respectively, before rising by 1.1% in the near future. In the near future, mid-future, and far future, respectively, yearly generation is predicted to rise by 4.3%, 3.6%, and 4.9% under the SSP245 Scenario. The yearly generation is expected to rise by 4.1%, 4.6%, and 4.7%, respectively, in the near future, mid-future, and far future, according to the SSP585 Scenario. The hydropower plant is intended to reach a capacity of 114 GWh at all times in the future.

Keywords: Climate Change; Hydropower; DHPS; SWAT; CMIP6; SSP245; SSP585

ACKNOWLEDGEMENT

I would like to thank the Department of Mechanical and Aerospace Engineering, Pulchowk Campus, Institute of Engineering, Tribhuvan University for offering me an important platform to materialize engineering knowledge gained during my Master's program. Regular encouragement from my thesis supervisors Prof. Dr. Laxman Poudel and Assist. Prof. Laxman Motra (DHOD), Department of Mechanical and Aerospace Engineering for their regular encouragement and guidance throughout the thesis works.

I am very grateful to Assoc. Prof. Dr. Hari Bahadur Darlami, and Assoc. Prof. Dr. Nawaraj Bhattarai, Department of Mechanical and Aerospace Engineering, and all department teachers helped me till the final term of my thesis work.

I express my humblest gratitude to Mechanical Section Chief Er. Mukesh Regmi and all staff of Devighat Hydropower Station helped me in providing the necessary data

and suggestions and support in my thesis-related works. Last, but not least, I am very thankful to my family members for their support, help, and encouragement in each and every step of my thesis works.

Bed Prakash Nepal

August 06, 2023

TABLE OF CONTENTS

LIST OF TABLES

LIST OF FIGURES

LIST OF EQUATIONS

NOMENCLATURE AND ABBREVIATIONS

AR5	Fifth Assessment Report
BRB	Bagmati River Basin
CC	Climate Change
CCCSN	Canadian Climate Data and Scenarios
CMIP	Coupled Model Intercomparison Project
DHM	Department of Hydrology and Meteorology
DHPS	Devighat Hydropower Station
ESRI	Environmental Systems Research Institute, Inc.
FDC	Flow Duration Curve
FF	Far Future
FY	Fiscal Year
GCM	Global Circulation Model
GHG	Green House Gas
GLOF	Glacial Lake Outburst Flood
GWh	Gigawatt Hour
HadCM3	Hadley Centre Coupled Model version 3
HEC-HMS	Hydraulic Engineering Center-Hydraulic Modeling System
HPP	Hydro Power Project
HRU	Hydrological Response Unit
ICIMOD	International Centre for Integrated Mountain Development
IPCC	Intergovernmental Panel on Climate Change
Km^2	Square Kilometers
KW	Kilowatt
m.a.s.l.	Meters above sea level
m^3/s	Cubic meter per second
MCM	Million Cubic Meters
MF	Mid Future
MW	Mega Watt
MWh	Mega Watt Hour
NEA	Nepal Electricity Authority
NF	Near future

NSE	Nash Sutcliffe Efficiency
PoE	Percentage of Exceedance
PP	Precipitation
Q	Discharge
QM	Quantile Mapping
RCM	Regional Climate Model
RCP	Representative Concentration Pathways
RMSE	Root Mean Square Error
ROR	Run of River
SD	Standard Deviations
SDSM	Statistical Downscaling Model
SOTER	Soil and Terrain
SRES	Special Report on Emission Scenario
SUFI-2	Sequential Uncertainty Fitting
SWAT	Soil and Water Assessment Tool
SWAT-CUP	SWAT Calibration and Uncertainty Program
T	Temperature
THPS	Trishuli Hydropower Station
UN	United Nations
WCRP	World Climate Research Program

CHAPTER ONE: INTRODUCTION

1.1 Background

Hydropower is a clean energy technology for the derivation of electrical energy from the stream flow. Most of the electrical energy harnessed in Nepal is from hydropower projects (Singh et. al. 2022). Hydro energy is mainly reliant on the discharge of the river flow which fluctuates due to the changing climate. Nepal has a huge hydro potential because of an ample number of hydro resources due to its steep gradient and southern mountainous topography (Regmi et. al. 2022). It possesses one of the largest per capita hydropower potentials in the world, with an estimated theoretical power potential of 83,000 MW, and the technically and commercially feasible capacity has been estimated at 43,000 MW (Shrestha et. al., 2018). Even so, it hasn't been able to utilize even 5% of these viable hydropower potentials. Currently, the nation produces roughly 3242.45 GWh of hydroelectricity, with a 1748 MW peak demand. (NEA Annual Report 2021/22). These large seasonal fluctuations in electricity generation are experienced because of the fact that the river discharge is at a very low level in dry seasons. The energy generation drops up to 16.66 % of the design level in the dry season because of which the power crisis is at its peak during these months (Sharma et. al., 2013). The mismatch in strength capacity generation appears because of the discharge- driven run-of-river scheme of most of the hydropower plants in Nepal.

On the other hand, climate change has been raising a serious challenge and is dependent on local, regional, and national circumstances. Human activity is anticipated to be responsible for around 1^0C of global warming beyond pre-industrial levels, with an anticipated rise in global temperature between 0.8^0C to 1.2^0C, according to the IPCC Special Report on the Impacts of Global Warming. If the current rate of growth continues, global warming could rise to 1.5^0C between 2030 and 2052 (IPCC 4 Singh). In the context of Nepal, climate alternate has been substantial over the past few decades. Between 1975 and 2014, the yearly maximum temperature increased at a rate of 0.056 ^{0}C each year. Additionally, the lowest temperature has been rising at a rate of 0.02 ^{0}C each year, with the most significant changes occurring during monsoon season (Singh et. al. 2022). As a result of the impacts of climate change, the pattern and amount of precipitation have also changed. Pre-monsoon and post-monsoon rainfall is shown to be decreasing, whereas monsoon rainfall is seen to be rising in the Gandaki river basin (Singh et. al. 2022). It is discovered that there is an unpredictable pattern in the rainfall

at several locations in the Kulekhani River Basin (regmi et. al.). The average annual rainfall is predicted to increase 8–12% over the long term and 2-6% over the coming years. The average annual mean temperature is anticipated to rise by 1.3–1.8^{0}C over the long term and by 0.9–1.1^{0}C during the medium term (Singh et. al. 2022). These researches point out the dynamic change in climate pattern viz. temperature and precipitation due to which river hydrology will be altering leading to risk hydropower projects. The Devighat Hydropower Project, which is located in the basin of the Gandaki river in Nepal, has seen its output affected by climatic parameter fluctuations, according to a research conducted there. (Singh et. al. 2022).

Currently, on the Trishuli River catchment, there are several projects that are operating viz. Trishuli Hydropower Station-24 MW, Trishuli 3A Hydropower Station-60 MW, Devighat Hydropower Station- 15 MW, Chilime Hydropower Station- 22 MW, Mailung Hydropower Project- 5MW etc. and some are under construction phase viz. Upper Trishuli 1, 216 MW, Rasuwagadhi Hydropower Project- 111 MW, Sanjen Hydropower Project 57 MW, Trishuli 3B Hydropower Project 37 MW, Langtang Khola Hydropower Project 10 MW. Rasuwa Bhotekoshi Hydropower Project 120 MW etc. As a result, cumulatively 677 MW, is generated currently for the duration of the whole operation of the commissioned hydropower plant and a tremendous amount of electricity may be generated from the upcoming projects. The Trishuli River is still without the necessary evaluation by hydropower developers, project managers, and other stakeholders to take into account possible risks and consequences related to the climate that might occur in the future as a result of climate change. Therefore, trishuli River Catchment's fluctuating climatic factors make it essential to evaluate the potential impacts of hydropower. The outcomes might then be used to risk assessments related to the climate, hydropower development and operation, and eventually incorporation into the design and execution of the nation's energy plans. This research effort is to examine the possible effects of climate change on the generation of hydroelectricity of the Devighat Hydropower Station through the modeling of watershed hydrology by the SWAT model.

1.2 Statement of Problem

In terms of Nepal, hydropower is and will be the country's main energy source. Energy demand is anticipated to rise, and since we only have a small number of hydropower plants, the Trishuli River Basin hydropower projects account for the

majority of Nepal's electricity output. Many hydroelectric projects are underway there, the majority of which are of the Run-of-River (Roar) and Peak Run-of-River (P-RoR) types. Due to the considerable seasonal variance in flows, these types of hydropower are already seeing a loss in power generation, especially during the dry season. For effective hydropower development and ultimately harnessing maximum generation, it is crucial to understand the variations in climate change scenarios, particularly of climatic parameters like temperature, precipitation, and discharge. This will allow for efficient hydropower planning and the achievement of maximum power generation capacity. A snow-fed Himalayan watershed's plans to create hydropower have been greatly concerned by climate change and its effects on river hydrology. The generation of hydropower will be impacted by the climate change-induced shift in hydrology, thus now is the time to conduct climate change foresight studies to prepare for the challenges to come. Hydropower projects can last for 50 to 100 years or longer, and over the long term, they are quite vulnerable to climate change. Typically, hydropower projects are built in Nepal.

1.3 Research Gap

Many studies explored how climate change may affect hydrology and hydropower on a global and national level. There are numerous studies whose study region is within Nepal's catchment area. While some studies have focused specifically on hydropower generation, including hydrology, the majority of studies and research have focused on the hydrological impact of climate change. However, none of the research has presented the adverse effects of climate change in the Devighat Hydropower Station based on the most recent generation data. Based on the predictions of the watershed model, this research is being done to close the gap between hydropower and climate change in the Devighat Hydropower.

1.4 Research Questions

The principal research inquiry for this study is listed below:

- How has the hydrology of the Trishuli Watershed been affected by the observable effects of climate change?
- How has the Devighat Hydropower Station's hydro production been affected by climate change.

1.5 Objectives

1.5.1 Main Objective

Identifying potential climate change effects on the Devighat Hydropower Station's ability to produce electricity is the main primary objectives of this research.

1.5.2 Specific Objectives

With the assistance of the following auxiliary objectives, the main objectives will be accomplished.

i. To Analyze if climate change may have an effect on the hydrology of the Trishuli Watershed.
ii. To project future climate by different climate change scenarios based on selected groups of global circulation models (GCMs).
iii. To relate the climate change data analysis to the Devighat Hydropower Station's hydropower perspective.

1.6 Limitations

- The non-existence of data and recent hydro-meteorological updates.
- Currently, there aren't many hydrological stations in use, and there are just a few meteorological stations.
- A few hydrological response units, depending to the monitoring stations.
- In the chosen catchment, the spatial distribution of stations was even poor.
- The model ensembles' future projections could not accurately capture all of the site's physiographic features.
- The parameter values chosen for the SWAT model's calibration and validation might not always be a perfect representation of the basin's physical properties.
- The absence of current data series makes it challenging to take into account the changes in hydrology brought on by recent climate change.

1.7 Organization of Thesis Works

This report is organized into six different chapters as described below;

Chapter One introduces this dissertation. This chapter covers the research's history, research gap, objectives, theme, scope, and restrictions.

Chapter Two describes the extensive literature consulted throughout the project. This covers earlier research in the hydropower and climate change fields. Studies on global climate forecast scenarios and studies on Nepali climate projections are also included. The literature on SWAT model setup, calibration, and validation, as well as investigations of GCMs, are included as well.

Chapter Three illustrates the thematic area and the series of study data sets.

Chapter Four outlines the process that was utilized for creating a model for the Arc SWAT interface, its calibration, validation, and bias correction for future climate datasets from CMIP6 models.

Chapter Five illustrates the findings and analysis of the research exertion, along with a thorough review and conclusions.

Chapter Six gives the conclusion of the thesis report and recommends future studies.

CHAPTER TWO: LITERATURE REVIEW

In this chapter, a few chosen research articles that are important and relevant to climate change in relation to hydropower generation are reviewed in detail. These papers were chosen from a variety of sources related to the project that had been gathered.

The average lifespan of a hydropower project is about 100 years. However, the key to the long-term survival of a hydro station is the constant availability of water, whether from runoff or a reservoir. The pattern and volume of precipitation throughout time, which are influenced by the effects of climatic fluctuation, determines the water flow or river discharge, as supported by a variety of literature. The literature review will concentrate on the connection between hydropower and climate change, Devighat Hydropower, hydrological modeling, techniques for selecting climate data, techniques for model calibration and validation, and finally, correlation studies between climate models and the generation of hydropower.

2.1 Climate Change and Hydropower in the global context

Berga L. (2013), stated that uncertainty on the future hydrological conditions is a challenge due to changing climate. Though the future climate projection may not be completely accurate but is very helpful for preliminary assessment due to the well-informed data, trends, and projections on hydropower generation.

Lehner B. et. al. (2005), noted that the altercation of hydrology will largely alter energy production. Hydrological variations like the variations in the river flow leading to altering the discharge will have great implications on hydropower generation in the future. It was concluded that climate change impact projection can be very fluctuating subject to flow systems.

Chianga et. al. (2013), observed that it was projected that climate change would affect the hydropower-producing capability. The various models predict erratic annual precipitation however, most concur with the fact that precipitation will be projected to be scattered in a non-uniform pattern with decreasing throughout the winter months and increasing during the monsoon season.

D. Anghileri et. al. (2018), asserted in their findings that the reduction in the availability of water is predicted to stimulate a decrease in hydroelectricity generation to -27% by the end of mid 21st Century.

Advait Godbole (2014), in his thesis, noted that the global climate is projected to show a warming signal whereby the European ensembles depict a likely increase of 1.5^0C and 2^0C in mean annual temperature. Likewise, the precipitation tends to increase by a small amount in autumn and winter and decrease in summer by the end of 2050s.

Shakya et. al. (2006), point out a significant decline in the winter and summer season flows in the rivers of Nepal. It poses a risk of the variability of discharge leading to extreme events like floods and unusual rainfall threats.

Sharma, R.H. (2013), stated that many river basins are already been affected by climate change like Koshi, Gandaki, and Bagmati. These basins have been facing climate-induced disasters like floods, drought, landslides, erosion, sedimentation, and many more extreme events. The supply of water is expected to be seriously threatened by the summer and winter seasons which will ultimately impact hydro energy generation in the lean season.

Bajracharya T. R. et. al. (2011), studies on the biggest river basin of Nepal depicted that hydroelectric production is greatly affected by increments in temperature and ever-changing patterns of rainfall. Though the study has been conducted on the Gandaki river basin where the majority of hydropower is run-off type, the study concluded that dam-type power plants are the need for firm electricity generation with a proper study of climate change. The authors have also noted that climate change is varying river hydrological characteristics thus a revision of the design capacity of corresponding hydropower stations is needed. There is high dependability of hydropower plants on expected streamflow characteristics.

Climate change will have an effect on Nepal's hydroelectric infrastructure, as shown by the literature review linking hydropower plants to its effects.

The majority of Nepal's river basins have been impacted by the scenario of climate change, including the hydrological properties of the river. The literature review's future climate estimates make evident how dramatic changes to weather parameters have occurred in several basins. According to climate forecasts, there will be significant and noticeable hydrological changes in the future, and these changes will be accompanied by irregular or rising variations in climatic parameters. Thus, future forecasts are made in order to examine the performance of hydropower plants in light of aspects related to climate change.

2.2 Hydrological Modeling

Harnett et. al. (2001), asserted that hydrological models have become an essential tool to analyze stream flows because of their potential to incorporate the physical dynamics underlying the basin. Hydrological models will fill holes in data series and forecast the proper modeling response to variations.

Yao and Georgakakos (2001), depicted that reliable forecasts of inflow and timely judgment methods can noticeably assist the functioning of basins and the processes of operation in handling climate change approaches.

Renji et. al. (2015), pointed out that the main objective and the main problem is to depict the rainfall-runoff processes within the basin properly. Many different hydrological models have been created to take all this complexities into account.. From the early 1960s, a number of model constructs is built and incorporated into the software, typically a mixture of linear function and non-linear function. Based on the use of input data and definition of physical processes, all watershed models can be classified as black-box models (e.g. Unit Hydrograph and Empirical Regression Approaches), conceptual models (e.g. SWAT, HEC- HMS and HYSIM), and physically based models (e.g. SHE and IHDM).

Black-box models are entirely focused on observational data and on the calibrated input-output relationship without the individual process being defined. Conceptual models in which the processes implied in the basin (snowmelt, infiltration, evapotranspiration, etc.) are to some degree isolated, but their input-output algorithms are tuned. Models that are based on physical based uses the mass and energy transfer equations. of mathematical physics in the river basin and are intended to reduce the need for calibration using observable catchment features.

Moriasi (2007), noted the statistical performance of indicators and the threshold limit for which the modeling system is categorized as good, very good, satisfactory and unsatisfactory. The hydrological system is considered reliable for the simulation of the water flow if PBIAS lies in the range of ±15% and NSE and R^2 is greater than 0.75.

Paudel R. C. et. al. (2019), pointed out that most of the streamflow including rivers and rivulets of Nepal is unmonitored. The ungauged, unmonitored or poorly gauged river flow is because of the absence of methodological and monetary support in collecting data, extremity, and complexity of the terrain, extreme climate scenario,

etc. The hydrological modeling techniques are very helpful to monitor the streamflow because of their simplicity in application and precision in projection.

Hansen et. al. (2007), stated that it is preferable to use the models of theoretical or conceptual types for water flow simulation, particularly in areas where data is lacking and various physical parameters and processes within the site are unmonitored. It is because these models are appropriate and easy to function where input data is very few. In addition, they are especially suitable for real-time prediction because of the calibration parameters and data set being very less, often providing results like those provided in operational situations by physically based models.

The conceptual method is used for hydrologic modeling in this study instead of the other two approaches to watershed models that are documented in the literature on the subject. For getting a real-time prediction from the limited observational data for the watershed, this method was used. A semi-distributed SWAT hydrologic model is used in this conceptual approach to hydrologic modeling for looking at the interactions between rainfall and runoff and its impacts on hydropower generation and water resources in Nepal's Trishuli River Basin. The basin-scale modeling program SWAT is widely used to forecast how soil, land use, and management will affect water and water quality. The study carried out by several scientists in various works has demonstrated the SWAT tool's capacity to correctly estimate the basin characteristics.

2.3 Selection of Global Climate Data

Horton et. al. (2006), pointed out that climate models are a set of computer codes that allows us to understand the earth's system and to project future climate. These models are used for various climate research around the world and are constantly updated to incorporate changing climatic scenarios. GCMs carry information about horizontal and vertical areas on Earth's surface. In addition, to represent extremes of the hydrological incident both on a temporal and spatial scale, meteorological and hydrological information from Global Climate Models is necessary.

Turner et. al. (2012), pointed out that it is an arduous job to select a suitable Global Climate Model (GCM) or Regional Climate Model (RCM) among several GCMs/RCMs for any site. For this reason, to reduce the ambiguity associated with the future projection of the climate model, an ensemble or the average projection value of multiple climate models is normally implemented.

Ayugi et. al. (2022), mentions that the Working Group on Coupled Modeling established the Coupled Model Inter-comparison Project (CMIP) in order to understand a multiple model situation in a better way. Currently, the project of the ensembled model arrived at its sixth level, or CMIP 6. where the modeling data sets used in it are based on the latest set of situations based on diverse shared socio-economic criteria.
Aryal K. (2022), used five independent CMIP6 models' predicted temperature and precipitation datasets are used viz - EC-EARTH3, INM-CM4-8, MPI-ESM1-2-LR MRI-ESM2-0 and NorESM2-MM. The result from the most recent model showed an alarming signal and additional warming of about 2°C, at a very faster rate than was projected by RCP8.5 of CMIP5. Similarly, change in precipitations hints to be more erratic with no specific trends.

Hausfather et. al. (2019), note that CMIP6 global circulation models are capable of predicting power generation with varied climate change scenarios since these models are predicted based on many socioeconomic predictions known as Shared socioeconomic pathways (SSPs). CMIP6 is a massive improvement over CMIP5 components its terms of modeling group participation, assessment of the projected future climate setups, and an amount of investigation conducted, all these components are enhanced immensely. It shows two alternative futures, one with a large share of renewable energy, low carbon emissions, and strong international collaboration, and the other with a high share of fossil fuels, low renewable energy, and fragmented cooperation.

In this study, calibration and validation are performed in SWAT-CUP after the SWAT model has been simulated. Following calibration and validation, the temperature and precipitation future values from five distinct CMIP6 models—INM-CM4, EC-EARTH3, MRI-ESM2, NoR-ESM2, and MPI-ESM1—are utilized.

2.4 Bias Correction

Because the data are coarse, with grid widths ranging from 100 to 500 km, and cannot take into account the variance of the local scale, several researchers have noted that the data from GCMs cannot be utilized directly at the regional level. Through the bias correction method, a link between regional climate characteristics and global climate features must be determined in order to remedy this issue. To make coarse GCM data more realistic at a finer scale, the bias correction procedure provides additional information to the data. In this study, after completion of validation, coarse Global

Climate Data CMIP6 was obtained from the CMIP6 archive (https://esgfnode.llnl.gov/search/cmip6/). The end coordinates that encompass the Trishuli River Basin are used to cut the coarse data from the CMIP6 database for our basin. Ubuntu is used. The Python interface was used to convert each rain gauge and temperature station's netCdf file into an Excel file format (.csv) once the research area's Shared Socioeconomic Pathways data had been collected. By comparing the historical baseline data of precipitation and temperature, the coarse GCM data were bias adjusted to the RCM.

Shrestha et al. (2017), carried out a relative assessment of several bias-correction techniques, including linear scaling and quantile mapping techniques. Linear Scaling is the simplest method of bias correction of climate change RCM models which have been applied for adjusting the average value of the regional climate model. The mean distinction between the averaged observed monthly data and averaged modeled data is used in the raw modeled data in order to obtain the fine bias-corrected climate data.

Hansen et al. (2007), stated that quantile mapping is the process in which the simulated and observed data cumulative distribution functions (CDFs) of the GCMs are matched with each other. The quantile value of precipitation's observed cumulative distribution function is matched with that of GCM's simulated variable.

Shrestha et al. (2017), noted that a comparison of the observed outputs has no significant difference in between linear scaling (a simpler technique of bias correction) and quantile mapping (a comparatively complex Technique of bias correction) and exhibited almost identical performances. The study led to a new result that a very simple technique like linear scaling for hydrological assessment at a monthly scale is sufficient for the Nepalese Basin.

In this work, the bias adjustment of coarse data for precipitation was carried out using an empirical linear scaling approach, whereas the bias correction for temperature was carried out using the delta change method. The correction factor used in this method of bias correction using the linear scaling method is the ratio of the mean of the observed data to the mean of the historical climate data. To obtain the corrected time series from the model matches that closely match the observed variable, this ratio is the correction factor or multiplication factor to be applied to all of the future raw climatic data of daily precipitation. Similar to this, the difference between the observed data and historical climate data is employed as a particular corrective change in the delta change.

technique of bias correction. In order to obtain the corrected temporal series and ensure that the model matches the observed minimum and maximum temperature data as closely as possible, this difference is the correction change or additional change that must be applied to all future daily raw maximum temperature and daily raw minimum temperature data.

2.5 Literature Summary

Reviewing previous research on a worldwide scale, particularly in Nepal, it was determined that the Trishuli River Basin, which has significant hydro-potential, requires adequate assessment. On the basis of several hydrological models, a few studies, most of which were theoretical in nature, have been conducted in the past about the effects of climate change. The future climatic data from previous GCMs/RCM models have been utilized to forecast the future extremes in terms of flow of water in the basin. Examinations of the influence on hydropower output in the future are insufficient in context with the estimates from the new generation model's increased climate sensitivity.

This study focuses primarily on the effects of climate change on the Trishuli Basin under the most recent CMIP6 scenarios, which consider two socio-economic paths and three future time horizons (2022-2047, 2048-2074, and 2075-2100). The goal of this research is to evaluate how the expected variations in precipitation and temperature in the future would affect hydrological changes and hydro-energy generation at the Devighat Hydropower Station.

CHAPTER THREE: STUDY AREA AND DATA

3.1 Study Area

The Devighat Hydropower Station, located in the Trishuli Watershed, is the subject of the research. The Trishuli River Basin (TRB) is located in the Bagmati Province of Nepal. It encompasses 32,000 square kilometers of Nepal's Central Development Region and accounts for around 13% of the Gandaki River Basin, one of the country's nine major river basins. Along the Trishuli River and its principal tributaries, there are six operational hydroelectric plants totaling 81 megawatts (MW). In addition, the Department of Electricity Development (DOED 2018) has given survey permits for at least 23 hydroelectric projects that are in the planning stage and seven hydropower projects totalling 286 MW that are now under construction. The latitude and longitude of Devighat Hydropower Station is 27.8881907°N and 85.1340051° E longitude respectively. The site is very near to the capital of Nepal, lying approximately 54 km to the northwest of Kathmandu. The catchment area has a wide range of fluctuation in altitude is seen in it ranging from approximately 450 masl to 7500 masl. The Trishuli power plant's cascade hydropower plant is Devighat Hydropower Station (DHPS). It was commissioned into operation in 1984 AD and is situated in Bagmati Pradesh, Battar, Nuwakot. It has an installed capacity of 14.1 MW with an annual design generation of 114 GWh. After successful renovation, modernization, and upgrading (RMU) of all 3 units in 2010–2011, the plant's capacity was increased to 15 MW. All three units are now operating properly. Since its initial operation, Devighat hydropower has produced 33243.99 GWh total as of FY 2078/79. The actual generation for the years 2078 and 2079 is 98.38 GWh, or 98.53% of the targeted generation. With assistance from the governments of India and Nepal, DHPS has been established for a total of NRs. 750 million, including transmission lines. Bharat Heavy Electricals Ltd. (BHEL), the contractor, successfully finished the restoration of all three units at a cost of INR 338.15 million and turned them back to NEA on July 13, 2011. The units' capacity has been upgraded to 15MW. The availability of the flow discharged by the upstream Trishuli Hydropower Plant determines the operational capacity.

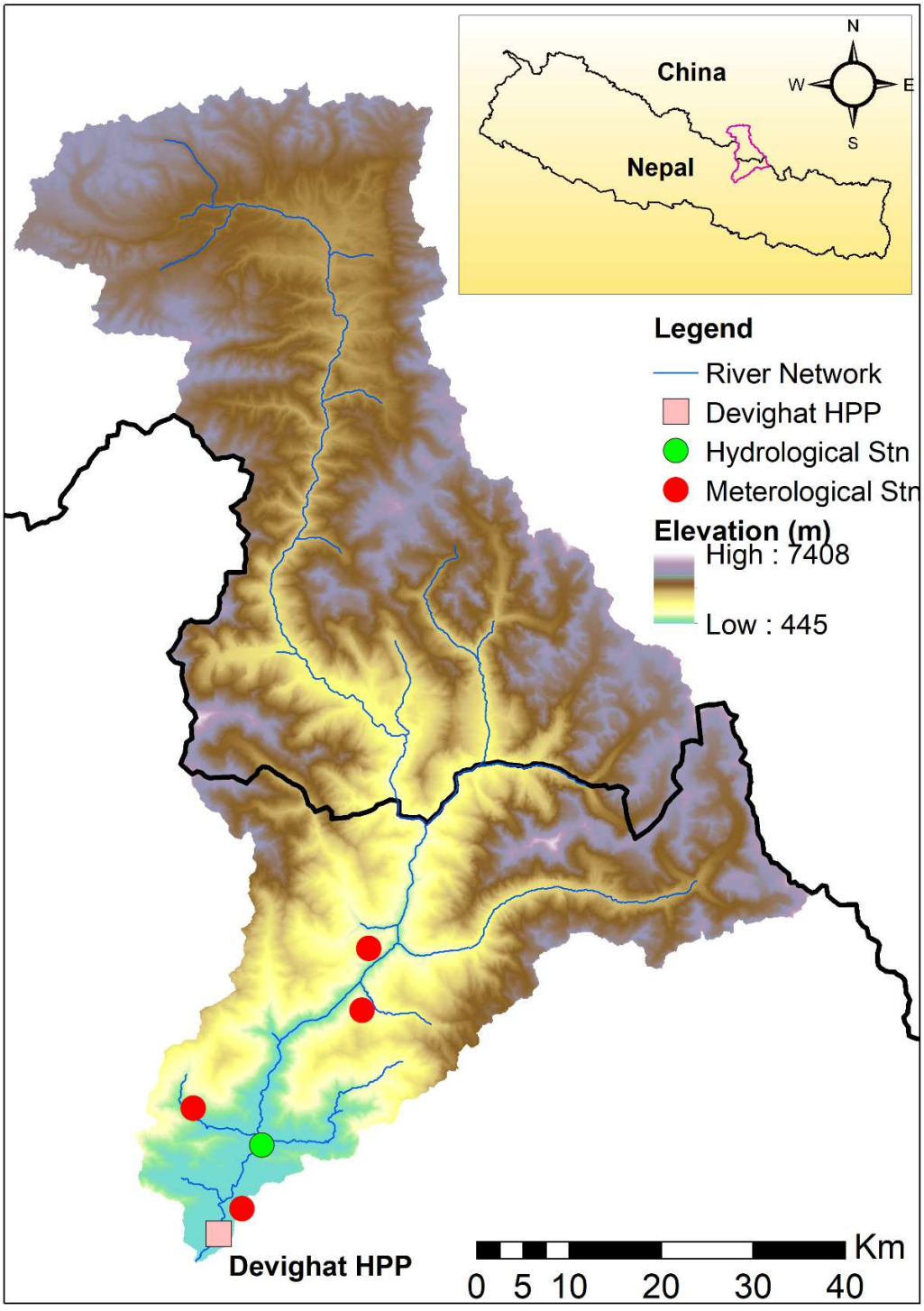

Figure 3.1: Geographic Area of Trishuli Watershed

Table 3.1: Salient Features of Devighat Hydropower Station (NEA, 2022)

Type	Trishuli Hydro Power Station's Cascade
Location	Battar Municipality, Charghare VDC, and Nuwakot District
Installed Capacity	(After rehabilitation) 15 MW
Annual Average Energy	114 GWh
Maximum Gross Head / Net head	40.5m, 39m
Catchment Area	4150 km^2 (upto Trishuli diversion)
Average Annual Flow	45.3 m3/s
Total length of the waterways	Trishuli HPS tailrace to Devighat HPS forebay is 4.5 kilometers away.
Penstock	3 Nos., Ø2.5m, steel lined
Turbine: Number and Type Rated discharge Rated output Rated speed	 3, Vertical Francis 14.3 m^3/sec 5.03 MW 333.3 rpm
Generator Rated output Rated voltage Rated frequency Power factor	 5 MW 6.6 kV 50 Hz 0.8
Power transformer	6.3MVA, 6.6/66kV, 3-phase, 3 Nos.
Transmission line	66kV, 37km (Devighat -Chabel), 28km (Devighat - Balaju), Double circuit

Figure 3.2: Satellite Map of Devighat Forebay-HPS

3.2 Data

Many data sets have been used in the model preparation process. The research attempt to utilized mainly four main types of datasets: geographical dataset, meteorological data, hydrological data, and future climate data. The geospatial data collection comprises soil maps, land use maps, and topographic maps (DEM). Temperature, precipitation, and projected climate data are all part of the baseline climate data. These numbers are produced to fit the basin and are gathered from various sources.

Figure 3.3: Devighat Hydropower Powerhouse with Sloping Penstock

3.2.1 Geo-Spatial Data Set

3.2.1.1 Topographic Data

The most important geospatial data for hydrological simulations in the SWAT model is a topographic dataset. The WGS 1984 referenced latitude and longitude in the Geo TIFF file format of the Digital Elevation Model (DEM) with a 30 m resolution was utilized (Pokharel et al., 2020). The sinks and pits that could unnecessarily capture water in the terrain are filled by raising the elevation of the pit's cells to that of surrounding cells. The topographical information is derived from DEM for the basin. The DEM in GIS helps identify the watershed, river network, drainage pattern, slope length, gradient, and sub-basin as well as generate other terrain-related data. DEM file with GIS operation generated initial input data to run Arc SWAT software. The elevation ranges from 445 to 7408 meters above sea level. as shown in figure 3.4.

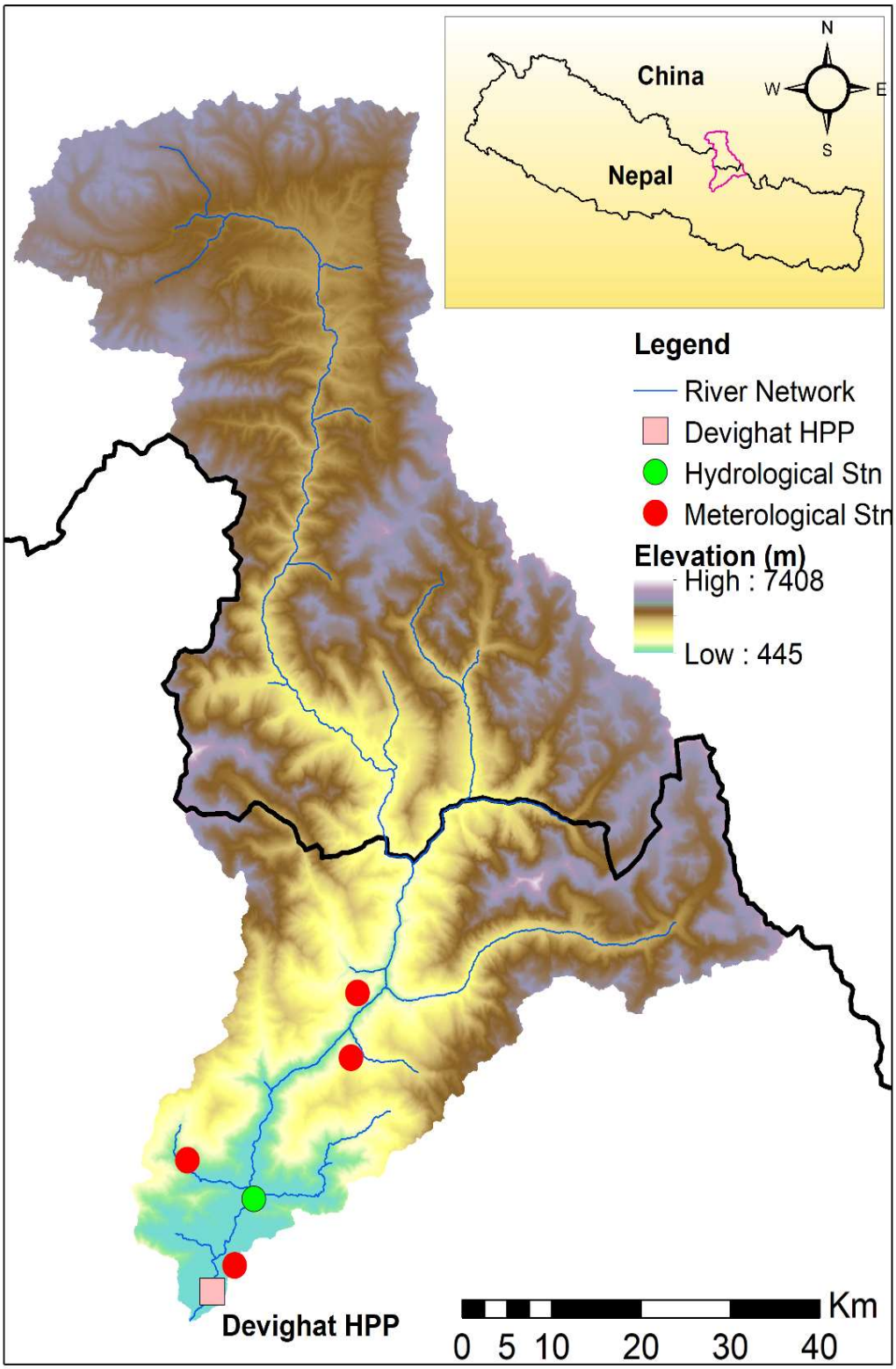

Figure 3.4: Digital Elevation Model of Trishuli River Basin

3.2.2 Land Cover Map

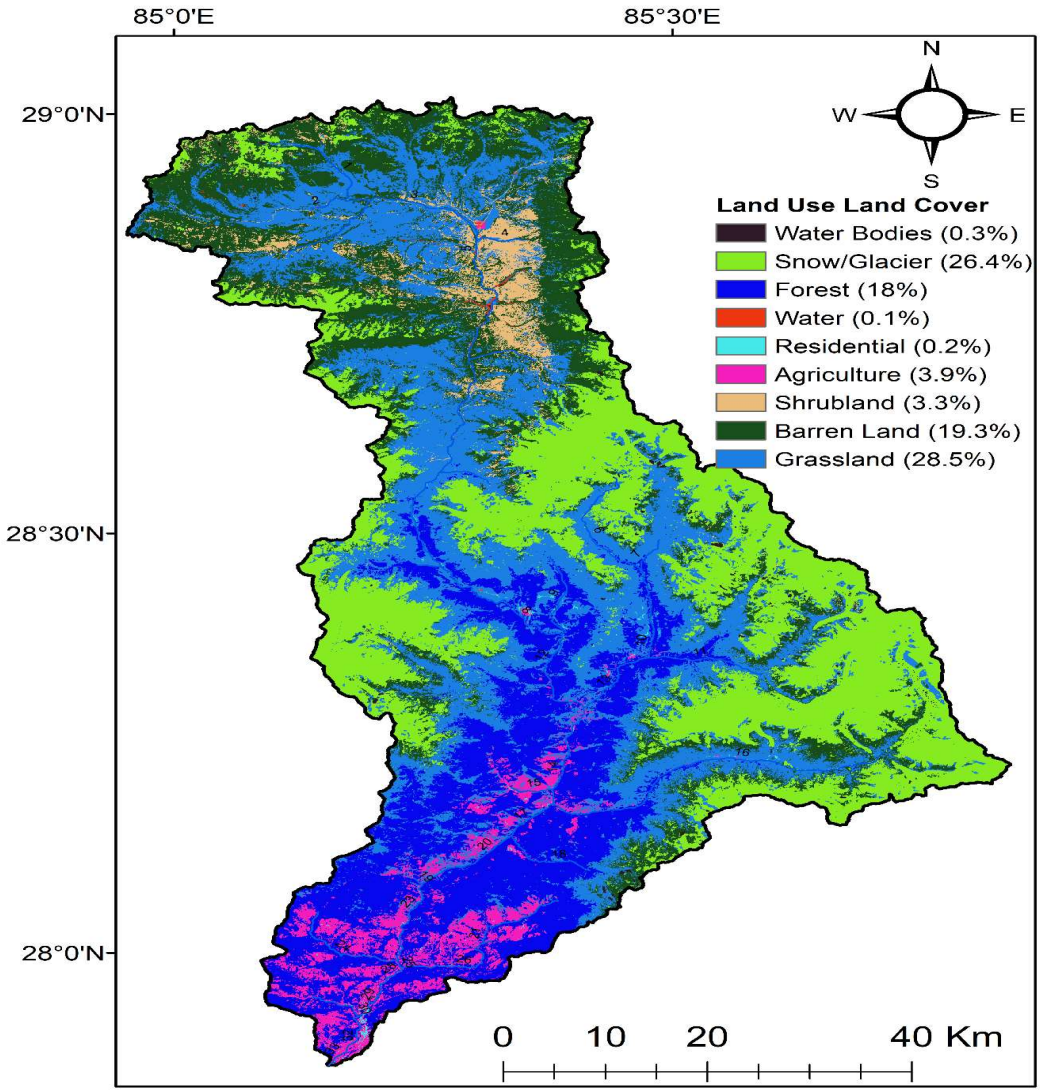

Figure 3.5: Land Use Map of Trishuli Catchment

The model shown in Figure 3.5 originated from using land cover data/map created by the International Center for Integrated Mountain Development (ICIMOD) and Department of Survey, which was accessible at a 30 m resolution. The main element affecting runoff, evapotranspiration, and soil erosion parameters in the basin is land cover. Nine different land use categories were found in the basin, with grasslands occupying a maximum of 28.5% of the area, followed by snow glaciers at 26.4%. Forest makes up 18% of the overall catchment area, followed by barren terrain, which makes up an intermediate 19.3%. The SWAT database has been utilized for rearranging the land use map based on the model parameters that correspond to different land use/cover categories as the raw land use map cannot be used for modeling.

3.2.3 Soil Map

The soil map of the Trishuli River Catchment shown in Figure 3.6 was created using a soil map at 1:1 million (Dijkshoorn, 2009) downloaded from the Soil and Terrain Database Program (SOTER). The map was compiled by FAO and Nepal's Survey Department. Three types of soil were found as shown in the catchment map.

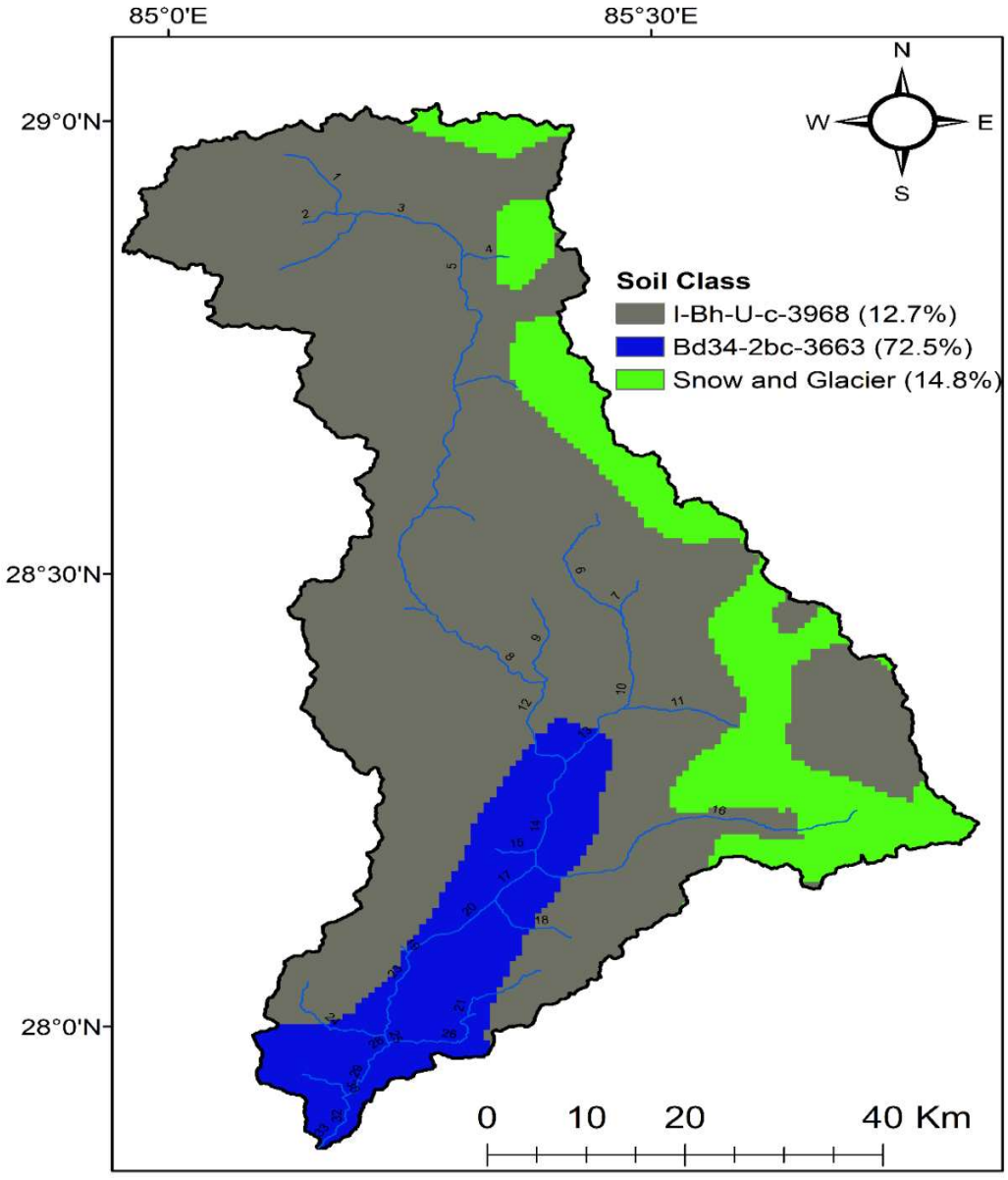

Figure 3.6: Soil Map of Trishuli River Basine

3.3 Baseline Climate Data

3.3.1 Meteorological Data

The Hydrological and Meteorological Department (DHM) of Nepal mentions that there are 282 meteorological stations in Nepal, four of which are close to the Trishuli River Basin. The maximum and minimal temperatures as well as the average daily precipitation were gathered from DHM for Nuwakot (1004), Pansayakhola (1057), Thamachit (1054), and Dhunche (1055). For the baseline period from 1997 to 2019, these stations were taken into account to determine the average basin precipitation and temperature. The meteorological information utilized for SWAT modeling purposes included daily rainfall data, daily maximum temperature data, and daily minimal temperature data. In order to ensure homogeneity across the research period, we used a collection of meteorological, temperature, and precipitation data for the basin over 20 years, from 2000 to 2019. The particulars of the meteorological stations are enlisted in Table 3.2.

Table 3. 2: List of Meteorological Stations Used in the Study

Se. No.	Station Name & No.	Latitude (N)	Longitude (E)	Elevation (masl)	Year	Available Data	Source	Remarks
1.	Nuwakot (1004)	27.91	85.16	1003	1970-2019	Climatology (Rainfall, Temperature)	DHM	Daily Data
2.	Pansayakhola (1057)	28.01	85.11	1240	1970-2019	Precipitation (Rainfall)	DHM	Daily
3.	Thamachit (1054)	28.16	85.31	1847	1970-2019	Precipitation (Rainfall)	DHM	Daily Data
4.	Dhunche (1055)	28.1	85.3	1982	1970-2019	Climatology (Rainfall, Temperature)	DHM	Daily Data

3.3.2 Hydrological Data

In total, there are 51 hydrological stations in all, one of which, Betrawati (Station number 447), is inside the basin. In order to replicate the current circumstances at the discharge point and to perform sensitivity analysis, calibration, and model validation, the discharge hydrological data were included in the model for both objectives. Arc SWAT version 12.10.5 was utilized for forecasting river flow using observed data on rainfall and temperature for the historical baseline period as well as future projections using bias-corrected GCM data. From 2000 to 2010, these data were utilized for calibration, and from 2011 to 2019, for validation. Table 3.3 displays the specifics of the hydrological stations close to the research location.

Table 3. 3: List of Hydrological Stations Used in the Study

Se. No.	Station Name & No.	Latitude (N)	Longitude (E)	Elevation (masl)	Year	Data Available	Source	Remarks
1.	Betrawati (447)	27^0 58' 08"	85^0 11' 00"		1970-2019	Hydrology (Discharge)	DHM	Daily

3.3.3 Future Climate Data

Future projections were made using the CMIP6 global climate model. The databank (https://esgf-node.llnl.gov/search/cmip6/) contained thirteen CMIP6 models arranged into four unique shared socioeconomic pathways: SSP126, SSP245, SSP370, and SSP585. There were four potential socioeconomic futures provided along with the historical data set for temperature and precipitation. We have utilized temperature and precipitation projections from five distinct CMIP6 models, including INM-CM4, EC-EARTH3, MRI-ESM2, NoR-ESM2, and MPI-ESM1, for the SSP245 and SSP585 pathways. The CMIP6 database had been utilized to download this data.

3.3.4 Data Processing

For watershed modeling and simulations, hydro-meteorological data processing is crucial. For any hydro-meteorological modeling project, this is the initial step in gathering trustworthy data (Sattari et al., 2017). The project's setup requires both geographical and temporal data, which was collected from numerous sources. The model requires the meteorological variables rainfall, high and low temperatures, relative humidity, solar radiation, and wind speed. Every data must be processed since incomplete data cannot be included into any hydrological model and the sequence of data that will be fed into SWAT must be accurate and complete.

The hydro-meteorological series of data are frequently insufficient for a variety of reasons, including geographical and technical restrictions, instrument errors, instrument damage, the incapability of the data collector to measure daily data, the compiler's error in storing and compiling data, the storage system's shortcomings, and so forth. Any study's reliability is significantly diminished by missing data. Checking each data and calculating the overall amount of missing data for each station comprise the data quality assessment. The data series given by the Department of Hydrology and Meteorology; Nepal was missing a significant amount of data. In several instances, the missing data was so significant that month-long gaps were apparent. The quality and amount of the figures should be regularly verified using a variety of different approaches in order to achieve the best results from the modeling requirements input data series to be given.

In this research, visual tracking of graphs and data reading were some of the different techniques used to assess data quality. There were several ways to complete the gaps in the data. The Normal Ratio Method, Long Term Average Method, Arithmetic Mean Method, etc. are a few of these well-known ones. When the amount of rainfall in a location change linearly over time, the long-term average filling approach is utilized. To fill up any gaps in the data, the arithmetic mean of the data figure corresponding to the following hydro-meteorological weather stations was computed. In our nation, where rainfall gauges are not evenly spread throughout a region, the arithmetic mean approach does not provide good results. The long-term average monthly temperature readings and the missing precipitation data from nearby stations were filled in using the normal Ratio approach. Based on the reliability of the data and its geographic dispersion, the Trishuli River Basin station was selected. The normal ratio has been the most widely used method for estimating missing rainfall

values, due to its simplicity and efficiency (Murhanuddin et al., 2017). The normal ratio approach is utilized, in which next-to stations were used to approximate missing data, for yearly precipitation exceeding 10% of the considered gauge compared to the surrounding gauges. This evaluates the impact of each nearby station. Calculations utilize typical precipitation as a baseline for comparison. A thirty-year average of rainfall is considered normal precipitation.

When the normal annual precipitation at other stations does not exceed the 10% threshold of the normal annual precipitation at station x, the arithmetic mean method is employed to determine Px.

$$P_x = \frac{1}{M}\sum_{i=1}^{m} p_i$$ Equation 3.1 Arithmetic Average

Where,

- P_X = Rainfall at missing station
- P_1, P_2, P_3, …. P_m = Annual precipitation values at stations 1, 2, 3, …m respectively
- M = Total number of stations

To approximate the missing series of data at the station, the weightage averages of all nearby stations are added up. If the average precipitation shows a significant gap, Px is approximated using the normal ratio method, which uses the weighted average method for calculating it.

$$P_X = \frac{1}{M}\sum_{i=1}^{m}\left(\frac{N_x}{N_i}\right)P_i$$ Equation 3.2 Weighted Average

Where,

- N1, N2, N3, ..., Nm = Normal annual precipitations at each 1, 2, 3, …, m stations
- Nx = Normal precipitation at station x

In this study, the long-term average technique was used to fill in the temperature data, and the Normal-ratio method was used to fill in the rainfall data. The range of useful data for precipitation and temperature had been established from 1997 to 2019. The SWAT uses all of this corrected data from selected gauge stations that are either nearby or inside the basin to run continuous event simulations.

3.4.5 Data Bias Correction

A better forecast of future climatic data depends on the selection of the bias correction. The linear scaling method is sufficient for hydrological analysis at monthly

resolution in the river basins of Nepal (Shrestha et al., 2017). The linear scaling approach is used to correct potential biases in future precipitation data based on this theory. The monthly mean bias of precipitation is corrected using the correction factor, which is the ratio of monthly means of observed and historical precipitation.

$$P'_{(\mathrm{F})} = P_{(F)} \frac{\mu_{(P_0)}}{\mu_{(P_h)}}$$ Equation 3.3: Linear Scaling Bias Correction

Where,

- P'(F)= Corrected Future Precipitation at station x
- P(F) = Coarse Future Precipitation at station x
- μ(Po)= Mean Monthly Observed Precipitation at station x
- μ(Ph)= Mean Monthly Historical Precipitation at station x

The delta approach is used to correct GCM data for bias in temperature.

$T'(F) = T(F) + [\mu(Th) - \mu(To)]$ Equation 3.4 Delta Change Bias Correction

Where,

- T '(F)= Corrected Future Temperature at station x
- T (F) = Coarse Future Precipitation at station x
- μ(To)= Mean Monthly Observed Temperature at station x
- μ(Th)= Mean Monthly Historical Temperature at station

CHAPTER FOUR: RESEARCH METHODOLOGY

The methodology flow diagram implemented for this study is detailed and illustrated in Figure 4.1.

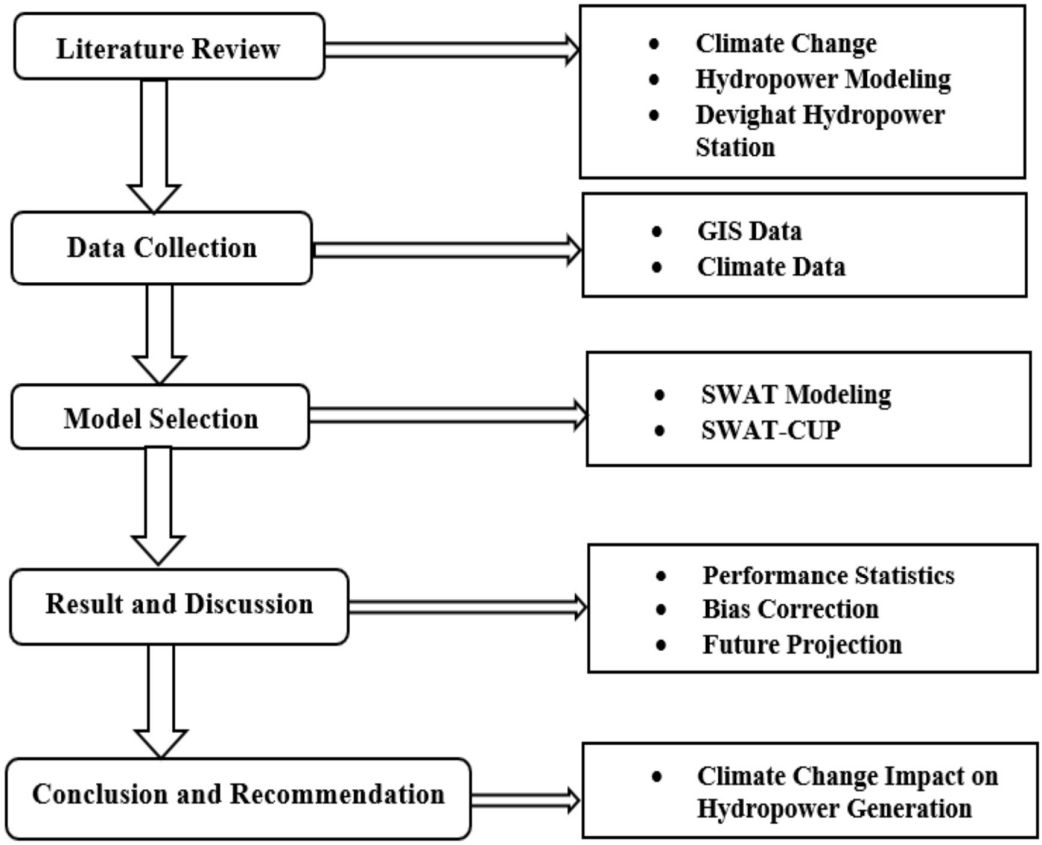

Figure 4.1: System Flow Diagram

4.1 Hydrological Model

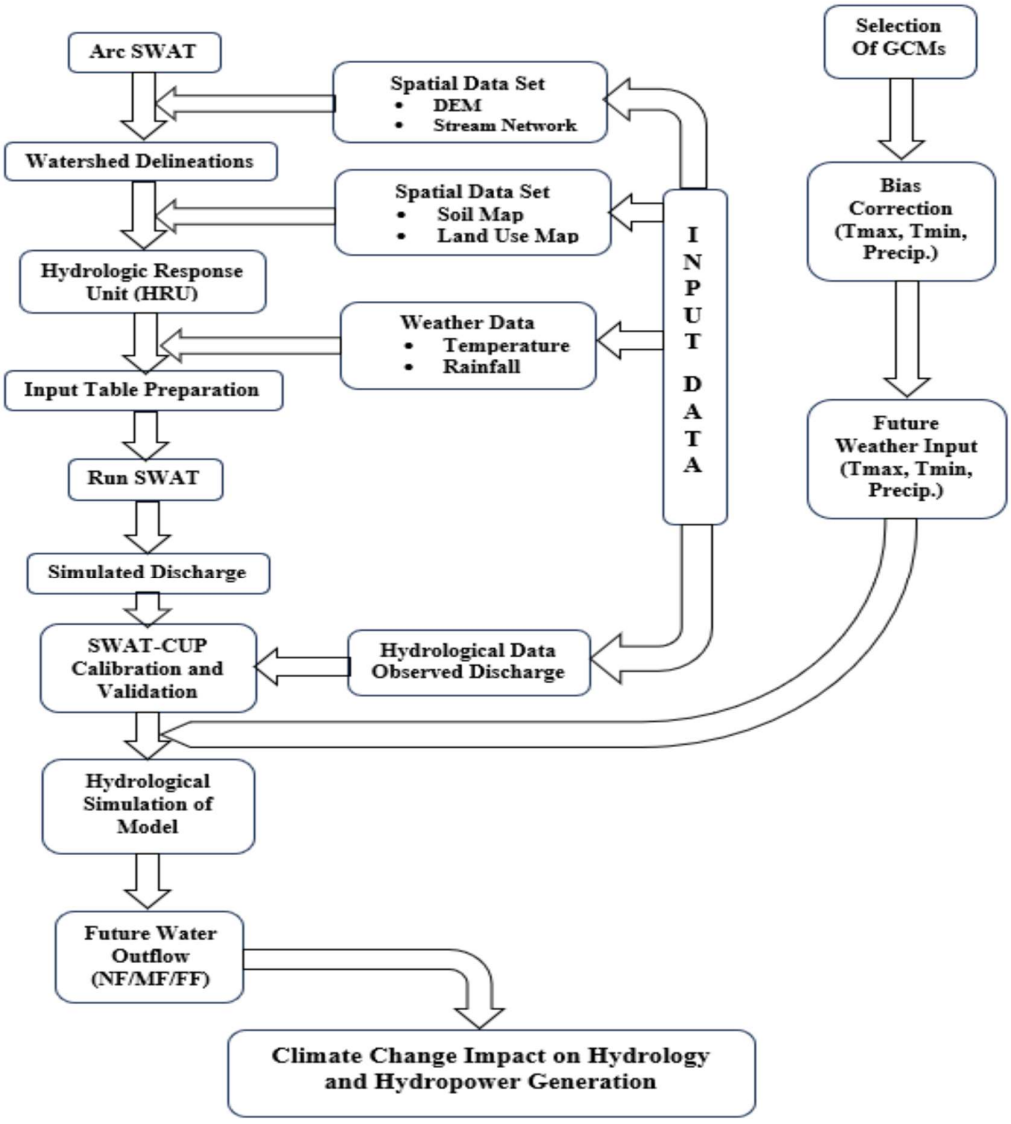

Figure 4.2: Detailed Methodology Flowchart

The hydrological model, which provides extensive insight into its implications, may be used to study the effects of climate change on water bodies (Praskievicz and Chang, 2009). Hydrological analysis with hydrological modeling is necessary for the proper analysis of climate impacts on hydropower projects (Bajracharya, et al., 2018). The selection of any water resource model is dependent upon the complexity, available resources and modeling objectives (US Environmental Protection Agency, 2009).

In this research, likely impacts on electricity production due to climate change in the Trishuli Watershed a sub-basin of Gandaki River Basin is investigated by analyzing outputs of the Arc SWAT (Arnold, et al., 1998) model and ArcGIS Platform. The SWAT model is created using the digital elevation model, land use data, and soil data. Statistical simulation is then carried out using the hydro-meteorological weather inputs that are accessible. It is necessary to assess the effectiveness of the developed SWAT model, and in order to do so, it must be calibrated and confirmed. Calibration and validation are done using the SWAT-CUP algorithm. For the uncertainty and sensitivity analysis, the sequential uncertainty fitting (SUFI-2) algorithm has been chosen from among the five SWAT-CUP approaches. Last but not least, the data series are analyzed based on the comparison analysis of output outcomes to provide future forecasts of weather scenarios and the research site's hydropower potential.

A simulation time is provided as input for the SWAT project set up in the Arc SWAT interface. The simulation's starting and end dates must be specified in the above context. The monthly scale is used to specify the printing settings. The stream network is then specified for the digital elevation model, which delineates the watershed. This involves selecting the output and input definitions as well as the stream requirements. The HRU Analysis dialog box is used to divide the sub-basins. The SWAT database is used to establish the types of soil and land use. The river basin was divided into a number of sub-basins that were then utilized in SWAT modeling to create the thirty-three sub-basins. The thirty-three sub-basins displayed the water's routing procedure to the basin's main channel clearly. Using the classification of the soil slope and the land use map, the input data from the 33 sequentially separated sub-basin are once more classified into various hydrological response units (HRUs). For the HRU analysis, five different slope class types are classified. The model classifies the land reach discharging into the sub-basin into a total of one hundred and eighty-four hydrological response units.

The balancing equation of water is the main crux theory of SWAT

$$SW(t) = SW(o) + \sum_{i=1}^{n}(R(i) - Q(si) - E(i) - W(i) - Q(gi))$$

Equation 4.1: SWAT Water Balance Equation

Where,

- SW(t) is the final soil water content on day t (mm),
- SW(o) is the initial soil water content (mm),
- R(i) is the amount of precipitation on the day i (mm),
- Q(si) is the amount of surface runoff on the day i (mm),
- E(i) is the amount of evapotranspiration on the day i (mm),
- W(i) is the amount of water entering the vadose zone from the soil profile on the day i (mm), &
- Q(gi) is the amount of return flow on the day i (mm).

Out of 198 HRUs, the streamflow of each HRU is forecasted simply to determine the watershed's overall runoff. The daily observed climatic data are used as inputs for the SWAT model while it runs. The model generates a variety of meteorological data for each reach of each of the 33 sub-basins.

4.1.1 SWAT model Setup

The splitting of a watershed into many sub-watersheds is the main step in modeling using SWAT. To separate the watershed into distinct land regions and stream reaches that flow to a single outlet, watershed delineation is utilized. A DEM is necessary for the delineation process since it is needed to calculate the definition of streams, flow directions, and flow accumulation at basin outlets. At the Devighat Tailrace Gate, the exit point was manually added to the watershed. The sub-basin parameter was established for each of the newly produced sub-basins once the watershed was defined. In the research region, 33 sub-basins developed shown in Figure 4.3.

Each sub-basin that has been defined is connected by a hydro network, which is again discretized in HRUs. A study watershed's fundamental component, an HRU, contains a distinctive blend of soil types, slope classifications, land uses, and land covers depending on user-defined limitations. The development of the HRUs utilized a mix of four GIS Layer maps, including the soil map, soil classes, and land use/land cover map. The dominant land use, the dominant soil, and the dominant slope can only be characterized as one HRU per sub-basin. On the other hand, SWAT also permits several HRUs per sub-basin that reflect all combinations of land use, soil, and slope.

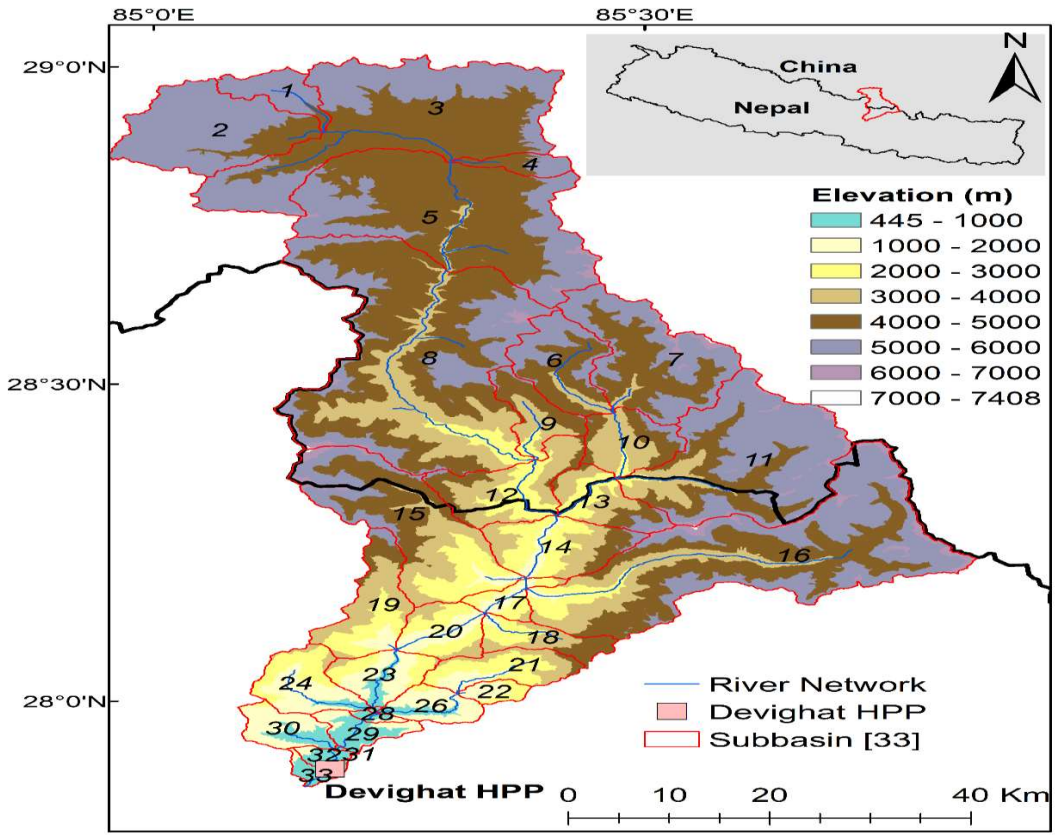

Figure 4.3: Sub Basins Delineation of Study Watershed

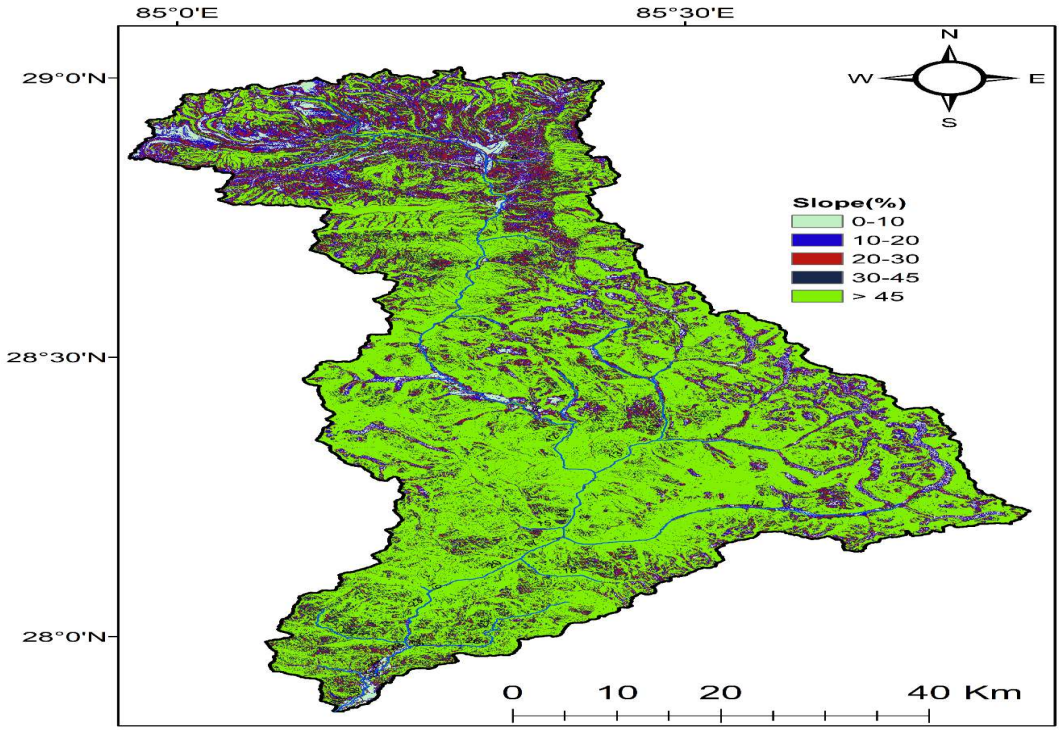

Figure 4.4: Land Slope Map of Study Watershed

Land use, soil, and slope class definitions were done individually to start the process of establishing HRU. With the help of the lookup tables for the land use map, soil map, and slope, the projected Raster GRID file of land use was loaded and cut to the watershed border, giving just raw land use. For the basin, five slope classifications were established. These maps were layered to construct HRU feature classes for slope reclassification, which was accomplished for slopes of 0–10%, 10–20%, 20–30%, 30-45%, and above 45%. A new full HRU layer is applied when the overlay is completed. In 33 sub-basins, 198 HRUs were constructed, and information about each HRU was gathered, as seen in the HRU analysis report.

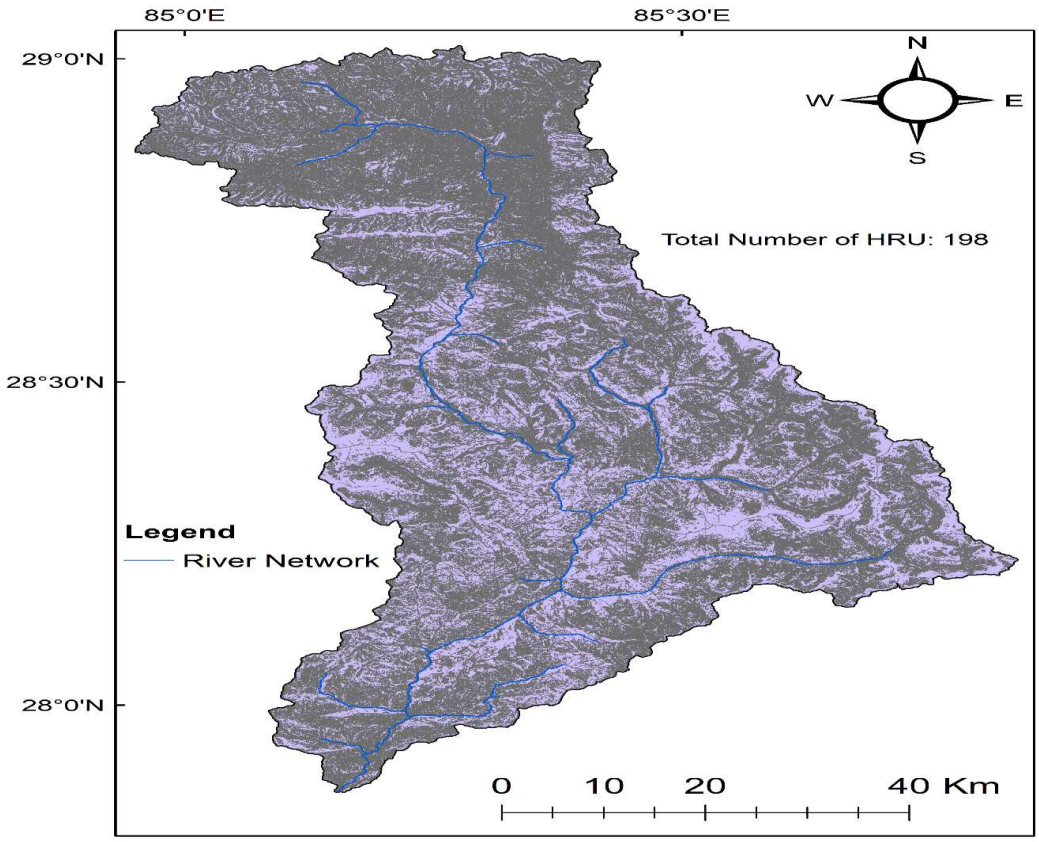

Figure 4.5: HRU Layer of Study Watershed

Following the acquisition of the HRU, SWAT requires meteorological data such as daily precipitation, maximum and minimal temperatures, solar radiation, and relative humidity for further computation. The temperature and precipitation missing data will be taken into consideration by the weather generator. The weather generator generates weather variables every day based on probabilities and statistical techniques, using average climatic statistics obtained nearby to predict the probability of rainfall on any

given day. For each sort of meteorological data, a gauge is attached to each sub-basin. Station data was loaded from input tables, and separate daily datasets for rainfall, maximum and minimum temperatures were created in.txt file format. The SWAT model needs input files with highly precise formatting. Sub-basins and HRUs were created from the collected data so that it could be converted into a SWAT-readable format. The SWAT model is run and outputs are produced using the SWAT prepared input files. The default information utilized in the construction, though, is probably not the most accurate. A better dataset for the watershed may be used as an input, and inputs from the user are written in SWAT-readable files and tables within the project geodatabase that was built. Separate SWAT input files were also made for each sub-basin or HRU. These files come with everything set to default, but you may change it later if you need to. The model was set to run after all the input files had been selected and written in text input files using the SWAT format.

4.1.2 SWAT model Run

After writing input files in SWAT format, the model is ready to run. Important decisions must be taken before running; the simulation period occurs first. Both the SWAT model's calibration and validation periods last for a specific number of years. The second step is choosing the appropriate type of rainfall distribution to be used in the precipitation generator and the time step (daily, monthly, or annual) for writing the outcome. The inputs are filed in a file.cio input file, also known as the watershed master control file as it controls the simulation. The SWAT model simulation is complete after all the parameters have been settled on. The simulation's time frame has been established with the years 1997 and 2014 as the beginning and end periods. The generator was chosen for its simplicity in the skewed distribution of rainfall used in the weather. For writing the output, a 64-bit SWAT executable version comprising a monthly time step was utilized. Finally, the SWAT model for the Trishuli River Basin was successfully run using the Arc SWAT 2012.10.5 interface.

Once the model has been set up using input data, it needs a set of parameters and a range of those values that can reproduce the observed flow. In order to calibrate and validate the model, SWAT employed SUFI-2, the SWAT CUP optimization software, as a further interface. The discharge data series at the manually selected outlet of the stream network is the result of the successfully completed model simulation. The performance of the SWAT model is determined by comparing the simulated and

observed discharges at the selected Devighat Tailrace (Sub-Basin Number 33) of the river basin. The future climatic data from the selected stations was provided as input into the calibrated and validated Arc SWAT interface for all five GCMs under both socio-economic paths. The SWAT model was ran for the future period of 2023-2100 after being given future meteorological data in order to anticipate future discharge. As a result, the five GCM discharge under the two scenarios was separated into three future periods. To get two sets of data for three upcoming periods, the average SSP245 across the five GCMS and the average SSP585 were merged. The discharge determined the availability of water in the future.

4.1.3 Calibration and validation in SWAT-CUP

A model's calibration involves fine-tuning its sensitive parameters within a suitable threshold in order to precisely match the model's output with the observed data, whereas a model's validation is a measurement of how accurately the output of the model corresponds to further observed data. Txtinout, the input file for calibration, is generated once the model has been successfully run. The automated model calibration process must properly reformulate the model's ambiguous parameters before the model is run a second time and its crucial outputs are extracted from its output files. Once the model has been built using input data, a set and range of those parameters that can duplicate the observed flow will be needed.

Figure 4.5: Tailrace diverging water into the main river stream (Sub-Basin No. 33)

The SWAT-CUP (SWAT Calibration and Uncertainty Program) interface created for SWAT is utilized to determine this. According to Abbaspour et al. (2017), it is an application made up of programmed algorithms that are used to alter the parameters such that a basin is accurately represented. The performance of the SWAT model can be analyzed using five optimization algorithms: SUFI-2, PSO, GLUE, ParaSol, and MCMC. These algorithms allow for parameter sensitivity analysis and performance analysis. Based on the statistical performance indicators used in this research study, the model has been calibrated and validated using the SUFI-2 algorithm.

For the calibration, a parameter set and its threshold ranges are set manually or between each auto-iteration. After the relevant data was gathered through reviewing related research conducted in the literature, parameterization a critical phase during calibration was carried out. The parameter sensitivities among the various parameters are an essential part of the calibration. The parameter set that affects the basin most responsively is selected. Only the most sensitive parameters from those selected were taken into consideration for further calibration in the SUFI-2 algorithm. According to SUFI-2, several rounds were carried out using the new set of parameter ranges until the ideal parameter range was identified. Only the most sensitive parameters from those selected were taken into consideration for further calibration in the SUFI-2 algorithm. According to SUFI-2, several rounds were carried out using the new set of parameter ranges until the ideal parameter range was identified. We discovered trustworthy outcomes after several repetitions in which the parameter range was decreased with each iteration. When results were received that were satisfactory, the model was set to validate for the validation period.

4.1.4 Model Evaluation

The relative comparison of the monthly simulated streamflow data with observed streamflow at the river basin's Sub-Basin Number 33 was carried out in order to calibrate and validate the SWAT's performance. Three statistical performance indicators Nash Sutcliffe efficiency (NSE), Coefficient of Determination (R^2), and Percentage Bias (PBIAS) were computed in order to analyze how well the simulated model representation performed in comparison to the basin's reality.

$$NSE = 1 - \frac{\sum^{n}(Qi^{0} - \mu Qi^{s})^{2}}{\sum^{n}(Qi^{0} - \mu Qi^{0})^{2}}$$

Equation 4.2: Nash Sutcliffe efficiency

$$PBIAS = 1 - \frac{\sum^{n}(Qi^{0} - Qi^{s})^{2} * 100}{\sum^{n}(Qi^{S})^{i}}$$

Equation 4.3: Percentage Bias

$$R^2 = 1 - \frac{\sum_{i}^{n}(Qi^{0} - \mu Qi^{0}) * (Qi^{S} - \mu Qi^{S})}{\sqrt{\sum_{i}^{n}(Qi^{0} - \mu Qi^{0})^{2} * (Qi^{S} - \mu Qi^{S})^{2}}}$$

Equation 4.4 : Coefficient Of Determination

Where,

Q^{O} = Observed Discharge

Q^{S} = Simulated Discharge

μQ^{O} = Average Observed Discharge

μQ^{S} = Average Simulated Discharge

NSE and R2 have values that vary from 0 to 1. This statistical performance indicator implies a model with more prediction ability when its values are close to 1. The Percentage Bias (PBIAS) with regard to the observed value measures the average tendency of the simulated values. If the PBIAS value is 0, it reflects the ideal simulation; otherwise, it indicates either a greater or lower number. The positive PBIAS number, on the other hand, reflects an underestimating of flow for the flow simulation whereas the negative PBIAS value indicates an overestimation of flow.

4.2 Estimation of Hydro Energy Generation

The function of head and discharge, which are provided in the equation, determines the power output of any hydroelectric plant utilizing the potential energy of water.

$P = \eta * \rho * g * H * Q$ Equation 4.5: Power Output

Where;

P = Power Output

H = Efficiency of the turbine

ρ = Density of water

g = Acceleration due to gravity

H = Effective Head

Q = Discharge

Any hydroelectric system produces energy as a function of power production and operating time. Power production from every hydropower source depends on the current flow rate under the conditions of constant head, total turbine runner efficiency, water density, and gravitational acceleration. The generation of hydropower will be impacted by the change in future discharge. As a result, the baseline discharge was used to calculate the influence of discharge on hydropower generation in this study. The discharge is the only factor controlling how much electricity is produced in hydropower stations. The forecasts of energy change will be based on the comparison of baseline discharge with future climatic data.

CHAPTER FIVE: RESULTS AND DISCUSSION

5.1 Hydrological Model Performance

The Arc SWAT interface was utilized to develop, adjust, and validate the hydrological model for the Trishuli Basin. The simulation covered a span of 23 years, running from 1997 to 2019. To establish accurate soil and ground conditions, a warm-up period of three years (1997 to 1999) was incorporated for calibration. Subsequently, the model underwent a ten-year calibration phase from 2000 to 2009 and validation was carried out for ten years span from 2010 to 2019. Monthly time series data was used for the simulations, with runoff as a variable. There were 33 sub-basins in the basin, also known as routing channels. Sensitive parameters were identified, signifying those slight fluctuations in their values significantly impacted the simulation outcomes. To investigate parametric sensitivity, the variables were manually adjusted, leading to immediate changes in the hydrograph results. All the adjusted variables were documented, and the model was rerun to examine the impacts of specific factors that had a greater influence on the discharge output.

Ten parameters were identified as the sensitive parameters for the basin. Base Flow Alpha Factor for Bank Storage (ALPHA_BNK.rte), Groundwater Delay from Soil to Channels Days (GW_DELAY.gw), Effective Hydraulic Conductivity in the Main Channel in mm/hr (CH_K2.rte), Snow Water Equivalent that corresponds to 50% Snow Cover (SNO50COV.bsn), Plant Uptake Compensation Factor (EPCO.hru), Soil Evaporation Compensation Factor (ESCO.hru), Threshold Depth of water in Shallow Aquifer Required for Return Flow in mm (GWQMN.gw), Temperature Lapse Rate in °C/km (TLAPS.sub), Maximum Melt Rate for Snow during the Year (SMFMX.bsn) and Average Slope Steepness in m/m (HRU_SLP.hru) was discovered to have a more significant impact on the Trishuli basin. Table 5.1 presents the calibrated parameters depending on their sensitivities determines ranking of those parameters.

Table 5.1: Parameter's Rank based on their sensitivities

Rank	Parameter Name	Description	t-stat	p-value	Initial Range	Fitted Value
1	ALPHA_BNK.rte	Base Flow Alpha Factor for Bank Storage	13.827	0.000	0 - 1	0.17
2	GW_DELAY.gw	Groundwater Delay From Soil to Channels (Days)	2.686	0.008	0 - 500	352.49
3	CH_K2.rte	Effective Hydraulic Conductivity in the Main Channel (mm/hr.)	-1.863	0.063	0 - 300	260.89
4	SNO50COV.bsn	Snow Water Equivalent that corresponds to 50% Snow Cover	-1.669	0.096	0 - 1	0.81
5	EPCO.hru	Plant Uptake Compensation Factor	1.639	0.102	0 - 1	0.61
6	ESCO.hru	Soil Evaporation Compensation Factor	-1.633	0.103	0 - 1	0.82
7	GWQMN.gw	Threshold Depth of water in Shallow Aquifer Required for Return Flow (mm)	1.633	0.104	0 - 2500	343.42
8	TLAPS.sub	Temperature Lapse Rate (°C/km)	1.605	0.110	(-8) - 0	-7.04
9	SMFMX.bsn	Maximum Melt Rate for Snow during the Year	-1.531	0.127	0-10	7.23
10	HRU_SLP.hru	Average Slope Steepness (m/m)	1.339	0.181	(-0.2) - 0.35	0.31

5.1.1 Model Performance Evaluation

The model's simulation span covered 23 years, starting from 1997 and ending in 2019. The assessment of the model's ability to accurately represent the hydrological simulation of the basin was based on three statistical parameters Nash Sutcliffe efficiency (NSE), Coefficient of Determination (R^2), and Percentage Bias (PBIAS). Figure 5.1 illustrates the hydrograph of the model, depicting its performance at the tailrace gate of the Devighat Hydropower Plant throughout the calibration and validation periods.

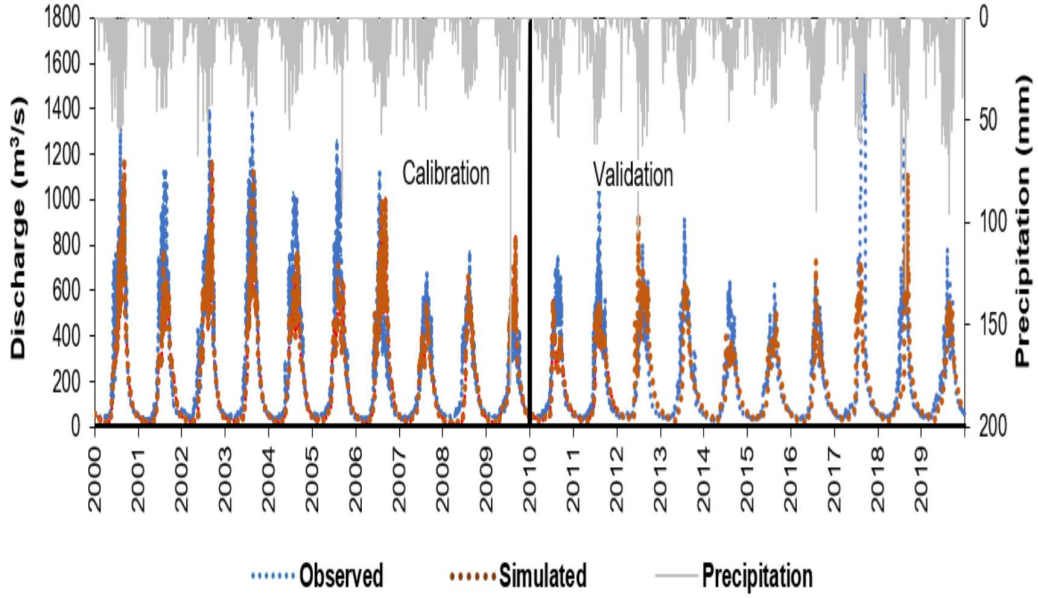

Figure 5.1: Observed Vs. Simulated Monthly Discharge Hydrograph for Calibration & Validation

Throughout the calibration and validation periods, there was a notable consistency between the simulated and actual discharges. The results of the SWAT model's simulation and validation in the Trishuli Watershed, specifically for the monthly discharge at the tailrace point of the Devighat Hydropower Station, demonstrate the model's accurate representation of the basin's hydrology, while also meeting the acceptable limits for statistical parameters. Table 5.2 provides a detailed presentation of the various statistical performance indicators of the SWAT simulation for the Devighat Hydropower Station tailrace point.

Table 5.2: Statistical Performance of Discharge during Calibration and Validation at Devighat HPS Tailrace Point (Sub- Basin No. 33)

S.N.	Period	Timeline	Performance Indicators		
			R^2	NSE	PBIAS
1	Calibration Period	2000-2010	0.78	0.76	14 %
2	Validation Period	2011-2019	0.70	0.69	5.5 %

The calibrated and validated performance statistics values are within the acceptable range. The statistical performance indicator shows the model has strong predictability capacity and reliability. The coefficient of determination (R^2) is used to identify the proportion of variance in the measured data whose value ranges from -1 to 1 if the model is valid. The optimal value of the coefficient of determination (R^2) is 1 but the model is rated satisfactory if its value is greater than 0.5. Similarly, the statistical parameter Nash Sutcliffe Efficiency (NSE) is been used to fix the relative degree of the residual variance (noise) in the model by comparing it with the measured data variance (information). It is also used as an indicative statistical sign to know how exactly the plot of simulated and observed data is fitting the 1:1 Line. Nash Sutcliffe Efficiency (NSE) value ranges from to 1 and the ideal value is 1. For the model statistical performance, the Nash Sutcliffe Efficiency (NSE) value higher than 0.5 is considered to be satisfactory. Lastly, to confirm the average tendency of the simulated data of the SWAT model to be larger or smaller than their observed counterpart, a statistical performance parameter known as the percentage of bias (PBIAS) is used. Based on the positive and negative percentage of the bias value of the model the underestimation and overestimation bias in the model are depicted. The best value of percentage of bias (PBIAS) is the least value of ±0% but for the model to be satisfactory, it can be in the range of ± 25%. The statistical rating is discussed in Table 5.3.

Table 5.3: Statistical Rating of Model (Moriasi et. al., 1998)

Rating of	Coefficient of	Nash Sutcliffe	Percentage of BIAS
Very good	$0.75 \leq R^2 < 1$	$0.75 \leq NSE < 1$	$PBIAS \leq \pm 10\%$
Good	$0.65 \leq R^2 < 0.75$	$0.65 \leq NSE < 0.75$	$10\% < PBIAS \leq \pm 15\%$
Satisfactory	$0.5 \leq R^2 < 0.65$	$0.5 \leq NSE < 0.65$	$15\% < PBIAS \leq \pm 25\%$
Unsatisfactory	$R+ < 0.5$	$NSE < 0.5$	$PBIAS > \pm 25\%$
Ideal Value	$R^2 = 1$	$NSE = 1$	$PBIAS = 0\%$

Last but not least, in order to validate an average tendency of the SWAT model's simulated data to be greater or smaller than its observed counterpart, a statistical performance parameter known as the percentage of bias (PBIAS) is used. The ideal percentage of bias (PBIAS) value is the least value of 0%, however for the model to be good, it can be in the range of 25%. Based on the positive and negative percentage of the bias value of the model, the underestimation and overestimation bias in the model are illustrated. Table 5.2 depicts the statistical rating of a model.

For the time period 2000–2010, the calibrated performance statistics value had a Coefficient of Determination (R^2) value of 0.78, which is greater than 0.75. The Nash Sutcliffe Efficiency (NSE) number is likewise more than 0.75, or above the allowable statistical performance limit, at 0.76. The Percentage Bias (PBIAS) value for the same calibration period is 14%, which is within the allowed range of 15%. The Coefficient of Determination (R^2) value for the 2011–2019 period of identified performance statistics was 0.70, which is in between of 0.65 and 0.75. The Nash Sutcliffe Efficiency (NSE) number is also 0.69, which is over the permissible statistical performance limit and higher than 0.75. The Percentage Bias (PBIAS) value over the same calibration period is 5.5%, which falls below 10% within the permitted range and is very good. The statistical performance indicator demonstrates the model's high capability for prediction and reliability.

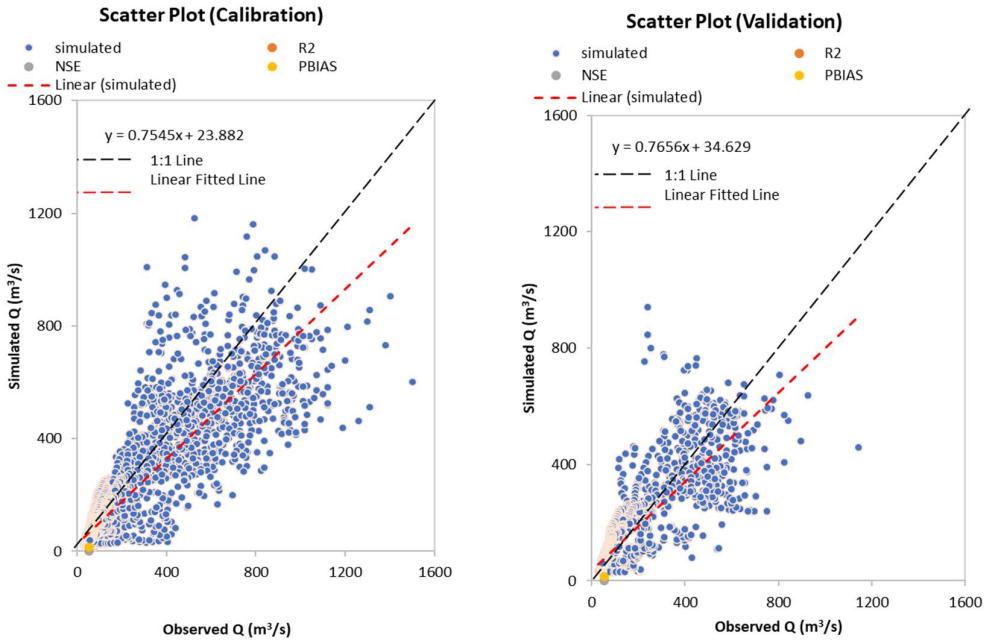

a) b)

Figure 5.2: Scatterplot of Simulated Versus Observed Discharge at Trishuli Basin a) Calibration b) Validation

Figures 5.2(a, b) show the scatter plots. The scatter plot in the figure depicts that the modeling estimates are correlating well throughout the flow period and somewhat spread out at the high flow period. It is clear from the hydrograph used for calibration and validation that the model predicts the flows preety well.

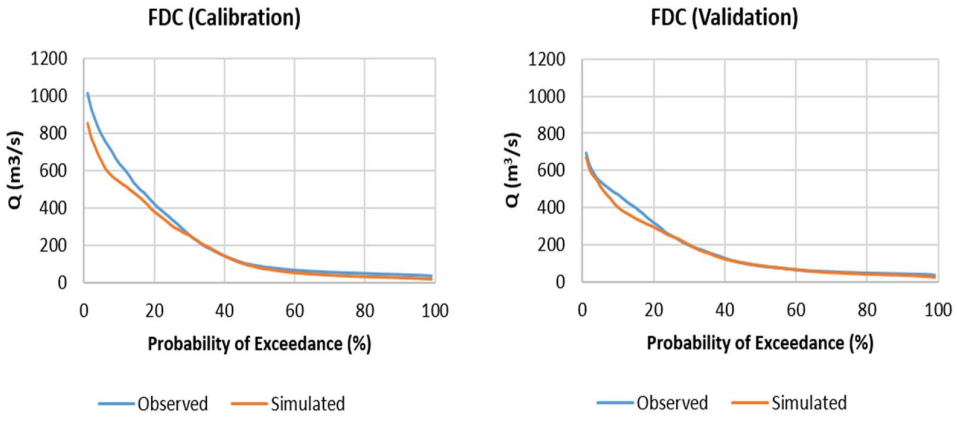

a) b)

Figure 5.3: Flow duration curve for observed discharge and simulated discharge a) Calibration b) Validation period.

It is clear from the hydrograph created for calibration and validation purposes that the model forecasts the flows preety well throughout all the seasons. The monthly hydrograph depicts higher precipitation during the months of June, July, August, and September with the highest precipitation in the month of August. The precipitation in the month of August is 460.87mm during the calibration period and it is 507.72 mm during the validation period. The observed discharge during the calibration period is at its peak during the month of August and it is 696.11 m^3/s while the simulated discharge is at its peak during the month of August and it is 599.44 m^3/s. The observed discharge during the validation period is at its peak during the month of August and it is 510.16 m^3/s while the simulated discharge is at its peak during the month of August and it is 444.13 m^3/s. The average monthly hydrograph is presented in Figure 5.4 below.

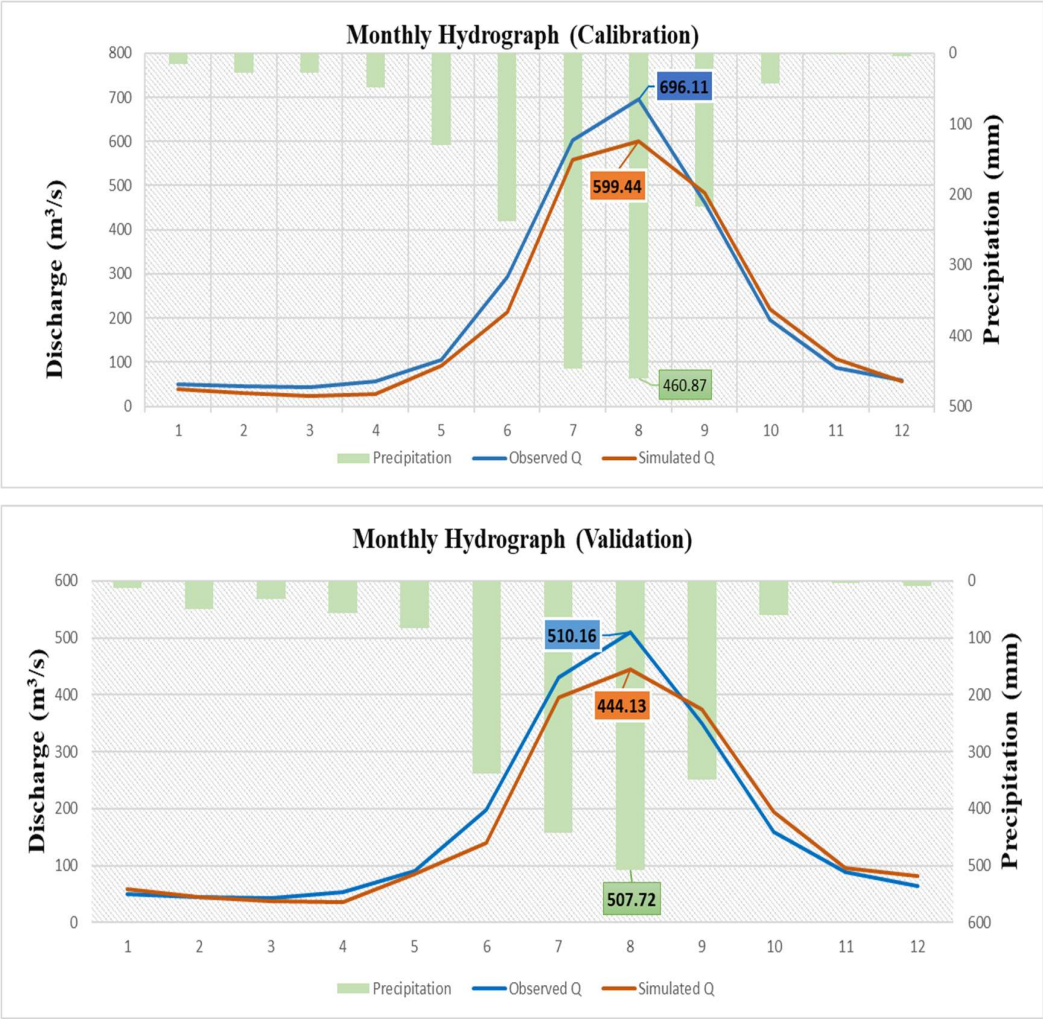

Figure 5.4: Average monthly hydrographs for observed and simulated discharge during calibration and validation period.

5.2 Projected Future Climate

The calibrated and validated SWAT model was run with projected future precipitation and temperature time series, based on SSP245 and SSP585 scenarios. The discharge from the simulated SWAT model used as the reference period's baseline data. An ensemble of 5 GCMs, INM-CM4, EC-EARTH3, MRI-ESM2, NoR-ESM2, and MPI-ESM1, had their simulated discharge from the future compared to the discharge derived from the reference period. The projected precipitation and temperature for the future time were examined using bias-corrected climatic data from the Trishuli River Basin. Three timelines, referred to as the near future (NF), mid-future (MF), and far future (FF), respectively, covering the years 2023 to 2048, 2049 to 2074, and 2075 to 2100, were created for the future period. Compared to the reference period (2000-2019), each period has 26 years of data. Under the circumstances of SSP245 and SSP585, the evaluation is carried out using forecasts from 5 CMIP6 models.

5.2.1 Projected Temperature

The most sensitive parameter and important factor in weather science is temperature. For all upcoming intervals NF, MF, and FF, the exchange will be expected month-to-month in addition to seasonally for both minimum and most temperatures in comparison to the starting month-to-month temperature. The estimate made using data from five different global climate models (GCMs) indicates a crucial temperature increase in both scenarios. For all GCMs, the majority of temperature rises look progressive over time. In Figure 5.6-5.11, the five models monthly forecasted temperatures for upcoming events are illustrated.

Among the five models considered, the highest average monthly temperature for the Nuwakot station in the future scenarios is recorded in the INM-CM4-8 model. According to projections, it is expected to reach 28.14°C within the month of June for the SSP245 scenario and 28.41°C within the month of August for the SSP585 scenario during the near future. On the other hand, the lowest average monthly temperature for the Nuwakot station in the future scenarios is also observed in the INM-CM4-8 model. It is projected to reach 15.65°C within the month of January for the SSP245 scenario and 15.79°C for the SSP585 scenario during the near future. The average monthly temperature projection of Nuwakot Station in the near future is presented in Figure 5.6.

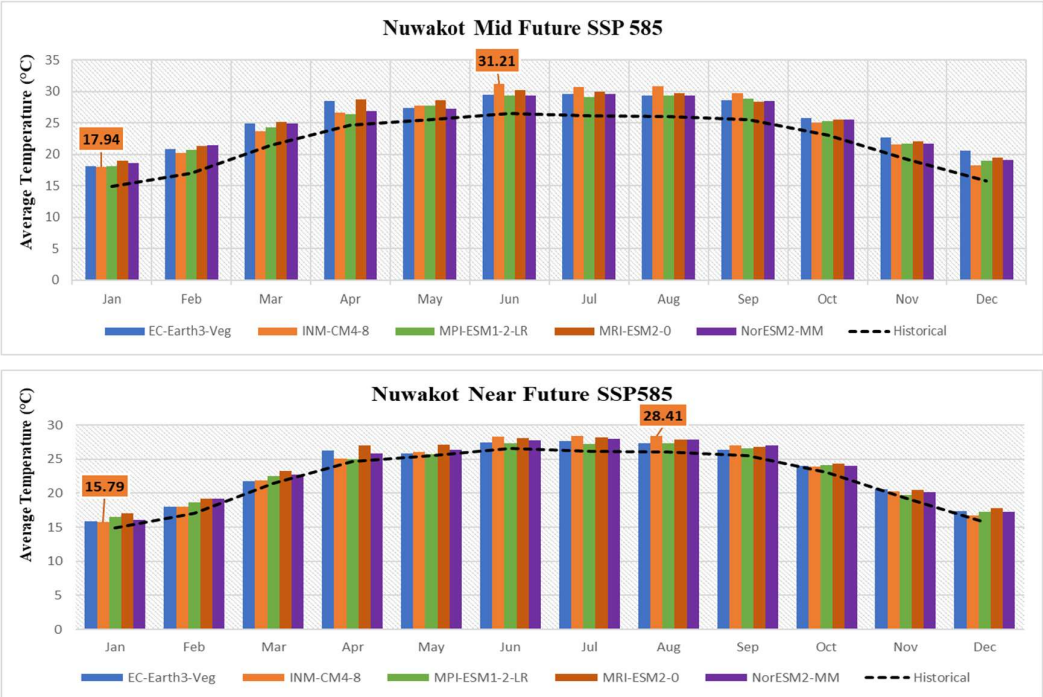

Figure 5.6: Projected Average monthly temperature (^{0}C) in Nuwakot Station in near future under two scenarios (a) SSP245 Scenario (b) SSP585 Scenario

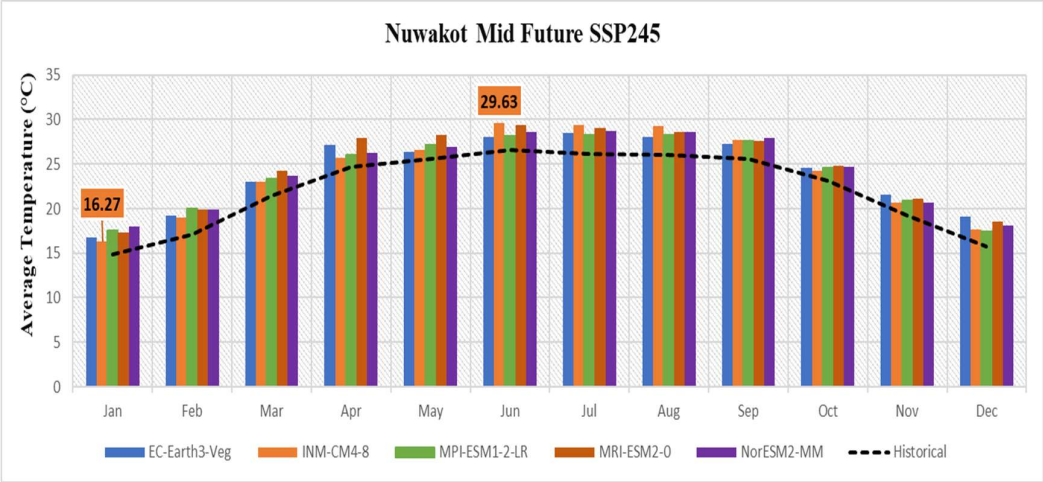

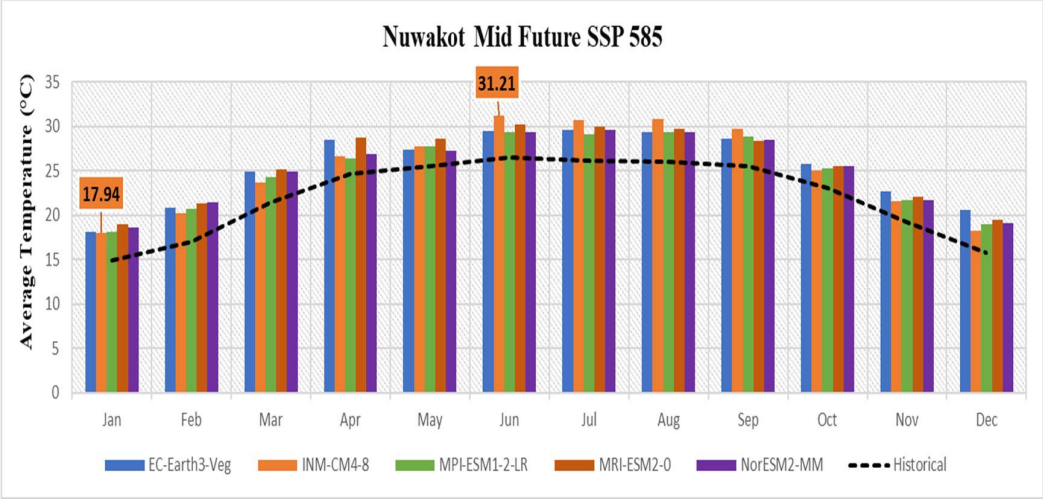

Figure 5.7: Projected Average monthly temperature (^{0}C) in Nuwakot Station in mid future undertwo scenarios (a) SSP245 Scenario (b) SSP585 Scenario

The INM-CM4-8 model exhibits the highest average monthly temperature for the Nuwakot station among the five models in the future scenarios. It is estimated to reach 29.63° within the month of June for the SSP245 scenario during the mid-future, and for the SSP585 scenario, it is projected to reach 31.21°C in the same month and time period. Similarly, the lowest average monthly temperature for the Nuwakot station among the future scenarios and five models is observed in the INM-CM4-8 model. The projection indicates that during the mid-future in the month of January, it is expected to reach 16.26°C for the SSP245 scenario and 17.94°C for the SSP585 scenario. The average monthly temperature projection of Nuwakot Station in the mid-future is presented in Figure 5.7.

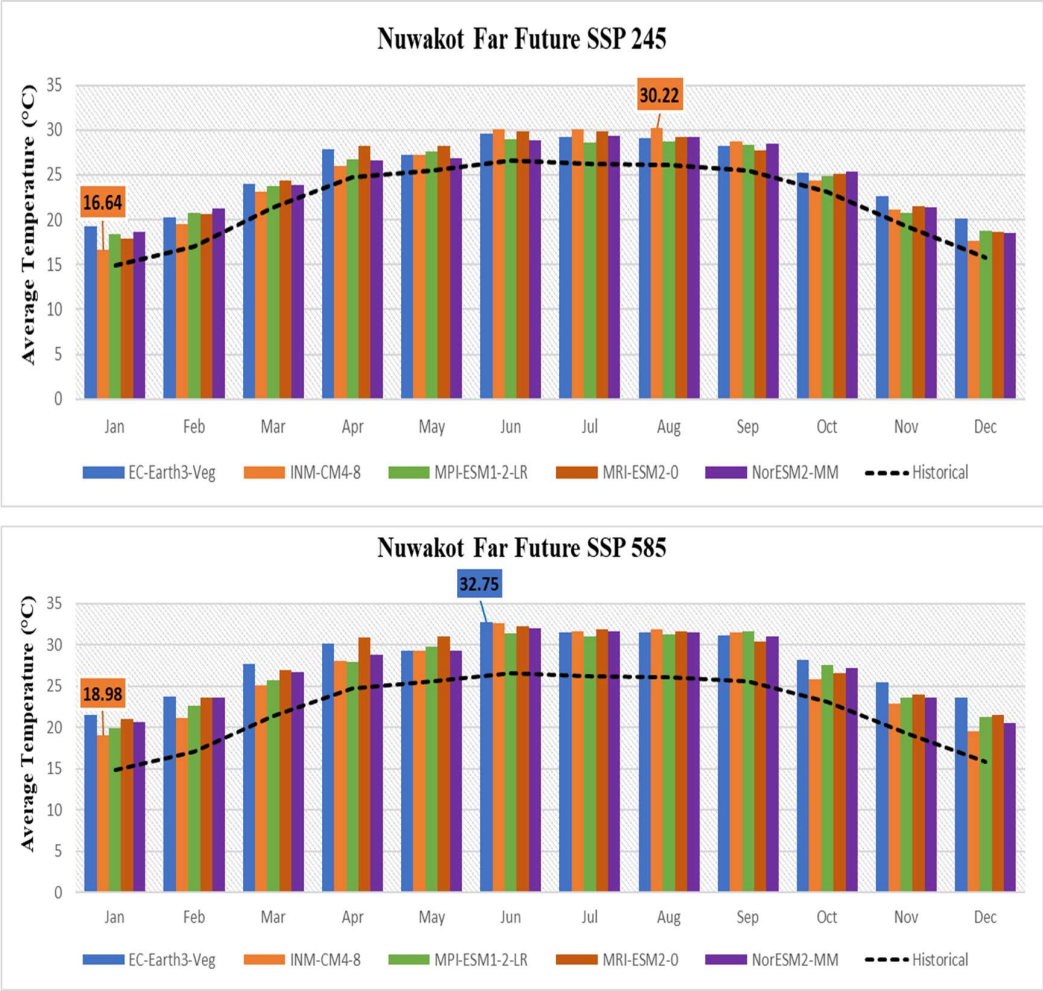

Figure 5.8: Projected Average monthly temperature (^{0}C) in Nuwakot Station in far future under two scenarios (a) SSP245 Scenario (b) SSP585 Scenario

The maximum average monthly temperature for the Nuwakot station for future scenarios among the five models is observed in the INM-CM4-8 model and is projected to reach 30.22°C during the far-future within the month of August for the SSP245 scenario and the maximum average monthly temperature for the Nuwakot station for future scenarios among the five models is observed in the EC-Earth3-Veg model is projected to reach 32.75°C in the far future within the month of June for the SSP585 scenario. Likewise, the minimum average monthly temperature for the Nuwakot station for future scenarios among the five models is observed in the INM-CM4-8 model and is projected to reach 16.64°C during the far future within the month of January for the SSP245 scenario and is projected to reach 18.98°C in the far future within the month of January for the SSP585 scenario. The average monthly temperature projection of Nuwakot Station in the far-future is presented in Figure 5.8.

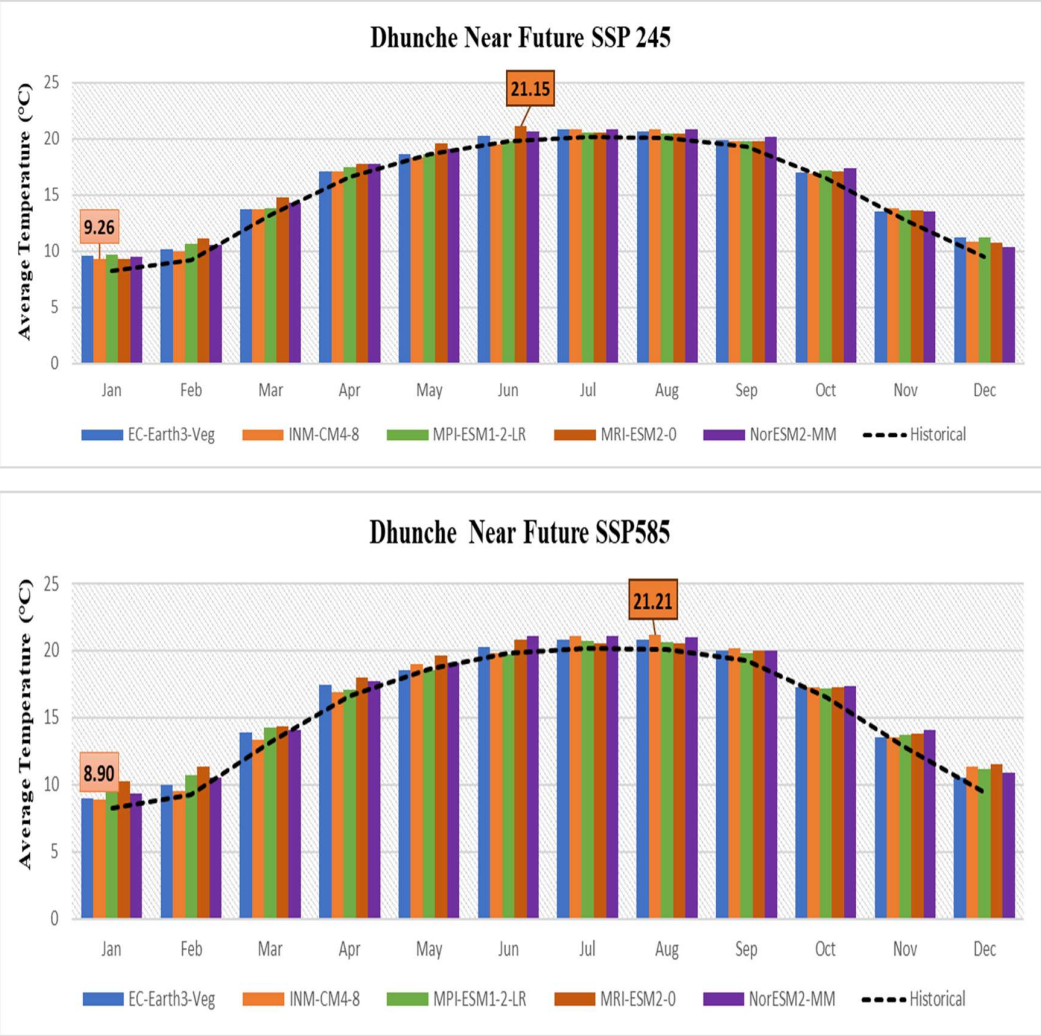

Figure 5.9: Projected Average monthly temperature (^{0}C) in Dhunche Station in near future undertwo scenarios (a) SSP245 Scenario (b) SSP585 Scenario

The maximum average monthly temperature for the Dhunche station for future scenarios among the five models is observed in the MRI-ESM2-0 model and is projected to reach 21.15°C during the near future within the month of June for the SSP245 scenario while the maximum monthly average is observed in the INM-CM4-8 model and is projected to reach 21.21°C during the near future within the month of August for the SSP585 scenario. Likewise, the minimum average monthly temperature for the Dhunche station for future scenarios among the five models is observed in the INM-CM4-8 model and is projected to reach 9.26°C during the near future within the month of January for the SSP245 scenario and is projected to reach 8.89°C in the near future within the month of January for the SSP585 scenario. The average monthly temperature projection of Dhunche Station in the near future is presented in Figure 5.9.

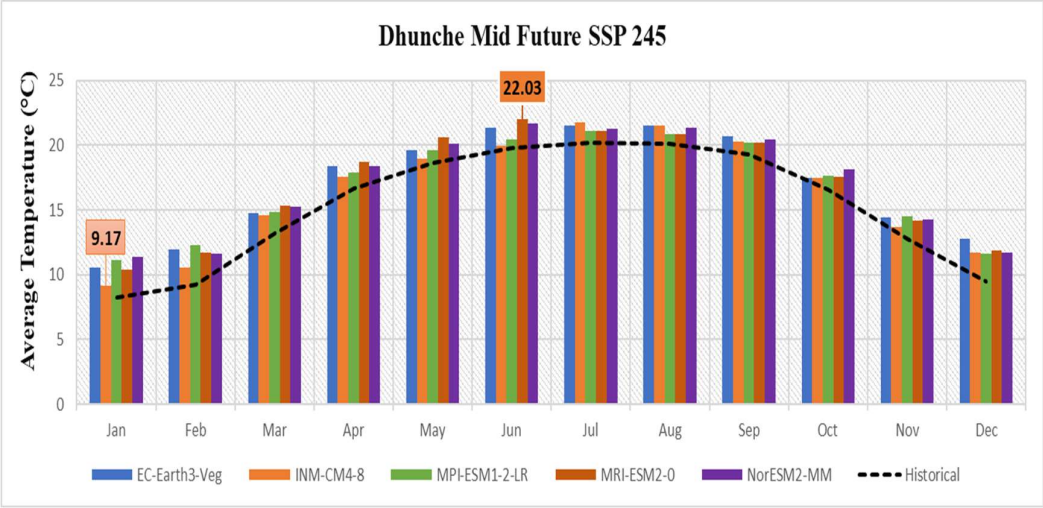

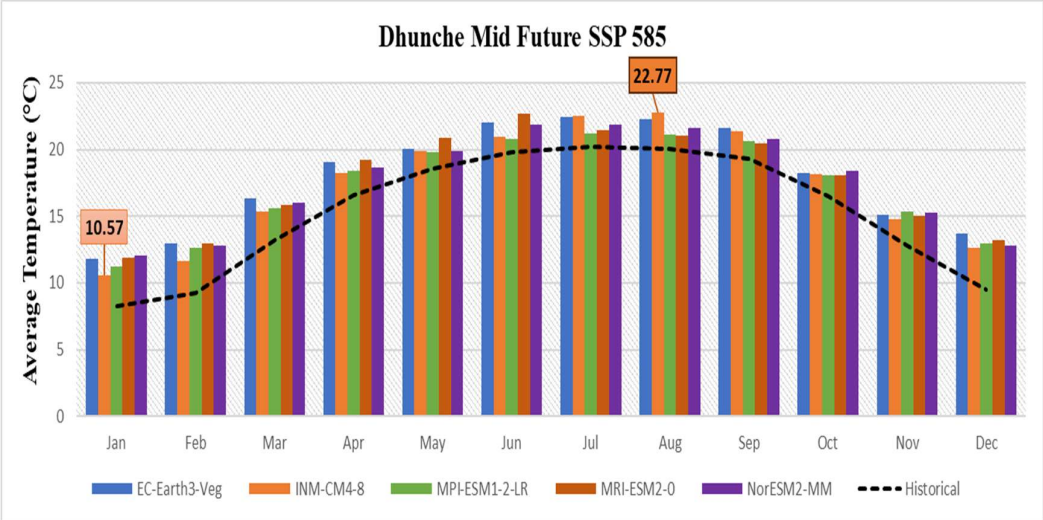

Figure 5.10: Projected Average monthly temperature (^{0}C) in Dhunche Station in mid future under two scenarios (a) SSP245 Scenario (b) SSP585 Scenario

The maximum average monthly temperature for the Dhunche station for future scenarios among the five models is observed in the MRI-ESM2-0 model and is projected to reach 22.02°C during the mid-future within the month of June for the SSP245 scenario while the maximum monthly average is observed in the INM-CM4-8 model and is projected to reach 22.78°C in the mid future within the month of August for the SSP585 scenario. Likewise, the minimum average monthly temperature for the Dhunche station for future scenarios among the five models is observed in the INM-CM4-8 model and is projected to reach 9.16°C during the near future within the month of January for the SSP245 scenario and is projected to reach 10.57°C in the mid future within the month of January for the SSP585 scenario. The average monthly temperature projection of Dhunche Station in the mid-future is presented in Figure 5.10.

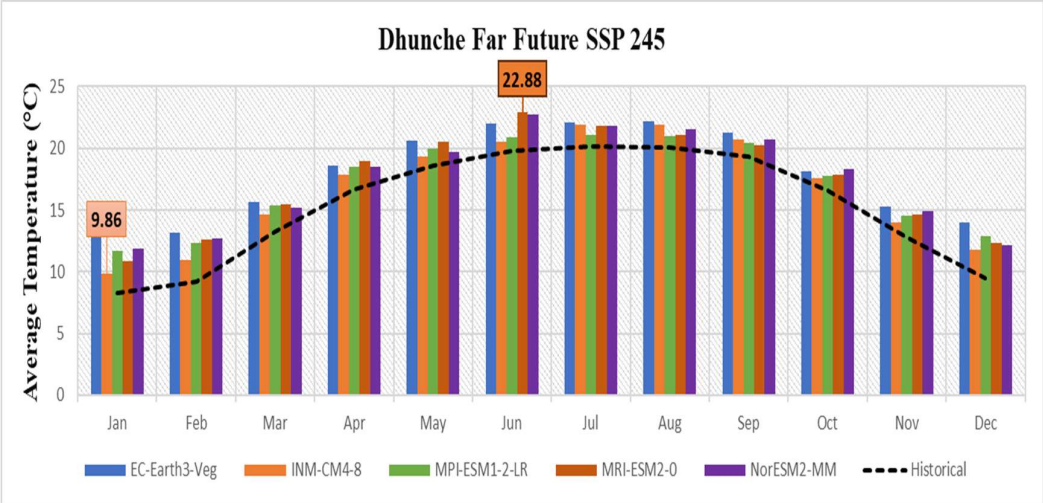

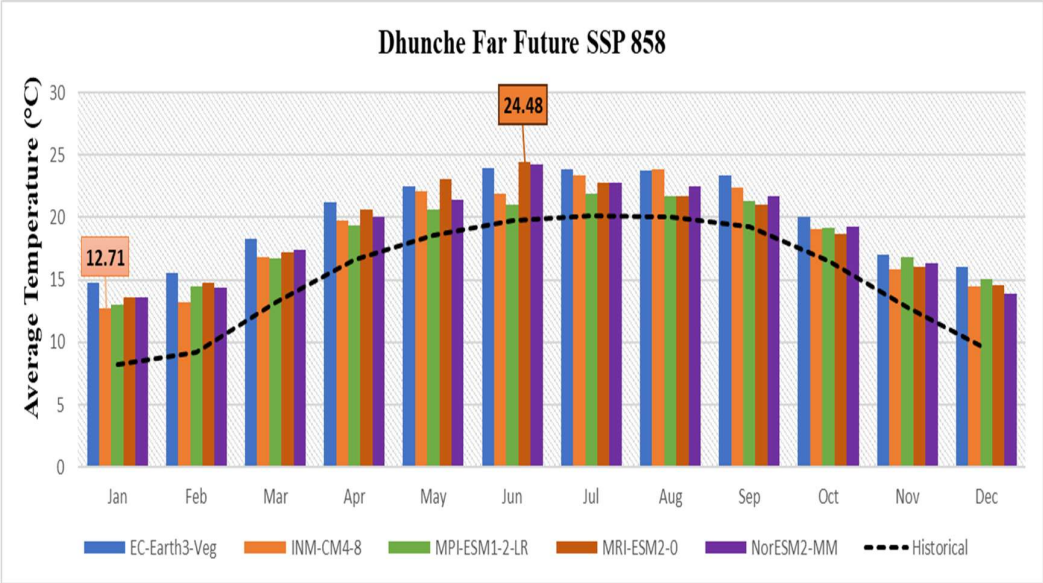

Figure 5.11: Projected Average monthly temperature (^{0}C) in Dhunche Station in far future undertwo scenarios (a) SSP245 Scenario (b) SSP585 Scenario

The maximum average monthly temperature for the Dhunche station for future scenarios among the five models is observed in the MRI-ESM2-0 model and is projected to reach 22.87°C during the far future within the month of June for the SSP245 scenario and is projected to reach 24.48°C in the far future within the month of June for the SSP585 scenario. Likewise, the minimum average monthly temperature for the Dhunche station for future scenarios among the five models is observed in the INM-CM4-8 model and is projected to reach 9.85°C during the far future within the month of January for the SSP245 scenario and is projected to reach 12.70°C during the far future in the month of January for the SSP585 scenario. Figure 5.11 provides the forecast for Dhunche Station's average monthly temperature in the far future.

5.2.2 Projected Precipitation

The projected average precipitation of the five CMIP6 models shows an increase in annual precipitations in all future periods though the decrease in monthly precipitations is observed in various months under both the SSP245 and SSP585 scenarios. There is erratic behavior in the change in precipitation on a monthly basis. The average monthly projected precipitation for future scenarios of the five models is presented in Figure 5.12-5.17.

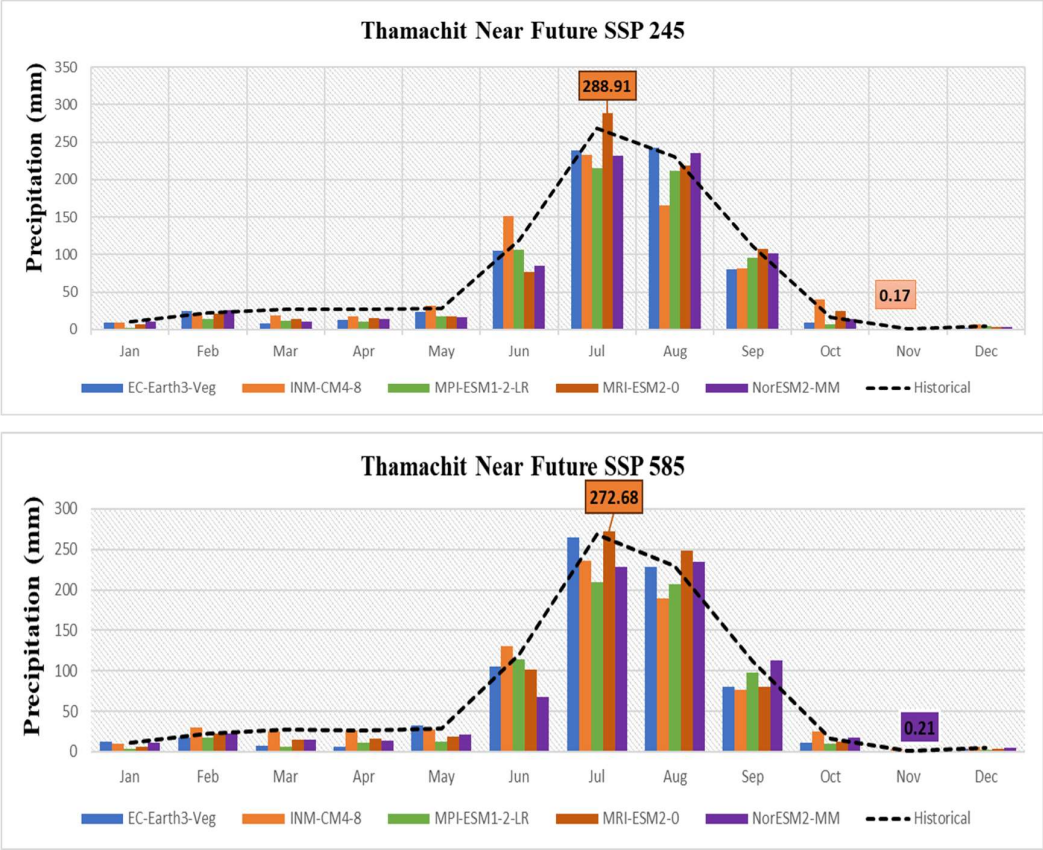

Figure 5.12 Average monthly precipitation (mm) in Thamachit Station in the near future under two scenarios (a) SSP245 Scenario (b) SSP585 Scenario

The MRI-ESM2-0 model shows the highest average monthly precipitation for the Thamachit station among the five models in the future scenarios. It is projected to reach 288.91mm within the month of July for the SSP245 scenario during the near future, and for the SSP585 scenario, it is projected to reach 272.68 mm in the same month and time period. Similarly, the EC-Earth3-Veg model demonstrates the lowest average monthly precipitation for the Thamachit station among the five models in the future scenarios. It is projected to reach 0.17 mm within the month of November for the SSP245 scenario

during the near future. Additionally, the NorESM2-MM model indicates the lowest average monthly precipitation for the Thamachit station among the five models in the future scenarios. It is projected to reach 0.21 mm in the month of November for the SSP585 scenario during the near future. The average monthly precipitation projection of Thamachit Station in the near future is presented in Figure 5.12.

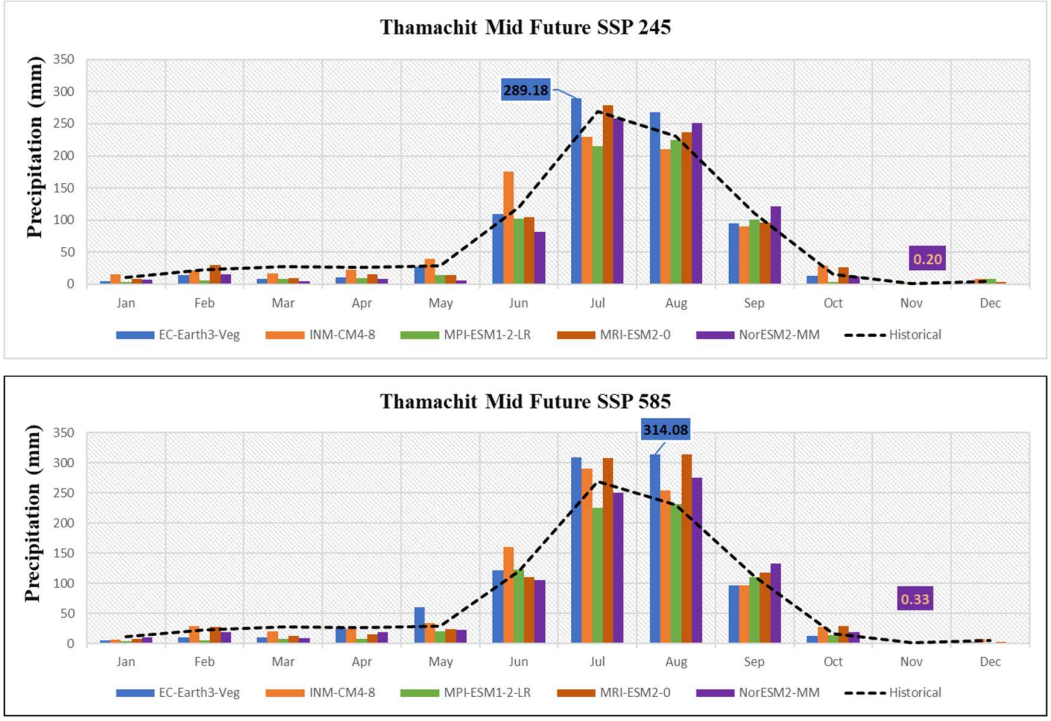

Figure 5.13 Average monthly precipitation (mm) in Thamachit Station in mid future under two scenarios (a) SSP245 Scenario (b) SSP585 Scenario

The maximum average monthly precipitation for the Thamachit station for future scenarios among the five models is observed in the EC-Earth3-Veg model and is projected to reach 289.18 mm during the mid-future in the month of July for the SSP245 scenario and is projected to reach 314.08 mm during the mid-future in the month of August for the SSP585 scenario. Likewise, the minimum average monthly temperature for the Thamachit station for future scenarios among the five models is observed in the NorESM2-MM model and is projected to reach 0.19 mm during the mid-future in the month of November for the SSP245 scenario and is projected to reach 0.33 mm during the mid-future in the month of November for the SSP585 scenario. The average monthly precipitation projection of Thamachit Station in the mid-future is presented in Figure 5.13.

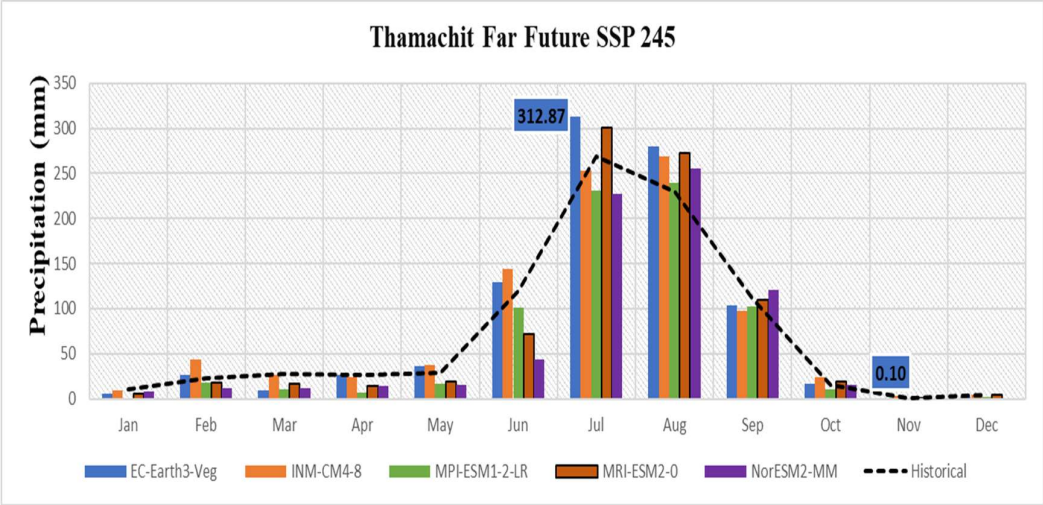

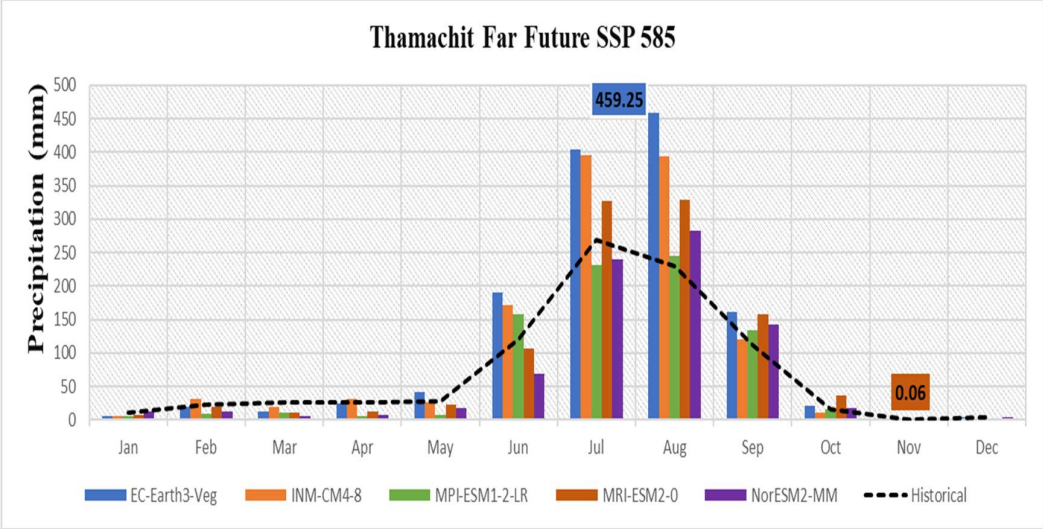

Figure 5.14 Average monthly precipitation (mm) in Thamachit Station in far future under two scenarios (a) SSP245 Scenario (b) SSP585 Scenario

The maximum average monthly precipitation for the Thamachit station for future scenarios among the five models is observed in the EC-Earth3-Veg model and is projected to reach 312.87 mm during the far future within the month of July for the SSP245 scenario and is projected to reach 459.25 mm during the far-future within the month of August for the SSP585 scenario. Likewise, the minimum average monthly temperature for the Thamachit station for future scenarios among the five models is observed in the EC-Earth3-Veg model and is projected to reach 0.10 mm during the far future within the month of November for the SSP245 scenario and is projected to reach 0.06 mm during the far-future within the month of November for the SSP585 scenario in the MRI-ESM2-0 model. The average monthly precipitation projection of Thamachit Station in the far future is presented in Figure 5.14.

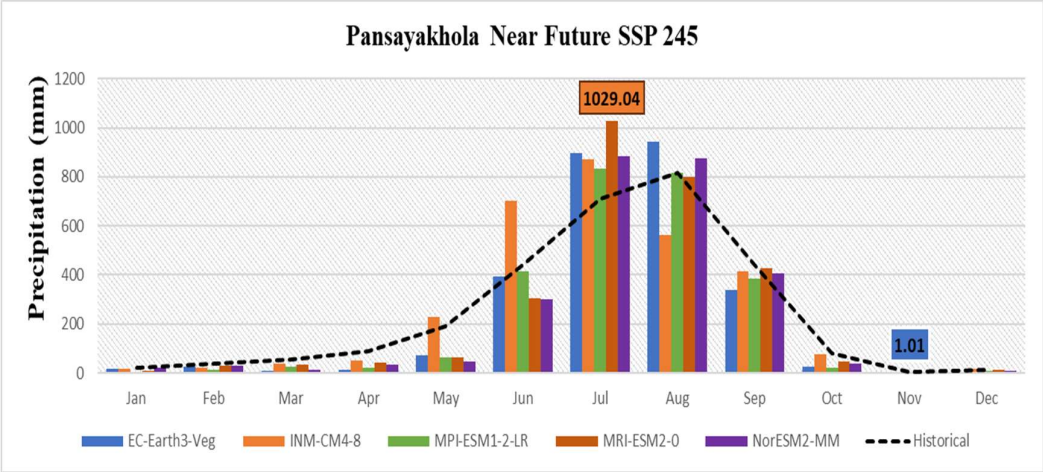

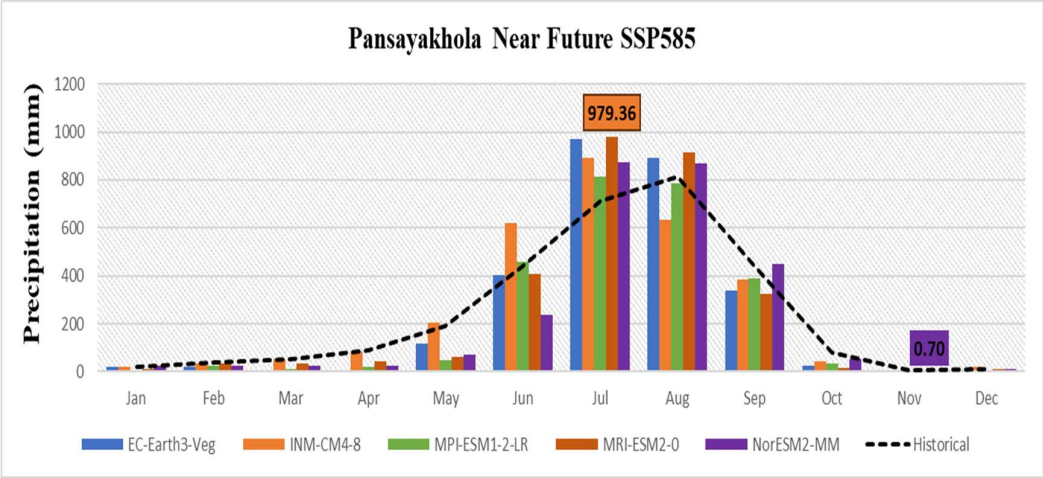

Figure 5.15: Average monthly precipitation (mm) in Pansyakhola Station in the near future under two scenarios (a) SSP245 Scenario (b) SSP585 Scenario

The maximum average monthly precipitation for the Pansayakhola station for future scenarios among the five models is observed in the MRI-ESM2-0 model and is projected to reach 1029.04 mm during the near future within the month of July for the SSP245 scenario and is projected to reach 979.36 mm during the near future within the month of July for the SSP585 scenario. Likewise, the minimum average monthly temperature for the Pansayakhola station for future scenarios among the five models is observed in the EC-Earth3-Veg model and is projected to reach 1.01 mm during the near future within the month of November for the SSP245 scenario. Similarly, the minimum average monthly temperature for the Pansayakhola station for future scenarios among the five models is observed in the NorESM2-MM model and is projected to reach 0.70 mm during the near future within the month of November for the SSP585 scenario. The average monthly precipitation projection of Pansayakhola Station in the near future is presented in Figure 5.15.

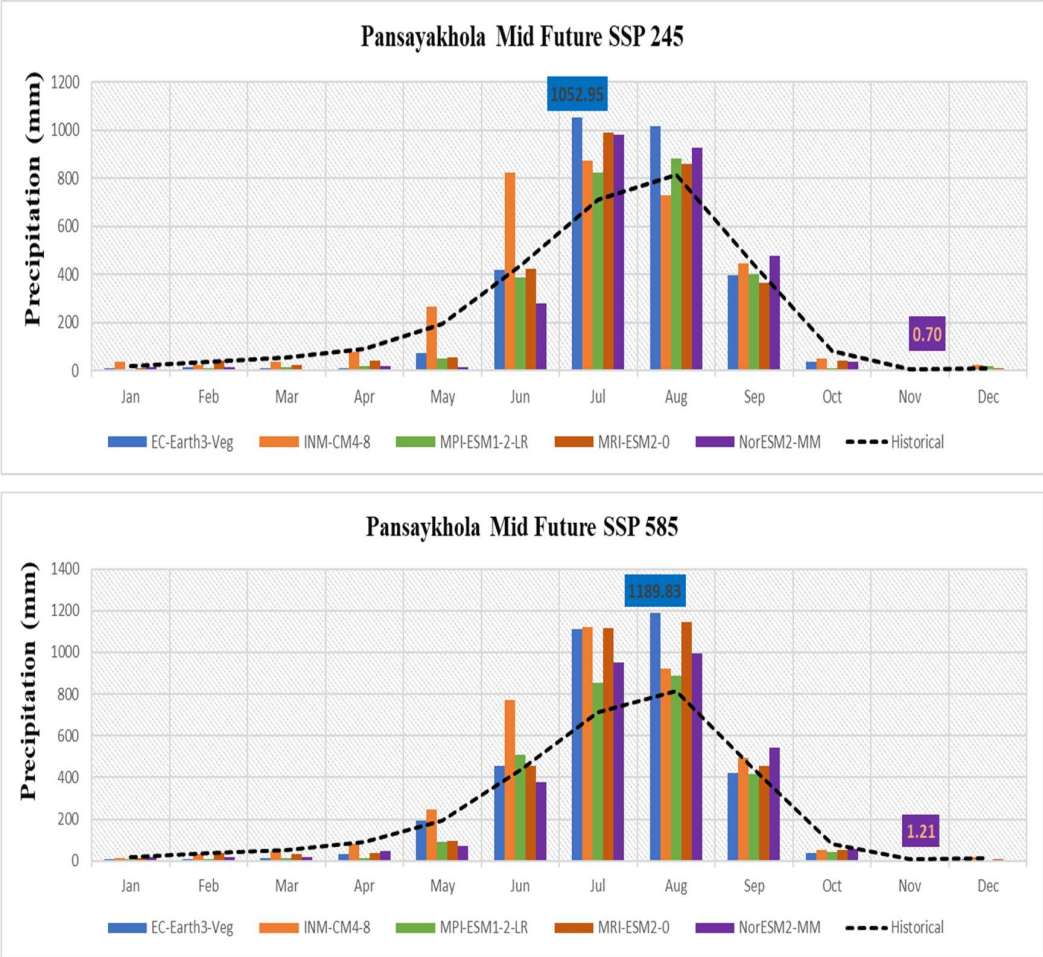

Figure 5.16: Average monthly precipitation (mm) in Pansyakhola Station in mid-future under two scenarios (a) SSP245 Scenario (b) SSP585 Scenario

The maximum average monthly precipitation for the Pansayakhola station for future scenarios among the five models is observed in the EC-Earth3-Veg model and is projected to reach 1052.95 mm during the mid-future within the month of July for the SSP245 scenario and is projected to reach 1189.82 mm during the mid-future in the month of August for the SSP585 scenario. Likewise, the minimum average monthly temperature for the Pansayakhola station for future scenarios among the five models is observed in the NorESM2-MM model and is projected to reach 0.70 mm during the mid-future in the month of November for the SSP245 scenario. Similarly, the minimum average monthly temperature for the Pansayakhola station for future scenarios among the five models is observed in the NorESM2-MM model and is projected to reach 1.21 mm during the mid-future in the month of November for the SSP585 scenario. The average monthly precipitation projection of Pansayakhola Station in the mid future is presented in Figure 5.16

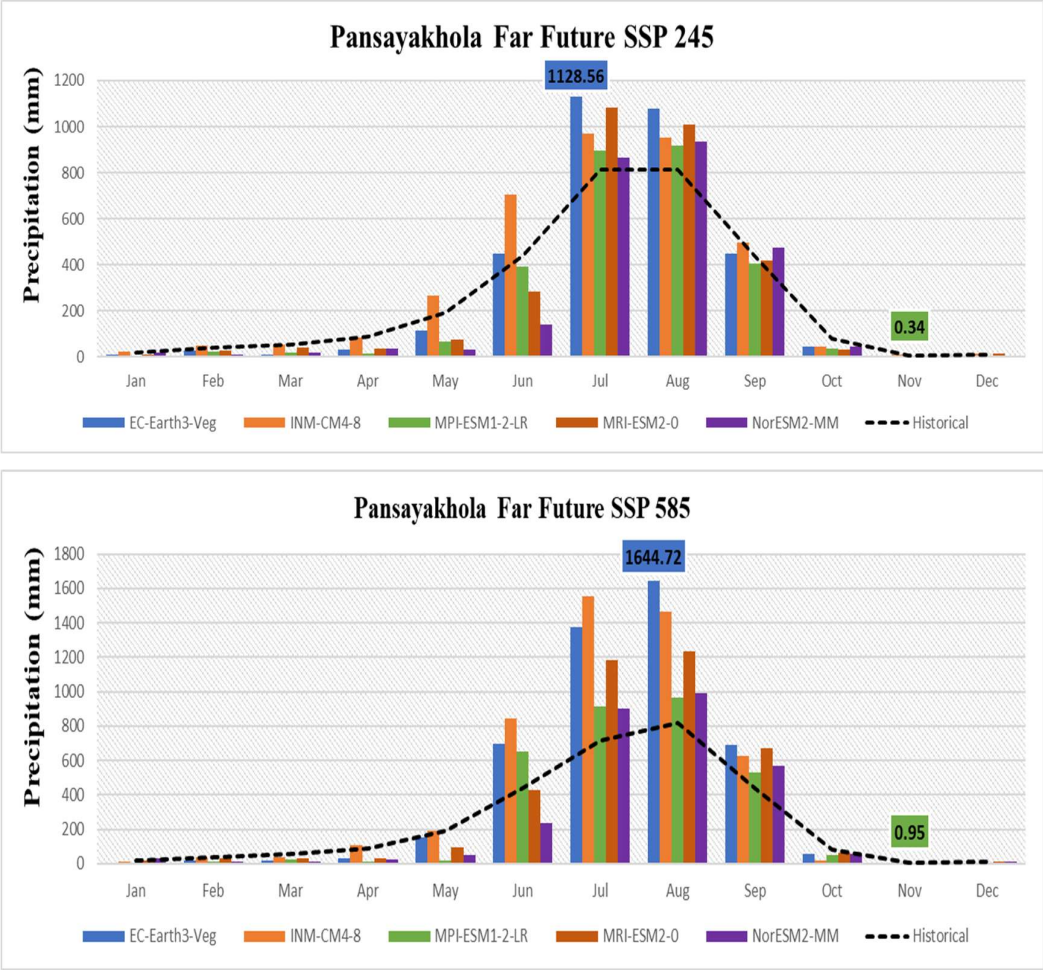

Figure 5.17: Average monthly precipitation (mm) in Pansyakhola Station in the far future under two scenarios (a) SSP245 Scenario (b) SSP585 Scenario

The maximum average monthly precipitation for the Pansayakhola station for future scenarios among the five models is observed in the EC-Earth3-Veg model and is projected to reach 1128.56 mm during the far future within the month of July for the SSP245 scenario and is projected to reach 1644.72 mm during the far-future within the month of August for the SSP585 scenario. Likewise, the minimum average monthly temperature for the Pansayakhola station for future scenarios among the five models is observed in the MPI-ESM1-2-LR model and is projected to reach 0.34 mm during the far future within the month of November for the SSP245 scenario. Similarly, the minimum average monthly temperature for the Pansayakhola station for future scenarios among the five models is observed in the MRI-ESM2-0 model and is projected to reach 0.94 mm during the far-future within the month of December for the SSP585 scenario. The average monthly precipitation projection of Pansayakhola Station in the far future is presented in Figure 5.17.

5.3 Climate Change Impact on Hydrology

The temperature and precipitation data, projected on a monthly basis using five chosen Global Climate Models (GCMs), was utilized as input for the SWAT model that had been calibrated and validated. The purpose was to evaluate how these projections would impact the hydrological characteristics of the basin. The analysis focused on examining alterations in hydrological features at the basin's outlet to comprehend the potential changes in discharge along the streamlines in response to the projected future climate conditions. The average monthly stream flow (m^3/s) and relative change in discharge under both scenarios is presented in Figures 5.18-5.26.

The historical discharge is being compared with the simulated discharge of five Global Climate Models (GCMs). In the near future period of the SSP245 Scenario, the relative change of discharge compared to the baseline varies significantly, ranging from a decrease of 52.87% to an increase of 69.53%. In the Nor-ESM2-MM model, during February in the SSP245 Scenario, the projected discharge is notably higher than the baseline, ranging from 45.42 m^3/s to 77 m^3/s. However, in June of the same scenario and model, the projected discharge declines rapidly, ranging from 295.11 m^3/s to 139.08 m^3/s.

For the SSP585 Scenario in the near future period, the extreme fluctuation of discharge compared to the baseline is even more pronounced, ranging from a decrease of 59.49% to an increase of 94.64%. In the INM-CM4-8 model, during the month of March in the SSP585 Scenario, the projected discharge is considerably higher than the baseline, ranging from 44.83 m^3/s to 87.26 m^3/s. On the other hand, in June of the same scenario and Nor-ESM2-MM model, the projected discharge experiences a sharp decline, ranging from 295.11 m^3/s to 119.53 m^3/s. The average monthly stream flow (m^3/s) and relative change in discharge under both scenarios in the near future is presented in Figure 5.18,5.19 and 5.20.

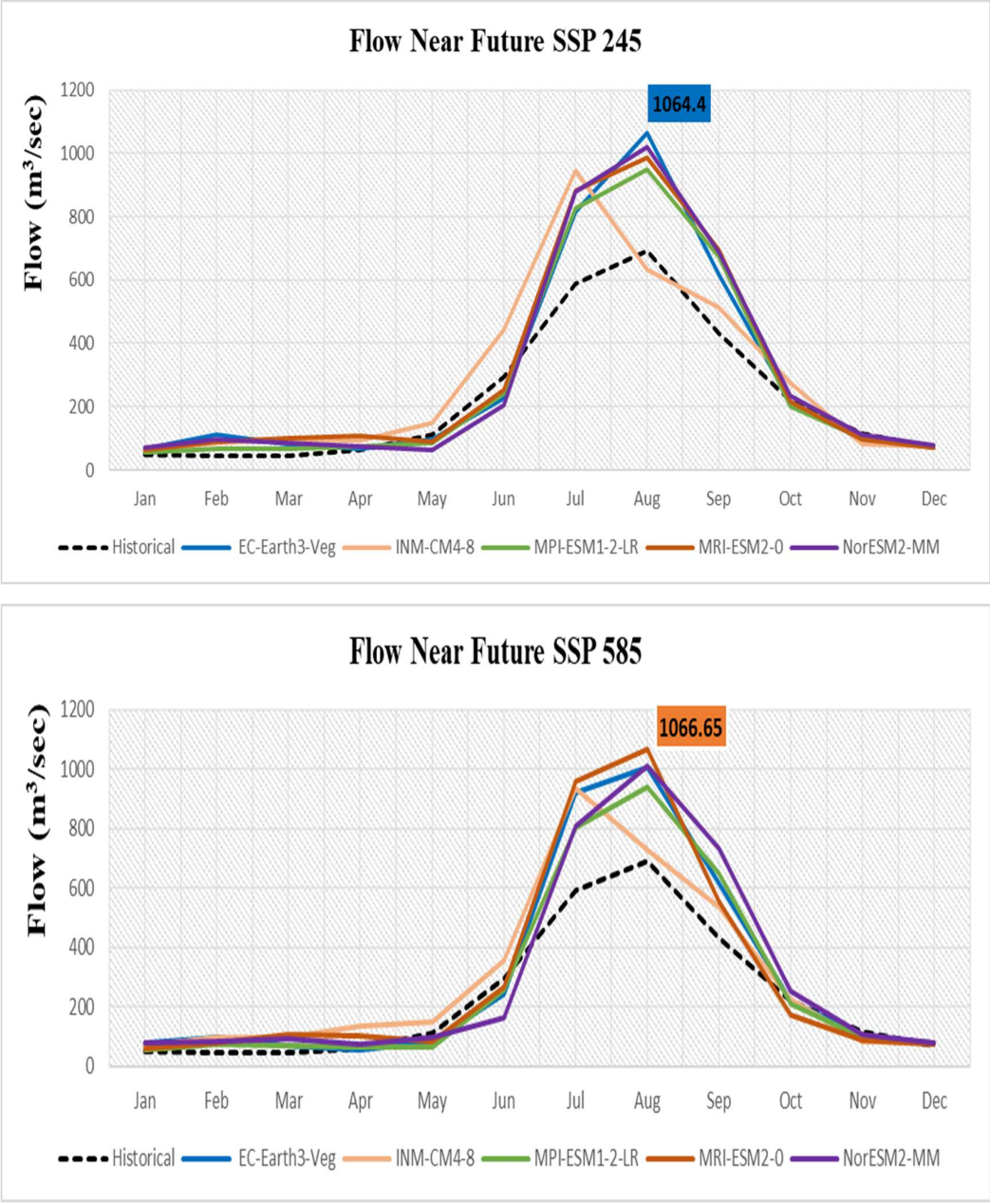

Figure 5.18: Average monthly stream flow (m^3/s) in the near future under two scenarios (a) SSP245 Scenario (b) SSP585 Scenario

The extreme RC in discharge during the mid-future period of the SSP245 Scenario, compared to the baseline, shows a wide range, varying from a decrease of 65.80% to an increase of 104.39%. In the MRI-ESM2-0 model, during the month of February in the SSP245 Scenario, the projected discharge is notably higher than the baseline, ranging from 45.42 m^3/s to 92.83 m^3/s. However, in May of the same scenario and NorESM2-MM model, the projected discharge declines rapidly, ranging from 112.54 m^3/s to 38.49 m^3/s.

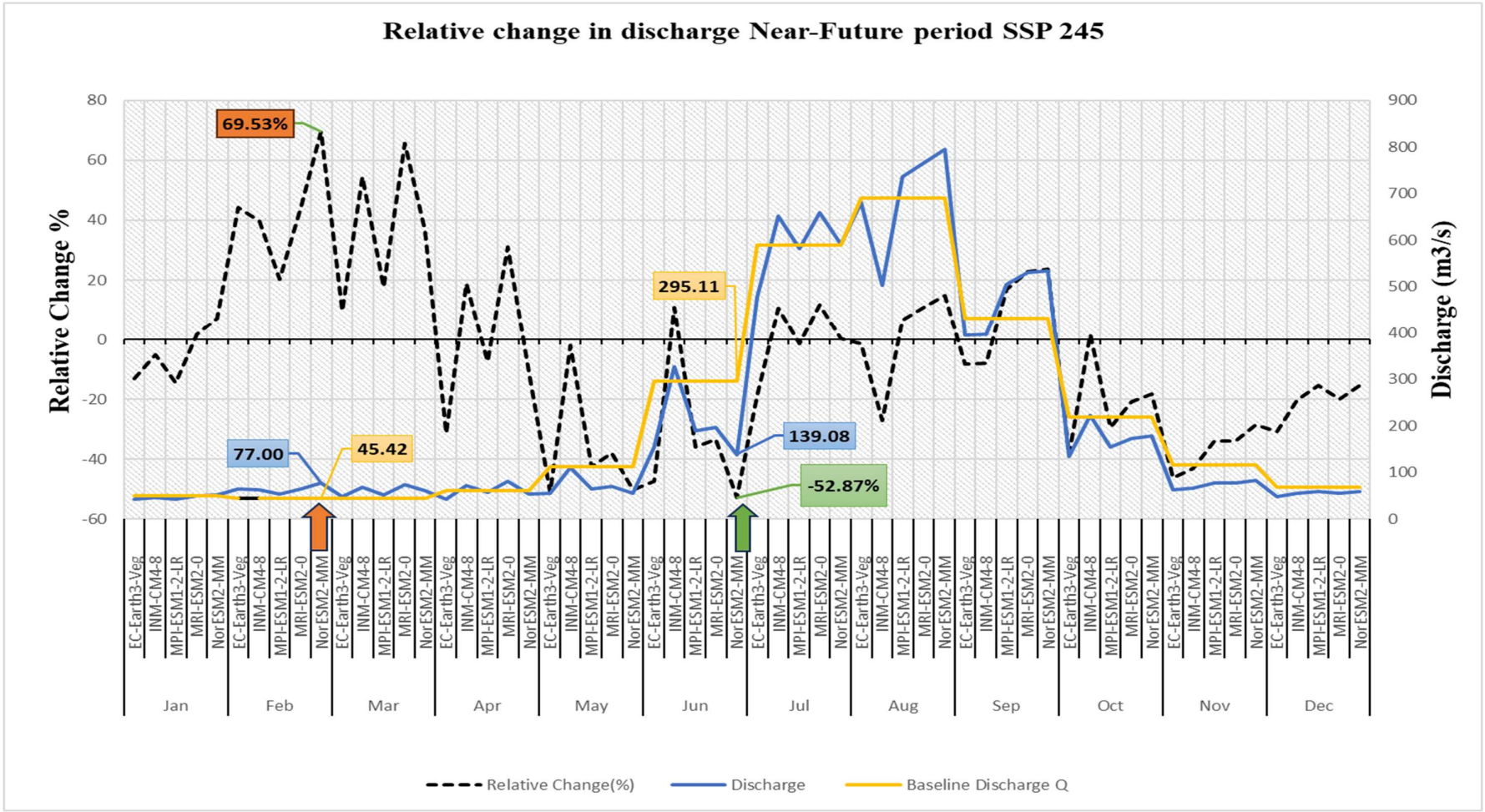

Figure 5.19: Relative change in discharge near future period SSP 245

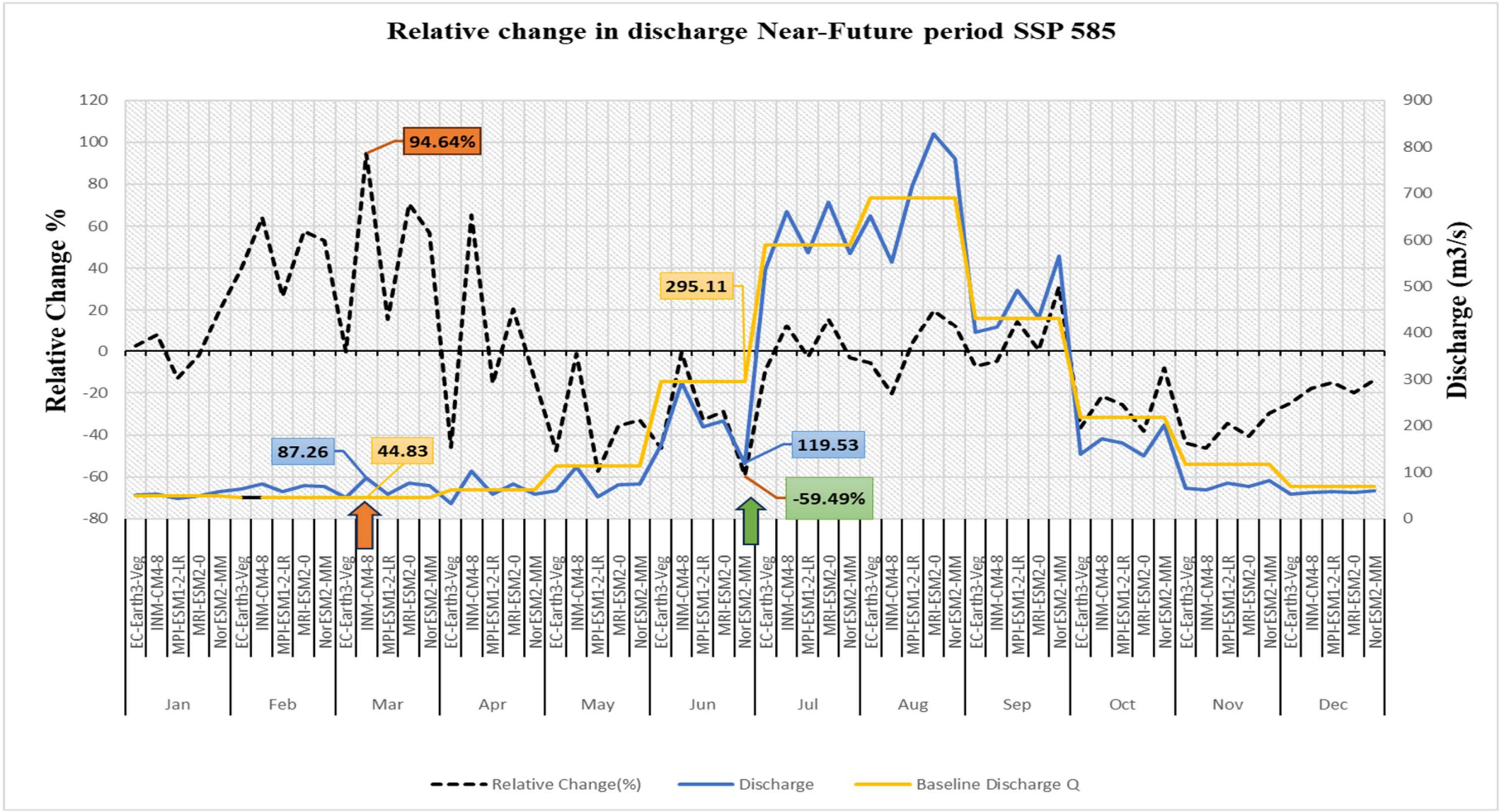

Figure 5.20: Relative change in discharge near future period SSP585

Similarly, in the mid-future period of the SSP585 Scenario, the extreme fluctuation of discharge, compared to the baseline, ranges from a decrease of 53.06% to an increase of 104.99%. In the MRI-ESM2-0 model, during the month of February in the SSP585 Scenario, the projected discharge is considerably higher than the baseline, ranging from 45.42 m^3/s to 93.10 m^3/s. Conversely, in May of the same scenario and MPI-ESM1-2-LR model, the projected discharge experiences a sharp decline, ranging from 112.54 m^3/s to 52.83 m^3/s. The average monthly stream flow (m^3/s) and relative change in discharge under both scenarios in mid future is presented in Figure 5.21, 5.22 and 5.23.

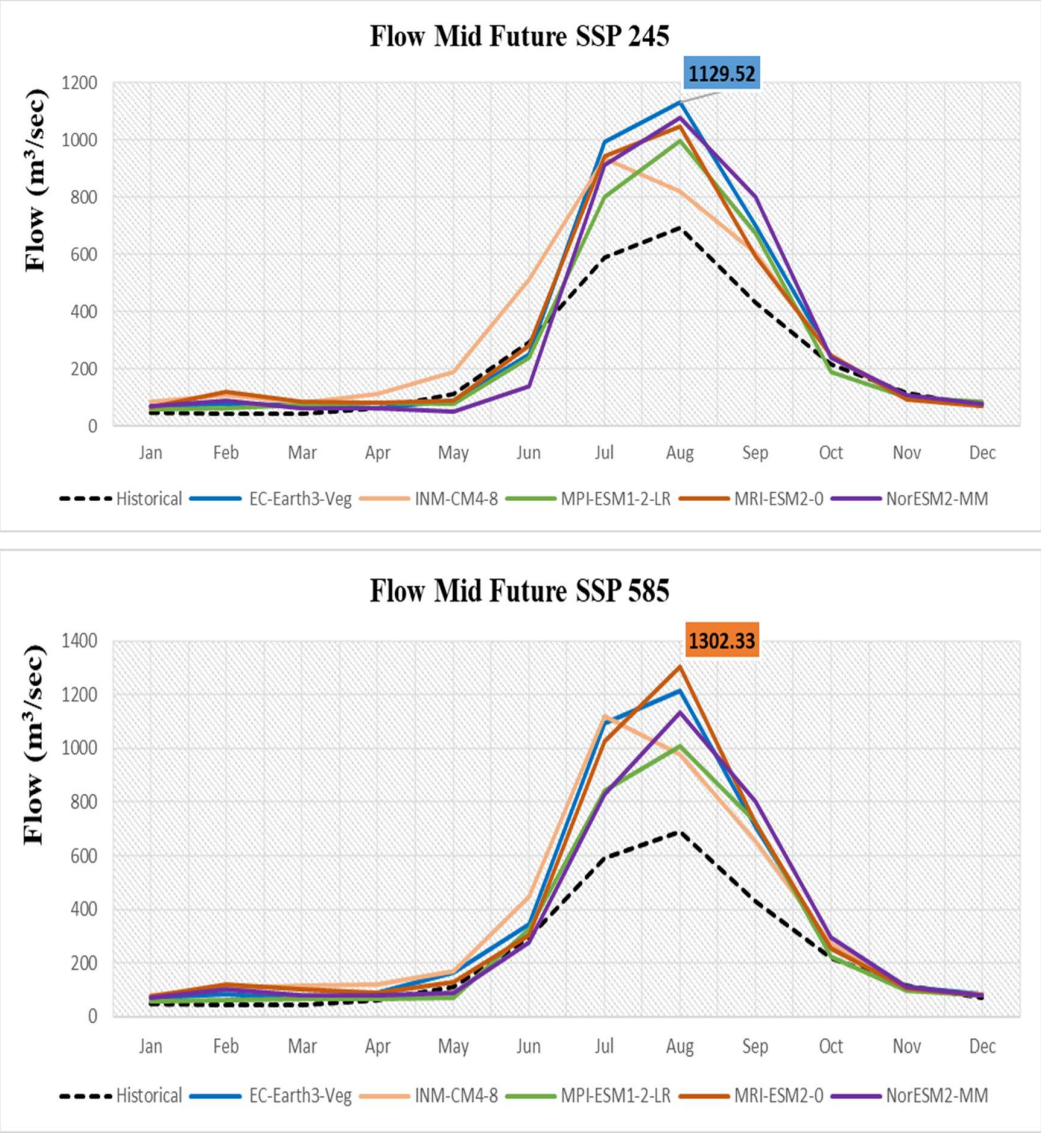

Figure 5.21: Average monthly stream flow (m^3/s) in mid-future under two scenarios (a) SSP245 Scenario (b) SSP585 Scenario

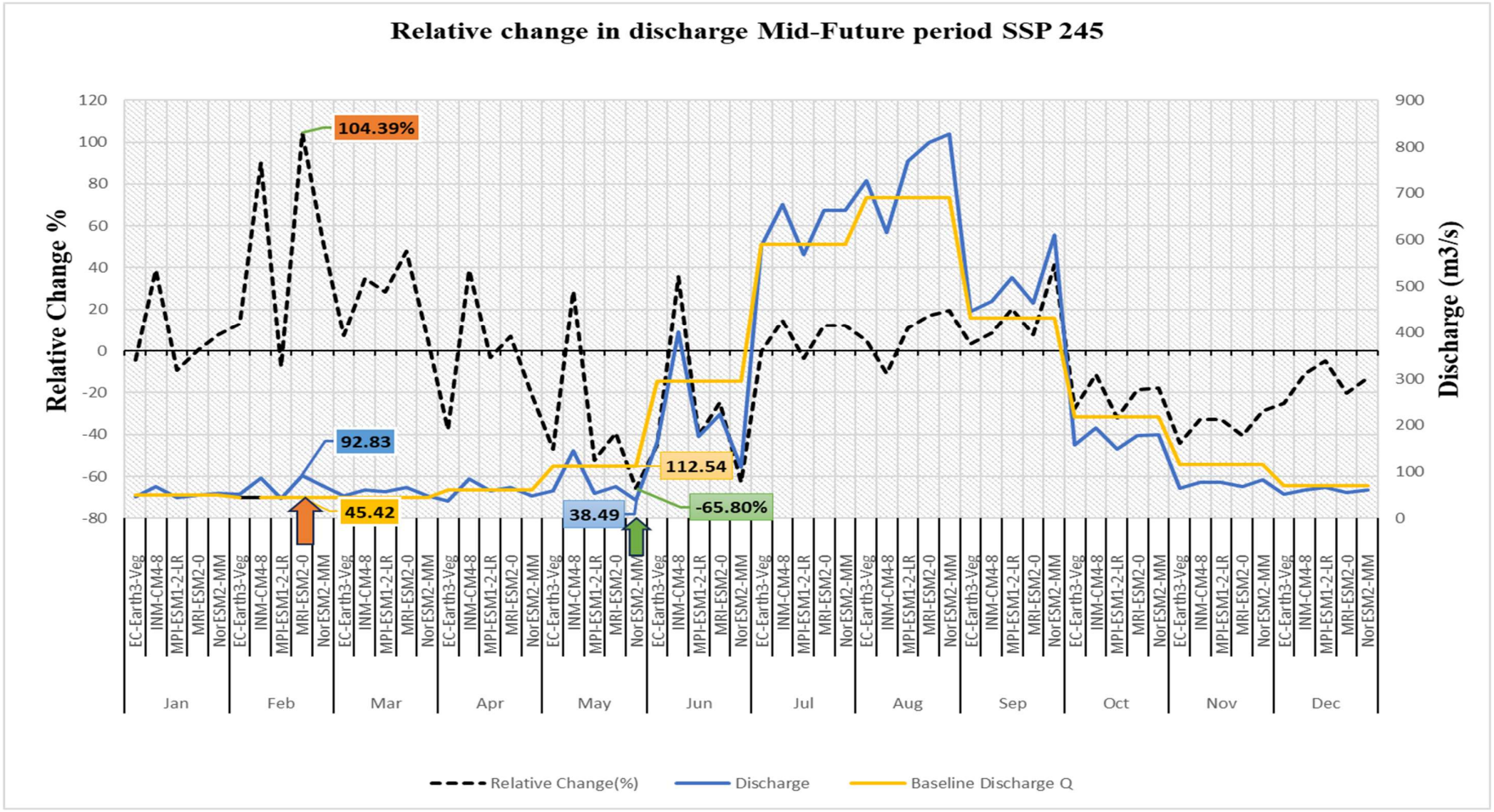

Figure 5.22: Relative change in discharge mid future period SSP245

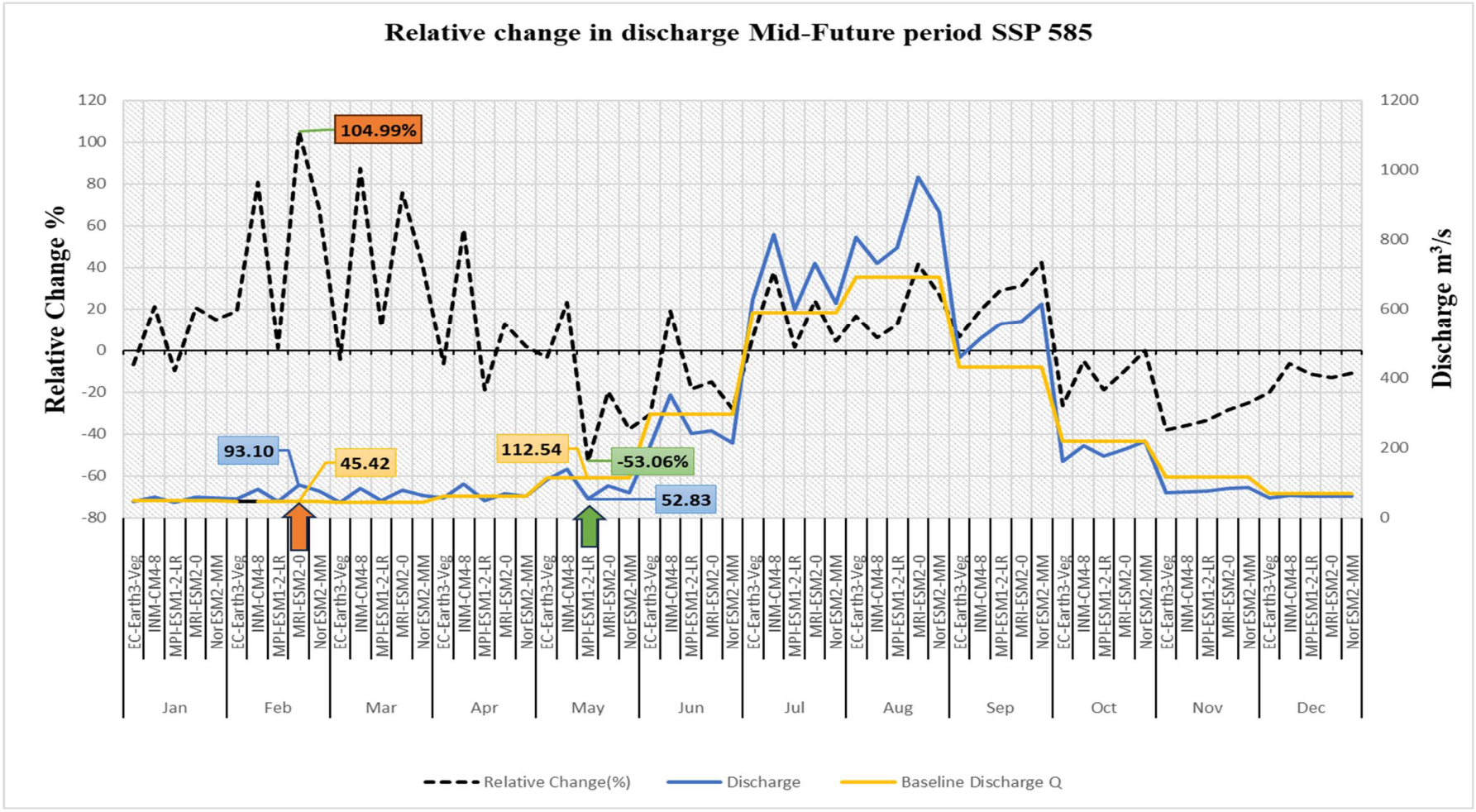

Figure 5.23: Relative change in discharge mid future period SSP585

The extreme relative change in discharge during the far-future period of the SSP245 Scenario, compared to the baseline, exhibits a significant range, varying from a decrease of 72.78% to an increase of 155.24%. In the INM-CM4-8 model, during February in the SSP245 Scenario, the projected discharge is notably higher than the baseline, ranging from 45.42 m^3/s to 115.92 m^3/s. However, in June of the same scenario and NorESM2-MM model, the projected discharge experiences a rapid decline, ranging from 295.11 m^3/s to 80.33 m^3/s. Likewise, in the far-future period of the SSP585 Scenario, the extreme fluctuation of discharge, compared to the baseline, ranges from a decrease of 65.44% to an increase of 152.16%. In the INM-CM4-8 model, during the month of February in the SSP585 Scenario, the projected discharge is significantly higher than the baseline, ranging from 45.42 m^3/s to 114.52 m^3/s. Conversely, in May of the same scenario and MPI-ESM1-2-LR model, the projected discharge experiences a sharp decline, ranging from 112.54 m^3/s to 38.89 m^3/s. The average monthly stream flow (m^3/s) and relative change in discharge under both scenarios in farfuture is presented in Figure 5.24, 5.25 and 5.26.

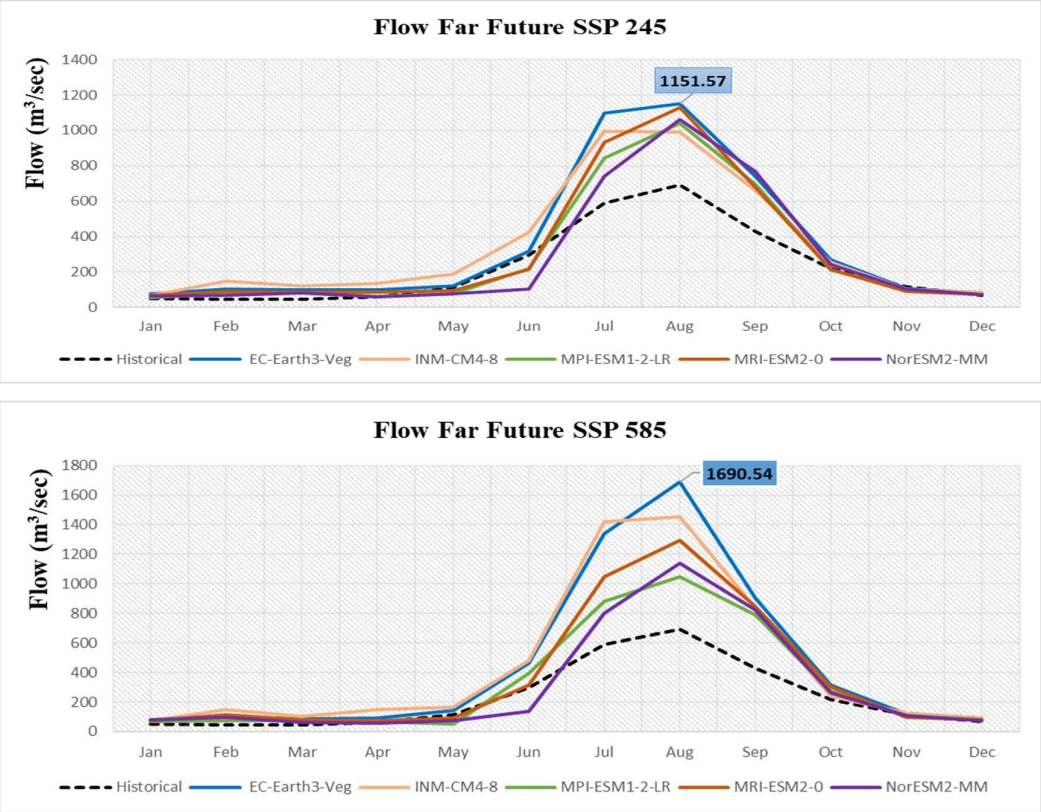

Figure 5.24: Average monthly stream flow (m^3/s) in the far future under two scenarios (a) SSP245Scenario (b) SSP585 Scenario

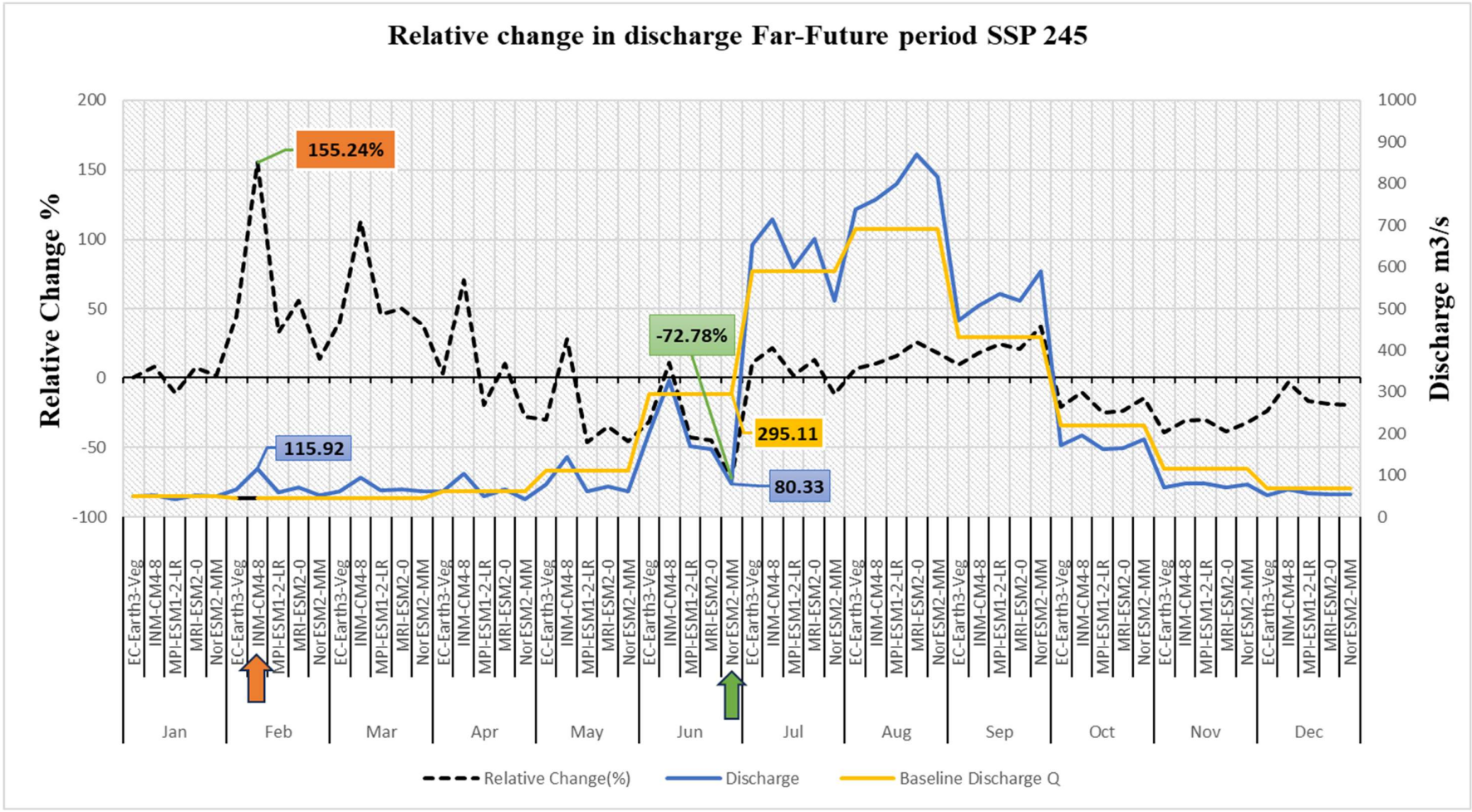

Figure 5.25: Relative change in discharge far future period SSP245

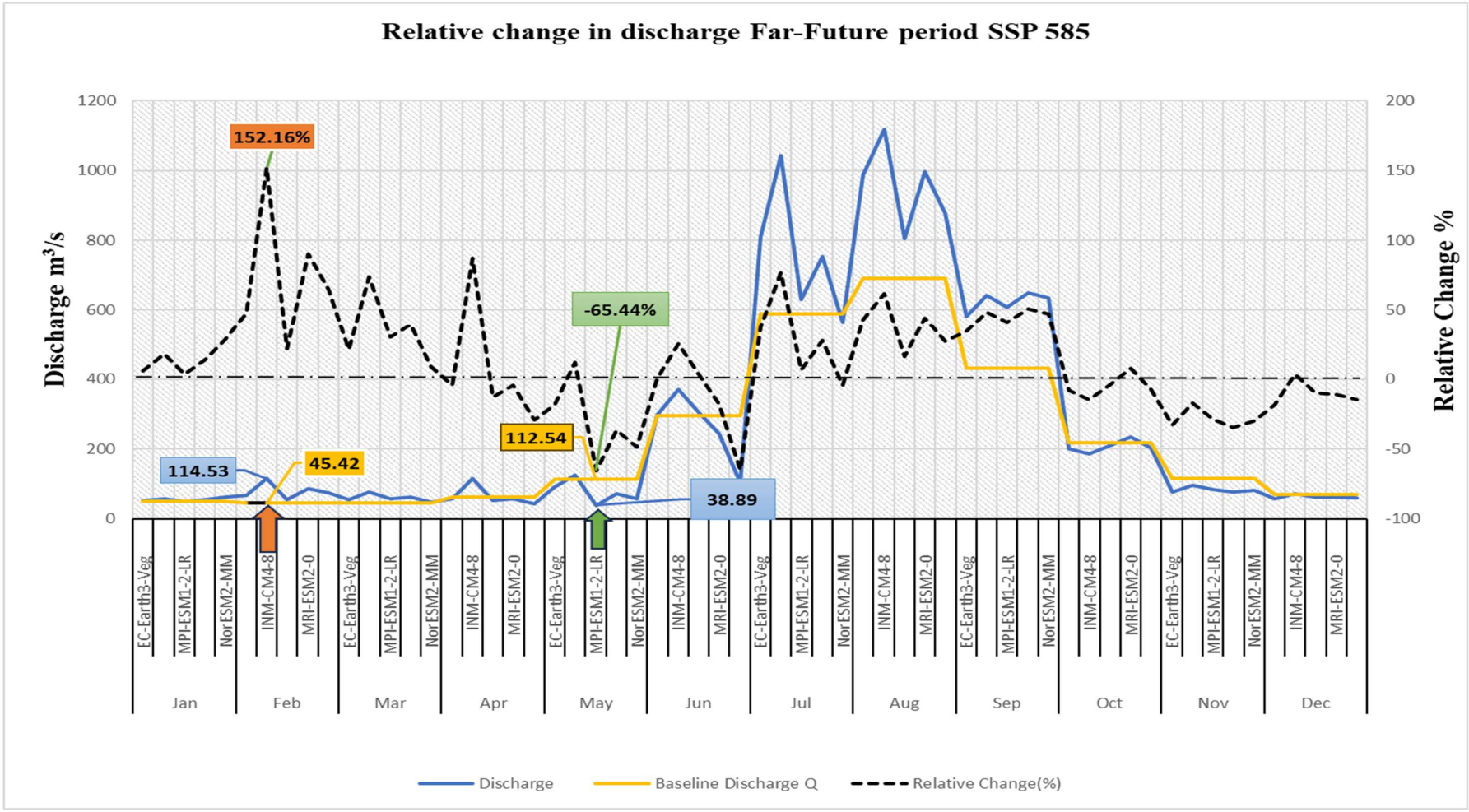

Figure 5.26: Relative change in discharge far future period SSP585

5.4 Climate Change Impact on Hydro Energy Generation

The baseline energy generators based on estimations of the long-term average stream flow are compared to the three future eras NF, MF, and FF energy production under two SSP245 and SSP585 scenarios. Based on the simulated discharge generation for future periods utilizing the power plant's efficiency of 85% and effective head of 39.5 meters, the hydro energy generation was computed. The maximum power plant capacity for each of the next periods is shown using the output of the simulated stream flow. The design capacity of the Devighat Hydropower Station is 15 MW after the rehabilitation project. The hydro plant's maximum capacity number demonstrates that, the power plant is capable of operating at full load capacity almost constantly in most of the future projections. The utmost energy generation (GWh) under both scenarios is presented in Figures 5.27-5.35.

The hydro power plant has the capacity to generate maximum energy in most months, with a few exceptions. Under the SSP245 Scenario in the near future, the projected generation output is minimum for the INM-CM4-8 Climate model having 9.82GWh in the month of January, 8.81GWh in the month of February, 10.51GWh in the month of November and 10.56GWh within the December as compared to rest of the climate models. Similar to this, the NorESM2-MM's generation of energy is lowest during the months of April, May, and June when compared to the other climate models. Additionally, all the Climate model, were able to achieve its peak generation in the months of July, August and October with the utmost generation of 10.89 GWh. All the models, falls short in regards to the utmost generation output in the month of January, February, March, April, June, September and November under the SSP245 Scenario in the near future.

Under the SSP585 Scenario in the near future, the projected generation output is minimum for the INM-CM4-8 Climate model having 9.85GWh in the month of January, 8.44GWh in the month of February, 10.36GWh in the month of November and 10.48GWh within the month of December as compared to rest of the climate models. Similarly, for the month of March, and May the energy output is minimum for the MPI-ESM1-2-LR compared to the rest of the climate models having 9.91GWh in the month of March and 9.05GWh in the month of May. Additionally, all the Climate model, were able to achieve its peak generation in the months of July, August and October with the utmost generation of 10.89 GWh. All the models, falls short in regards

to the utmost generation output in the month of January, February, March, April, June, September and November under the SSP245 Scenario in the near future.

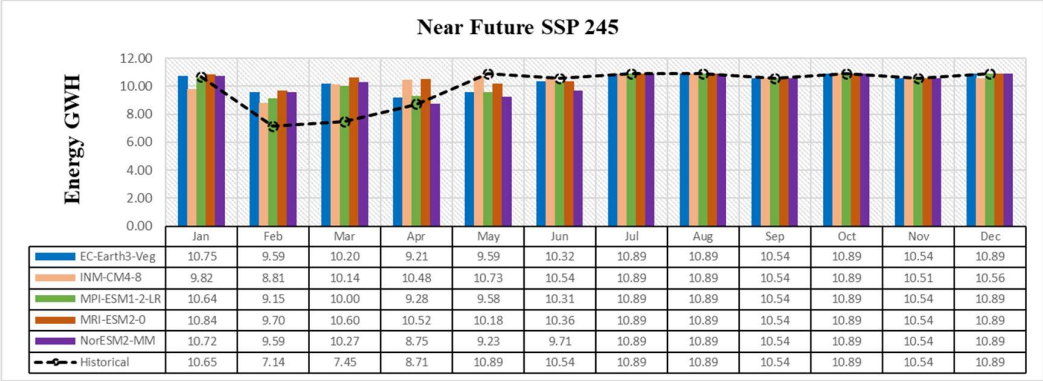

	Jan	Feb	Mar	Apr	May	Jun	Jul	Aug	Sep	Oct	Nov	Dec
EC-Earth3-Veg	10.75	9.59	10.20	9.21	9.59	10.32	10.89	10.89	10.54	10.89	10.54	10.89
INM-CM4-8	9.82	8.81	10.14	10.48	10.73	10.54	10.89	10.89	10.54	10.89	10.51	10.56
MPI-ESM1-2-LR	10.64	9.15	10.00	9.28	9.58	10.31	10.89	10.89	10.54	10.89	10.54	10.89
MRI-ESM2-0	10.84	9.70	10.60	10.52	10.18	10.36	10.89	10.89	10.54	10.89	10.54	10.89
NorESM2-MM	10.72	9.59	10.27	8.75	9.23	9.71	10.89	10.89	10.54	10.89	10.54	10.89
Historical	10.65	7.14	7.45	8.71	10.89	10.54	10.89	10.89	10.54	10.89	10.54	10.89

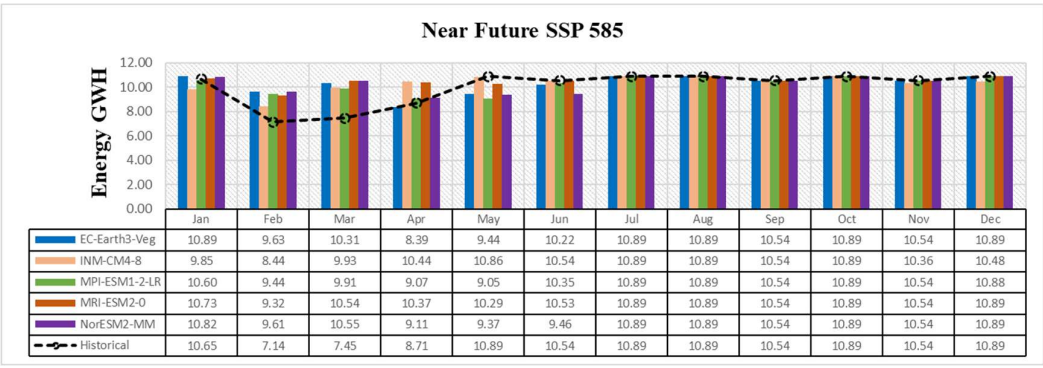

	Jan	Feb	Mar	Apr	May	Jun	Jul	Aug	Sep	Oct	Nov	Dec
EC-Earth3-Veg	10.89	9.63	10.31	8.39	9.44	10.22	10.89	10.89	10.54	10.89	10.54	10.89
INM-CM4-8	9.85	8.44	9.93	10.44	10.86	10.54	10.89	10.89	10.54	10.89	10.36	10.48
MPI-ESM1-2-LR	10.60	9.44	9.91	9.07	9.05	10.35	10.89	10.89	10.54	10.89	10.54	10.88
MRI-ESM2-0	10.73	9.32	10.54	10.37	10.29	10.53	10.89	10.89	10.54	10.89	10.54	10.89
NorESM2-MM	10.82	9.61	10.55	9.11	9.37	9.46	10.89	10.89	10.54	10.89	10.54	10.89
Historical	10.65	7.14	7.45	8.71	10.89	10.54	10.89	10.89	10.54	10.89	10.54	10.89

Figure 5.27: Average energy generation (GWh) in the near future under two scenarios (a) SSP245Scenario (b) SSP585 Scenario

The hydro power plant has the capacity to generate maximum energy in most months, with a few exceptions. Under the SSP245 Scenario in the mid future, the projected generation output is minimum for the MPI-ESM1-2-LR Climate model having 10.64Wh in the month of January and 9.15GWh in the month of February as compared to rest of the climate models. Similarly, for the month of April, and June the energy output is minimum for the EC-Earth3-Veg model compared to the rest of the climate models. Additionally, all the Climate model, were able to achieve its peak generation in the months of July, August and October with the utmost generation of 10.89 GWh. All the models, falls short in regards to the utmost generation output in the month of February, March, April, May, June, September and November under the SSP245 Scenario in the mid future.

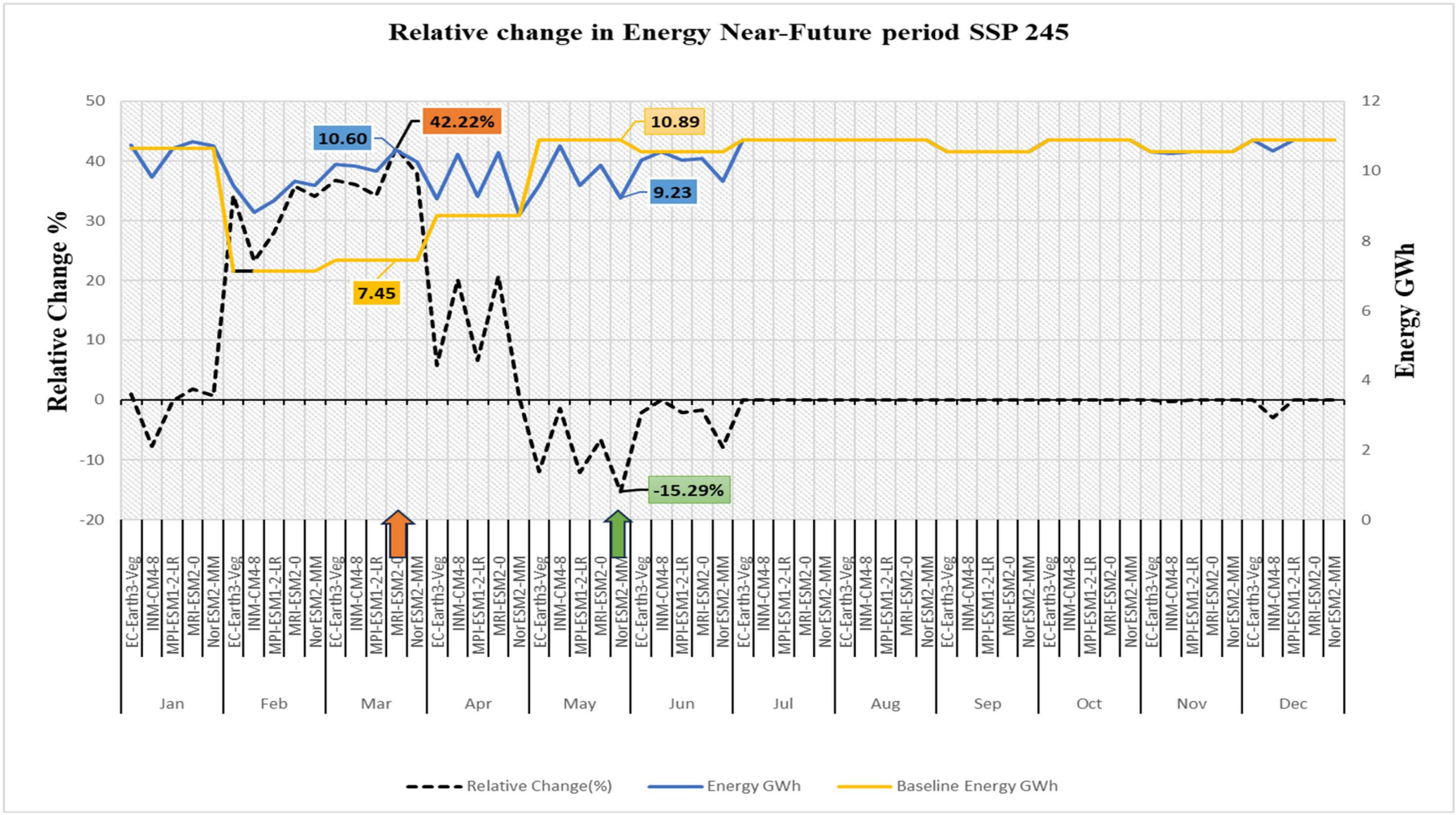

Figure 5.28: Relative change in energy near-future period SSP 245

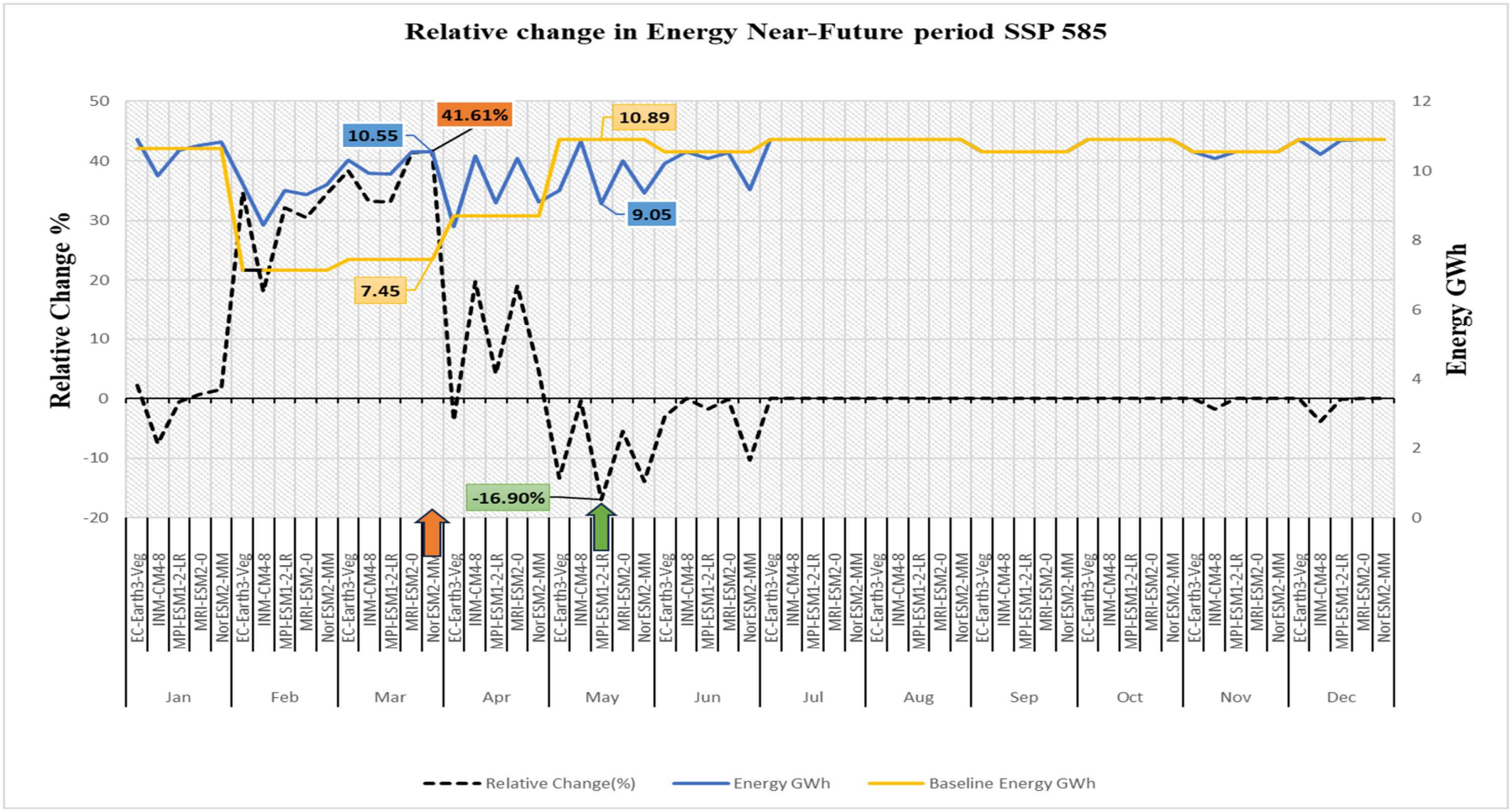

Figure 5.29: Relative change in energy near-future period SSP 58

Under the SSP585 Scenario in the mid future, the projected generation output is minimum for the MPI-ESM1-2-LR Climate model having 9.21GWh in the month of February, 9.78GWh in the month of March, 8.90GWh in the month of April and 8.91GWh in the month of May as compared to rest of the climate models. Similarly, for the month of January, November and December the energy output is minimum for the INM-CM4-8 model compared to the rest of the climate models having 10.60GWh in the month of January, 10.48GWh in the month of November and 10.69GWh in the month of December. Additionally, all the Climate model, were able to achieve its peak generation in the months of July, August and October with the utmost generation of 10.89 GWh.

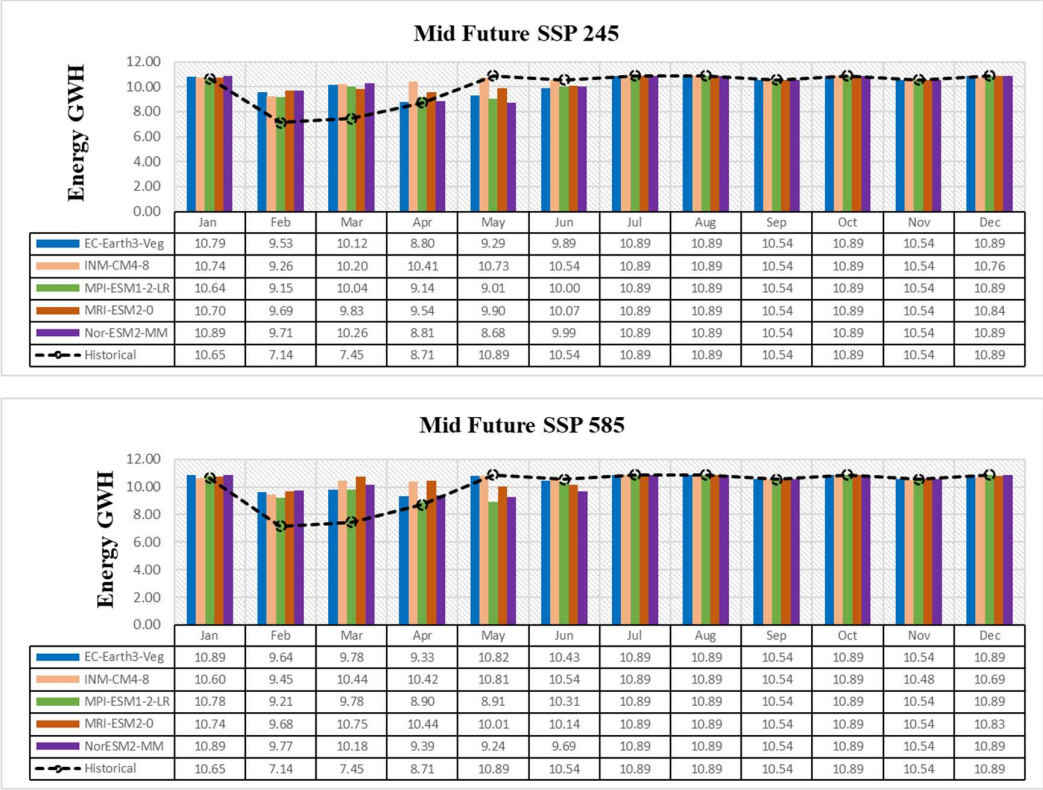

Figure 5.30: Average energy generation (GWh) in the mid future under two scenarios (a) SSP245Scenario (b) SSP585 Scenario

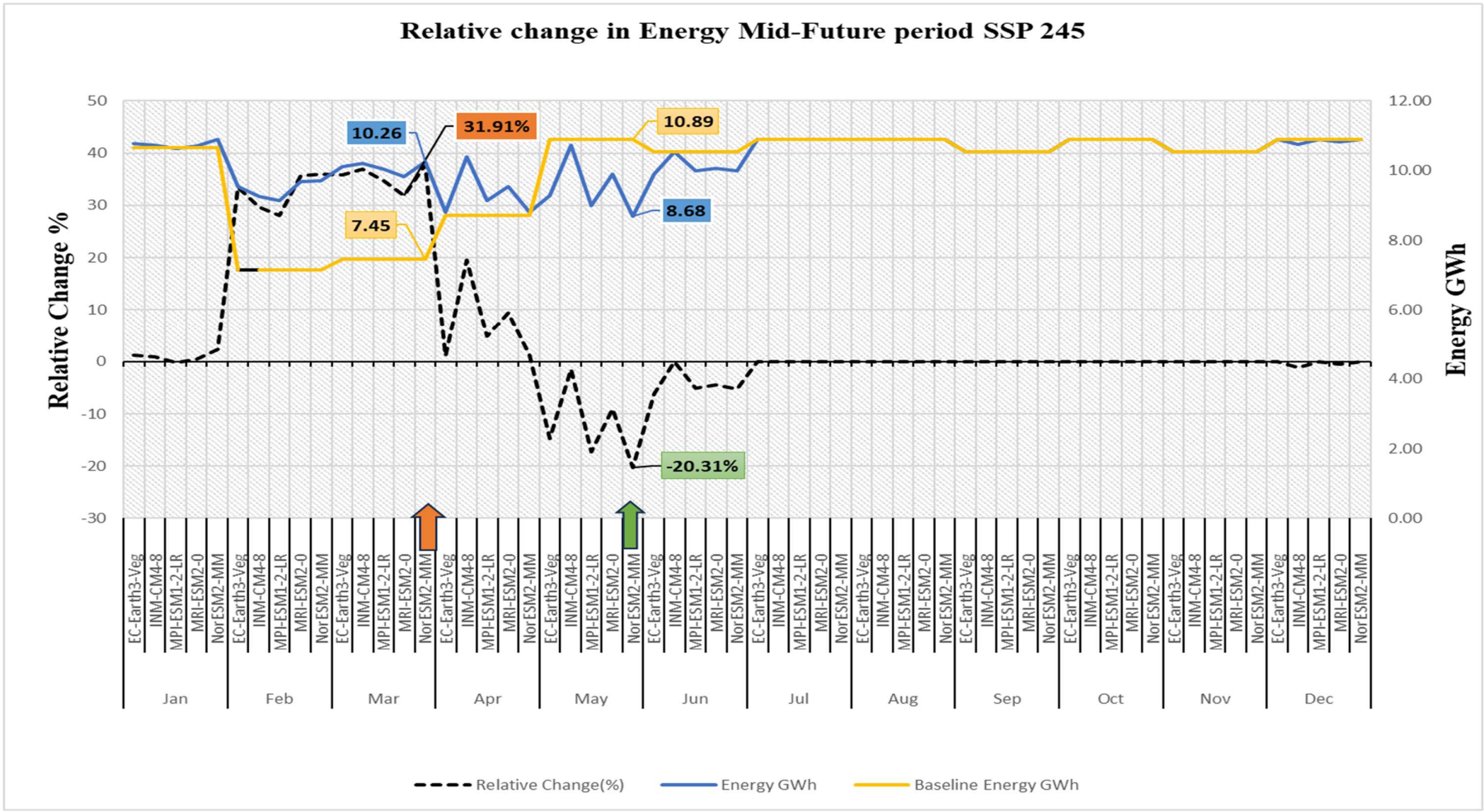

Figure 5.31: Relative change in energy mid-future period SSP 245

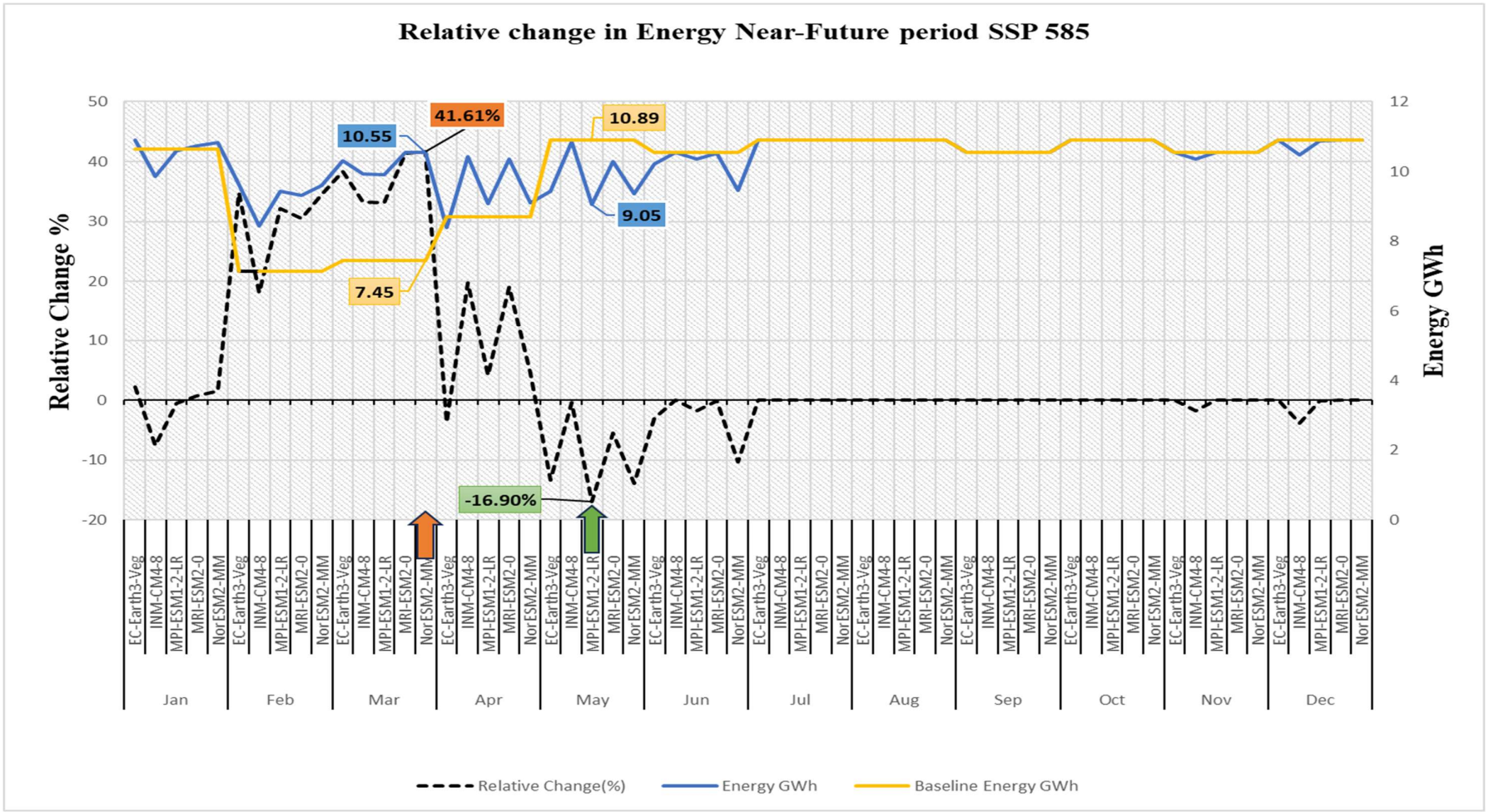

Figure 5.32: Relative change in energy near-future period SSP 585

The hydro power plant has the capacity to generate maximum energy in most months, with a few exceptions. Under the SSP245 Scenario in the far future, the projected generation output is minimum for the MRI-ESM2-0 Climate model having 10.60Wh in the month of January and 9.21GWh in the month of February as compared to rest of the climate models. Similarly, for the month of March, April, and June the energy output is minimum for the NorESM2-MM model compared to the rest of the climate models having 9.67GWh in the month of March, 8.41GWh in the month of April and 9.50GWh in the month of June. Additionally, all the Climate model, were able to achieve its peak generation in the months of July, August and October with the utmost generation of 10.89 GWh. All the models, falls short in regards to the utmost generation output in the month of February, March, April, May, June, September and November under the SSP245 Scenario in the far future.

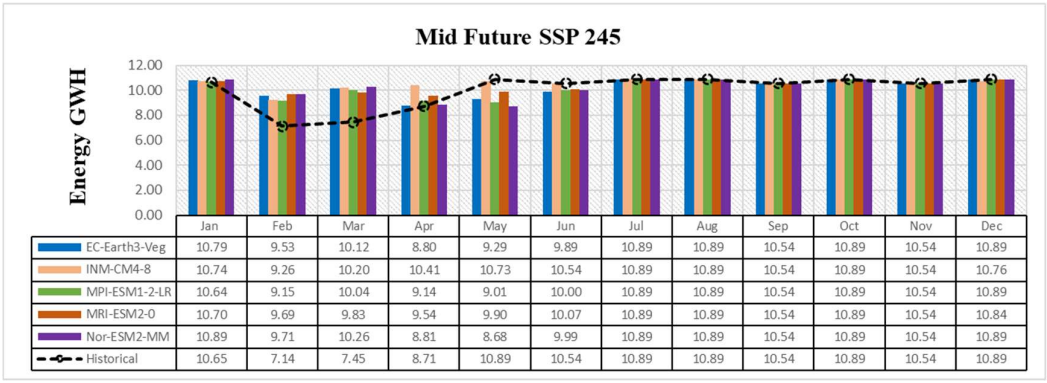

	Jan	Feb	Mar	Apr	May	Jun	Jul	Aug	Sep	Oct	Nov	Dec
EC-Earth3-Veg	10.79	9.53	10.12	8.80	9.29	9.89	10.89	10.89	10.54	10.89	10.54	10.89
INM-CM4-8	10.74	9.26	10.20	10.41	10.73	10.54	10.89	10.89	10.54	10.89	10.54	10.76
MPI-ESM1-2-LR	10.64	9.15	10.04	9.14	9.01	10.00	10.89	10.89	10.54	10.89	10.54	10.89
MRI-ESM2-0	10.70	9.69	9.83	9.54	9.90	10.07	10.89	10.89	10.54	10.89	10.54	10.84
Nor-ESM2-MM	10.89	9.71	10.26	8.81	8.68	9.99	10.89	10.89	10.54	10.89	10.54	10.89
Historical	10.65	7.14	7.45	8.71	10.89	10.54	10.89	10.89	10.54	10.89	10.54	10.89

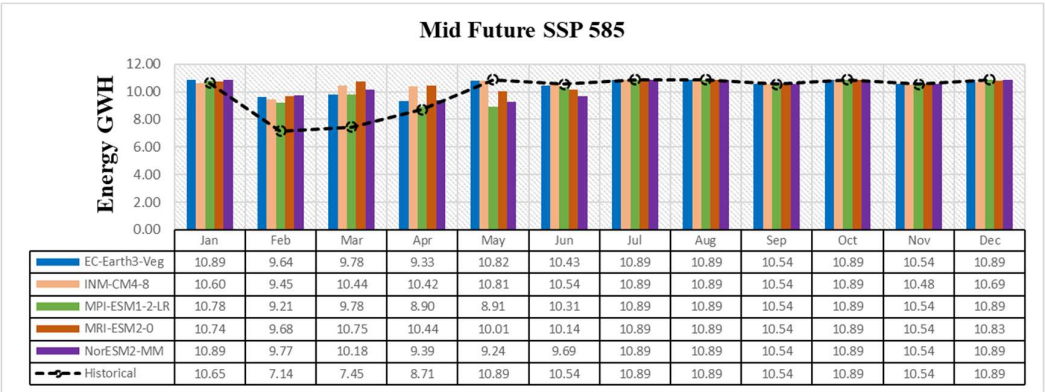

	Jan	Feb	Mar	Apr	May	Jun	Jul	Aug	Sep	Oct	Nov	Dec
EC-Earth3-Veg	10.89	9.64	9.78	9.33	10.82	10.43	10.89	10.89	10.54	10.89	10.54	10.89
INM-CM4-8	10.60	9.45	10.44	10.42	10.81	10.54	10.89	10.89	10.54	10.89	10.48	10.69
MPI-ESM1-2-LR	10.78	9.21	9.78	8.90	8.91	10.31	10.89	10.89	10.54	10.89	10.54	10.89
MRI-ESM2-0	10.74	9.68	10.75	10.44	10.01	10.14	10.89	10.89	10.54	10.89	10.54	10.83
NorESM2-MM	10.89	9.77	10.18	9.39	9.24	9.69	10.89	10.89	10.54	10.89	10.54	10.89
Historical	10.65	7.14	7.45	8.71	10.89	10.54	10.89	10.89	10.54	10.89	10.54	10.89

Figure 5.33: Average energy generation (GWh) in the far future under two scenarios (a) SSP245Scenario (b) SSP585 Scenario

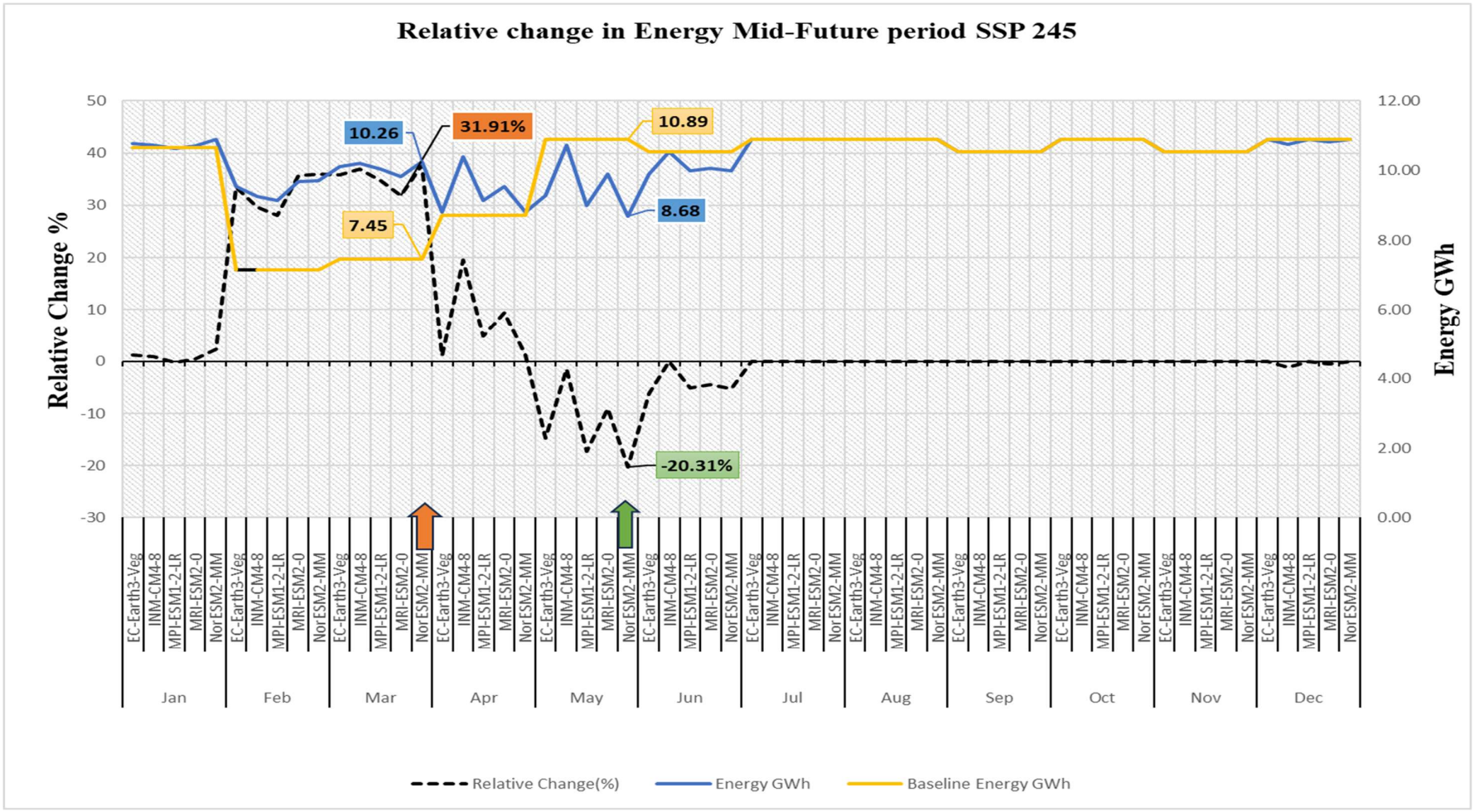

Figure 5.34: Relative change in energy mid-future period SSP 245

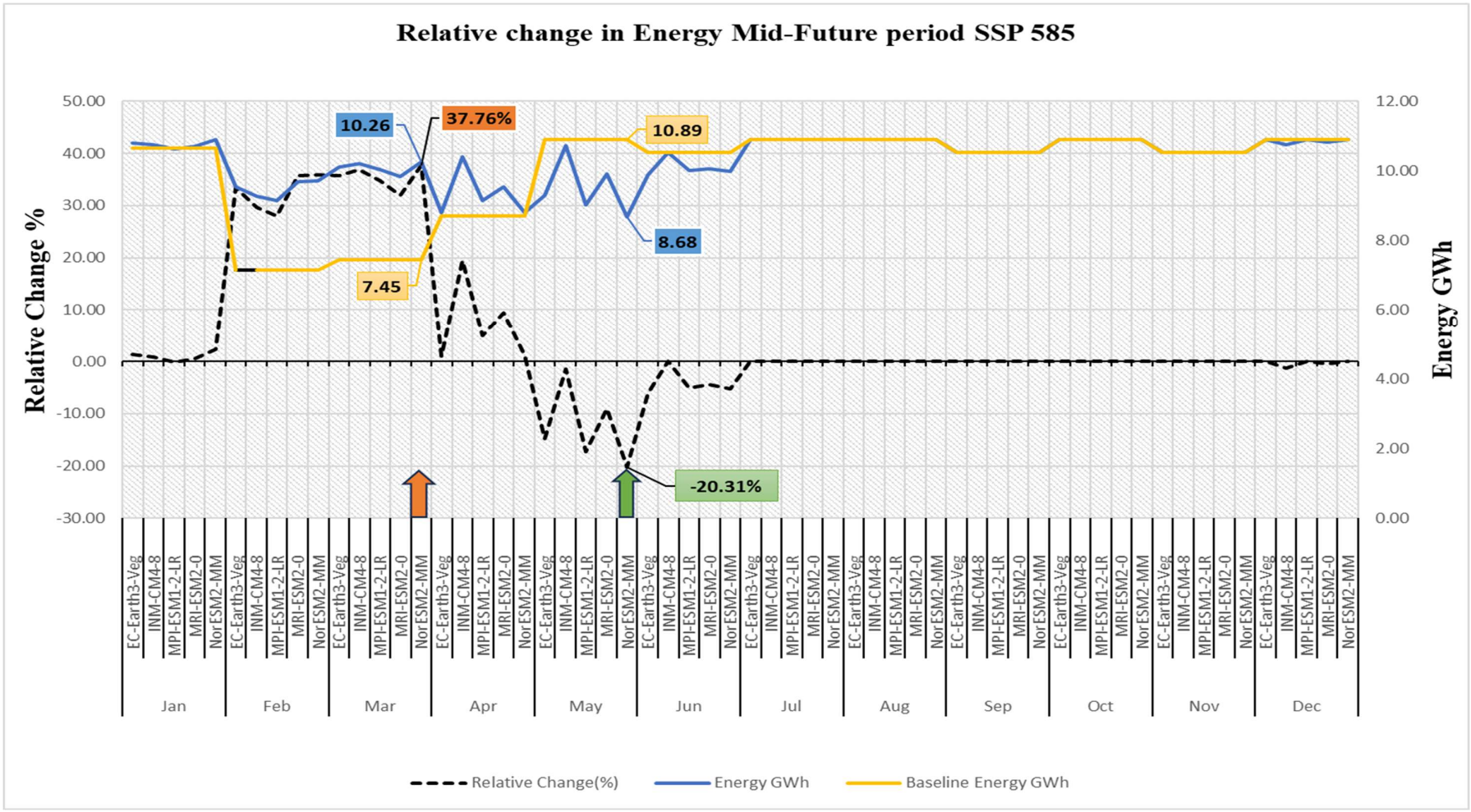

Figure 5.35: Relative change in energy mid-future period SSP 585

Under the SSP585 Scenario in the far future, the projected generation output is minimum for the NorESM2-MM Climate model having 10.77GWh in the month of January, 9.57GWh in the month of February, 9.47GWh in the month of March, 8.10GWh in the month of April, 8.67GWh in the month of May and 9.79GWh in the month of June as compared to rest of the climate models. Additionally, all the Climate model, were able to achieve its peak generation in the months of July, August, October and December with the utmost generation of 10.89 GWh.

5.5 Discussion

Hydropower projects can operate for up to a century, but their prolonged lifespan depends on a steady flow of water through runoff. The operation of Devighat Hydropower Station, which is a cascade hydropower plant, is dependent on the operation of Trishuli Hydropower Station. While Devighat Hydropower Station's high-capacity utilization rate of nearly 90% in contrast to the average capacity utilization rate of almost 56% of the power plants in Nepal (NEA Gen. 2020), is vital to the energy infrastructure at present scenario, there is uncertainty about its future operation due to theeffects of climate change

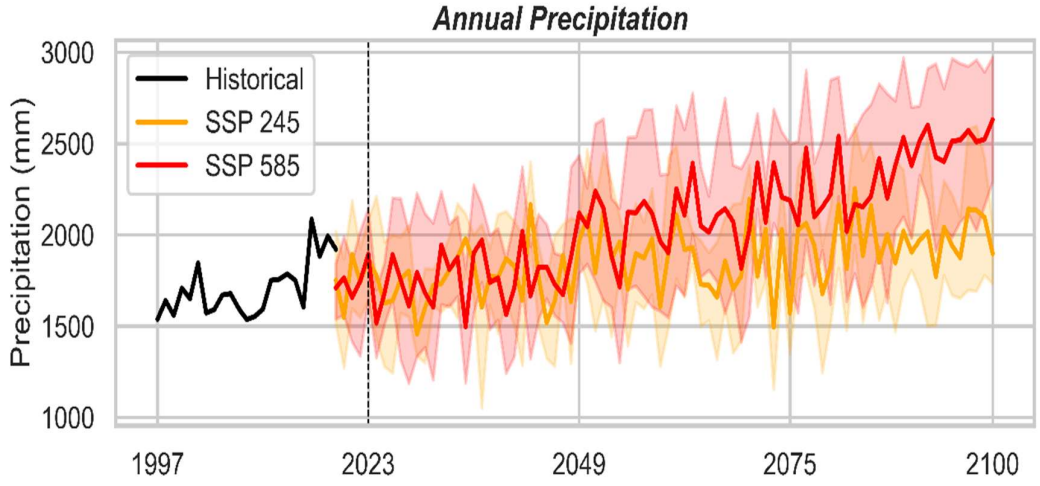

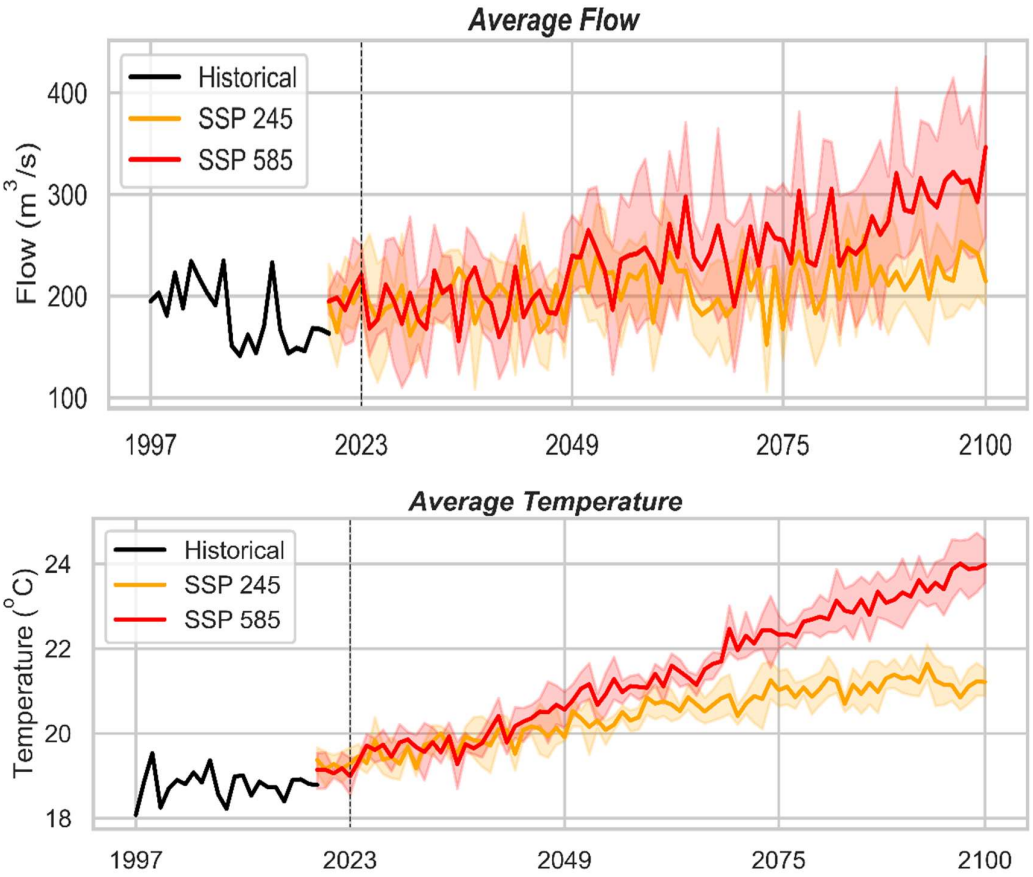

Figure 5.36: Timeline Curve a) Average Temperature b) Annual Precipitation c) Average Flow

This study utilizes five different climate models to project potential climate changes, each producing a unique outcome. The hydro energy generation outlook is based on the combined results of all five climate models. Based upon the individual climate projection climate change is clearly evident in the mid and far-future periods. Although the water flow needed for the power plant is expected to be adequate for all units to operate at full capacity in future scenarios, there is a clear indication that water-related disasters such as floods will likely occur due to extreme precipitation and stream runoff resulting from significant climate change. Undertaking site- specific research on cascade projects like this will provide a more accurate feasibility analysis during the planning and construction stages of hydropower projects, especially with regard to the impacts of climate change in the future. The timeline Figure 32 illustrates the average annual temperature, precipitation, and stream flow from the historical baseline period to the future period.

CHAPTER SIX: CONCLUSIONS AND RECOMMENDATIONS

6.1 Conclusions

The objective of the research was to analyze how climate change may affect the Trishuli Basin's hydrology and its potential risks of generating electricity. After conducting the analysis, several key findings were identified and can be summarized as follows:

In the Trishuli Basin, the impacts of climate change are evident, with noticeable fluctuations observed in climatic factors. There are clear projections indicating a substantial rise in both temperature and precipitation within the basin.

In all future periods and under both SSP245 and SSP585 Scenarios, the Trishuli Basin experiences a notably strong warming trend according to all five climate models. The basin's dominant snow-covered land contributes significantly to the escalation of river runoff due to this warming effect. The projections indicate a consistent temperature rise in the future, with a more rapid increase in the mid-future and far future compared to the near future. In the basin, the average annual discharge is expected to undergo a significant increase. When considering the SSP245 Scenario, the annual flow is predicted to decrease by 1.4% in the near future, but then increase by 4% and 7.4% in the mid and far future, respectively. Similarly, under the SSP585 Scenario, the annual flow is projected to decrease by 1.1% in the near future, and then rise by 14.5% and 26.5% in the mid and far future, respectively.

When evaluating the potential hydropower output at Devighat Hydropower Station, it is found that a consistently almost full generation level is maintained in all upcoming periods, irrespective of whether the SSP245 or SSP585 Scenario is utilized. The average annual hydro energy generation in the basin is expected to increase significantly. Under the SSP245 Scenario, annual generation is forecasted to increase by 4.3%, 3.6%, and 4.9% in the near future, mid-future, and far future, respectively. Likewise, under the SSP585 Scenario, the annual generation is predicted to increase by 4.1%, 4.6%, and 4.7% in the near future, mid-future, and far future, respectively. Throughout all upcoming periods, the hydropower station is designed to attain a capacity of 114 GWh.

6.2 Recommendation

The following suggestions are put forward:

- This research covers the operational Devighat Hydropower. However, the approach and conclusions from the study will be useful to analyze the energy generation of other hydroelectric plants and other water-related projects to assess future water availability and formulate future basin regulations under CC circumstances.
- Climate change might maximize catchment utilization of water. However, an unpredictable rise in precipitation will lead to flash floods, which may cause flood-induced disasters in the area, therefore flood analysis will be an important topic of study in the future.
- For upcoming projects, a comprehensive study of weather climate change, based on long-term hydro-meteorological data, must be included, and these measures should be made mandatory at the policy level.
- Different models can be evolved to project the reservoir records in an extra bodily way by putting in and incorporating the present hydrological information data stations.

REFERENCES

Shrestha, R. S., Biggs, S., Justice, S., & Gurung, A. M. (2018). *'A Power Paradox: Growth of the Hydro Sector in Nepal'*, Hydro Nepal, (23). SJVN Arun-3 power development company Pvt. Ltd.

Vimal Mishra, Udit Bhatiya & Amar Deep Tiwari (2020). *'Bias-corrected climate Projections for South Asia from Coupled Model Intercomparison Project-6.'* https://www.nepjol.info/index.php/HN/article/view/20821/17098 (pp. 5–17). Almazroui,

M., Saeed, S., Saeed, F., Islam, M., Ismail, M., (2020). *Projections of precipitation and temperature over the South Asian countries in CMIP6.* Earth Systems and Environment, 4, 297-320

Arnold, J. G., Srinivasan, R., Muttiah, R. S., Williams, J. R.(1998). *arge area hydrologic modeling and assessment part I: model development* 1. JAWRA Journal of the American Water Resources Association, 73-89.

Mishra, V., Bhatia, U., & Tiwari, A. D. (2020). *Bias-corrected climate projections for South Asia from coupled model intercomparison project-6. Scientific data*, 7(1), 1-13.

Poudyal, R., Loskot, P., Nepal, R., Parajuli, R., Khadka, S. K., ;, & ;. (2019). *Mitigating the current energy crisis in Nepal with renewable energy sources.* Renewable and Sustainable Energy Reviews, 109388.

Khadka, D., & Pathak, D. (2016). *Climate change projection for the marsyangdi river basin, Nepal using statistical downscaling of GCM and its implications in disasters*. Geoenvironmental Disasters, 3, 150-162.

Hydro Nepal: Journal of Water, Energy and Environment, 2012. Y. Mishra, *"Impacts of Climate Change on Irrigation Water Management in the Babai River Basin, Nepal,"* hydrology, 2021.

B. Dhami, *"Evaluation of the SWAT model for water balance study of a mountainous snow Fed river basin of Nepal,"* Environmental Earth Sciences, 2018.

T. Nakamura, *"Impact of Climate Change on Water Resources of the Bheri River Basin, Nepal,"* water, 2018.

Singh, R.; Bhattarai, N.; Prajapati, A.; Shakya, S. *Impact of variation in climatic parameters on hydropower generation: A case of a hydropower project in Nepal*, Heliyon 2022, 8,12240. https://doi.org/10.1016/j.heliyon.2022.e12240

Regmi, M. *Impact of Climate Change on Hydropower Generation: A case study of Kulekhani First Hydropower Station*. Masters of Science in Climate Change and

Development, Tribhuvan University, Nepal, 2022
Shrestha, R. S.; Biggs, S.; Justice, S.; Gurung, A. M. *A Power Paradox: Growth of the Hydro Sector in Nepal*. Hydro Nepal 2018, 23, 5-21
NEA (Nepal Electricity Authority), Annual Report 2021/2022. Available online: https://www.nea.org.np/annual_report, 2022 (accessed on August 2022)
IPCC (Intergovernmental Panel on Climate Change), *An IPCC Special Report on the Impacts of Global Warming of 1.5^{0}C.* Available online: https://www.ipcc.ch/site/assets/uploads/sites/2/2019/06/SR15_Full_Report_High_Res.pdf. (accessed on 17 September 2021)
DHM (Department of Hydrology and Meteorology), *Observed Climate Trend Analysis in the Districts and Physiographic Zones of Nepal* (1971- 2014), 2017. Available online: https://www.dhm.gov.np/uploads/climatic/467608975Observed%20Climate%20Trend%20Analysis%20Report_2017_Final.pdf. (accessed on 19 March 2021)
J. Panthi, P. Dahal, M. Shrestha, et al., *Spatial and temporal variability of rainfall in the Gandaki River Basin of Nepal Himalaya*, Climate 3 (2015) 210226.
MOFE (Ministry of Forests and Environment), Climate Change Scenarios for Nepal, 2019.http://mofe.gov.np/downloadfile/MOFE_2019_Climate%20change%20scenarios%20for% 20Nepal_NAP_1562647620.pdf. accessed 8 September 2021.
Bajracharya, T. R., Acharya, S., & Bahadur Ale, B (2011). *Changing climatic parameters and its possible impacts in hydropower generation in Nepal: A case study on Gandaki River basin.* Journal of the Institute of Engineering, 8(1), 160–173 https://doi.org/10.3126/jie.v8i1-2.5108
International Finance Corporation. 2018. *Cumulative Impact Assessment and Management: Hydropower*. Available online: https://www.ifc.org/wps/wcm/connect/d9ba169a-3642-4928-a2b5a7d567583f9d/Report_CIATrishuli_May2020_ExecutiveSummary.pdf?MOD=AJP RES&CVID=ns6PHB7(accessed on 29 January 2023).
Nepal Water Resource Portal. Available online: https://www.nwrmap.info/hydropower/devighat-hydropower-station-1 (accessed on 29 January 2023).
Shrestha, Rajendra & Dahal, Suraj. (2013). *Operation Optimization and Performance Evaluation of Devighat Hydropower Plant.*

Pokharel, N.; Sherchan, B.; Basnet, K.; Thapaliya, D. *Assessment of Hydropower Potential using SWAT modeling and Spatial Technology in the Seti Gandaki River, Kaski, Nepal*. *IEEE SEM* 2020*,* 8, 87–102.

ICIMOD. Available online: http://rds.icimod.org/Home/Data?any=landuse%20data&Category=datasets&&themkey=Nepal&&page=1 (accessed on 11 July 2022).

Dijkshoorn, K.; Huting, J. *Soil and Terrain database for Nepal, 2009 ed.;* ISRIC-World Soil Information: Wageningen, the Netherlands, 2009; pp. 1-21. Open Data Nepal. Available online:https://opendatanepal.com/dataset/meteorological-stations-of nepal/resource/4c4da8db-2540-48dd-9c41-6fd4440c7e8c/view/0ea57ff6-768f-4283-a716-c377e131f3b2 (accessed on 1 June 2022

APPENDIX A: Projected Average monthly temperature (^{0}C) in Dhunche and Nuwakot station in near, mid and far future under SSP 245 and SSP 585

Model	EC-Earth3-Veg		INM-CM4-8		MPI-ESM1-2-LR		MRI-ESM2-0		NorESM2-MM	
Month	Dhunche (Tavg) °C	Nuwakot (Tavg) °C	Dhunche (Tavg) °C	Nuwakot (Tavg) °C	Dhunche (Tavg) °C	Nuwakot (Tavg) °C	Dhunche (Tavg) °C	Nuwakot (Tavg) °C	Dhunche (Tavg) °C	Nuwakot (Tavg) °C
Jan	9.62	16.16	9.26	15.65	9.64	16.45	9.31	15.98	9.54	16.28
Feb	10.14	17.80	9.98	17.71	10.61	18.43	11.13	18.92	10.56	19.01
Mar	13.75	21.83	13.72	22.03	13.80	21.98	14.74	23.48	14.27	22.65
Apr	17.07	25.73	17.04	25.16	17.47	25.34	17.77	26.75	17.80	25.89
May	18.67	25.91	18.33	26.15	18.59	25.79	19.58	26.96	19.12	26.00
Jun	20.28	27.20	19.44	28.14	19.80	27.16	21.15	27.98	20.64	27.48
Jul	20.81	27.32	20.84	27.88	20.57	27.10	20.59	27.85	20.78	27.63
Aug	20.64	27.14	20.83	27.78	20.45	27.14	20.45	27.36	20.86	27.47
Sep	19.86	26.15	19.82	26.91	19.79	26.59	19.81	26.74	20.17	26.71
Oct	17.02	23.76	16.93	23.85	17.14	23.63	17.08	24.01	17.33	23.49
Nov	13.49	20.49	13.78	20.42	13.66	19.96	13.64	20.36	13.51	19.86
Dec	11.18	17.47	10.85	16.44	11.20	17.35	10.72	17.25	10.39	16.85

Projected Average monthly average temperature (⁰C) in Dhunche and Nuwakot Station in near future under SSP 585										
Model	**EC-Earth3-Veg**		**INM-CM4-8**		**MPI-ESM1-2-LR**		**MRI-ESM2-0**		**NorESM2-MM**	
Month	**Dhunche (Tavg) °C**	**Nuwakot (Tavg) °C**	**Dhunche (Tavg) °C**	**Nuwakot (Tavg) °C**	**Dhunche (Tavg) °C**	**Nuwakot (Tavg) °C**	**Dhunche (Tavg) °C**	**Nuwakot (Tavg) °C**	**Dhunche (Tavg) °C**	**Nuwakot (Tavg) °C**
Jan	9.02	15.82	8.90	15.79	9.61	16.50	10.26	17.02	9.32	16.03
Feb	10.01	18.00	9.51	18.04	10.70	18.65	11.33	19.17	10.51	19.13
Mar	13.86	21.78	13.39	21.87	14.28	22.49	14.39	23.25	14.06	22.77
Apr	17.46	26.23	16.94	25.11	17.04	25.00	18.00	27.01	17.70	25.81
May	18.57	25.82	18.95	26.05	18.57	25.71	19.63	27.13	19.12	26.33
Jun	20.28	27.40	19.81	28.24	19.74	27.35	20.84	28.07	21.05	27.71
Jul	20.81	27.67	21.08	28.40	20.71	27.20	20.52	28.15	21.11	27.99
Aug	20.77	27.28	21.21	28.41	20.59	27.32	20.54	27.86	20.98	27.84
Sep	19.97	26.31	20.21	27.05	19.84	26.61	19.96	26.84	20.01	27.00
Oct	17.24	23.97	17.23	23.88	17.13	24.12	17.30	24.27	17.38	23.96
Nov	13.52	20.53	13.57	20.24	13.68	19.74	13.77	20.49	14.07	20.19
Dec	10.56	17.39	11.39	16.72	11.16	17.23	11.51	17.78	10.86	17.23

Projected Average monthly average temperature (^{0}C) in Dhunche and Nuwakot Station in mid future under SSP 245										
Model	**EC-Earth3-Veg**		**INM-CM4-8**		**MPI-ESM1-2-LR**		**MRI-ESM2-0**		**NorESM2-MM**	
Month	**Dhunche (Tavg) °C**	**Nuwakot (Tavg) °C**	**Dhunche (Tavg) °C**	**Nuwakot (Tavg) °C**	**Dhunche (Tavg) °C**	**Nuwakot (Tavg) °C**	**Dhunche (Tavg) °C**	**Nuwakot (Tavg) °C**	**Dhunche (Tavg) °C**	**Nuwakot (Tavg) °C**
Jan	10.58	16.75	9.17	16.27	11.11	17.49	10.38	17.34	11.39	17.99
Feb	11.94	19.22	10.54	19.00	12.33	20.05	11.72	19.86	11.65	19.91
Mar	14.80	23.00	14.60	23.00	14.83	23.37	15.32	24.19	15.28	23.67
Apr	18.39	27.11	17.59	25.73	17.89	25.99	18.74	27.96	18.37	26.20
May	19.60	26.39	18.92	26.55	19.62	27.16	20.62	28.23	20.08	26.93
Jun	21.34	28.09	19.92	29.63	20.42	28.19	22.03	29.36	21.66	28.64
Jul	21.50	28.49	21.73	29.41	21.08	28.26	21.13	29.03	21.24	28.73
Aug	21.52	28.10	21.53	29.25	20.86	28.26	20.84	28.62	21.32	28.62
Sep	20.66	27.25	20.26	27.67	20.22	27.56	20.23	27.62	20.45	27.95
Oct	17.51	24.61	17.47	24.20	17.65	24.57	17.56	24.77	18.11	24.70
Nov	14.45	21.62	13.68	20.63	14.54	20.84	14.18	21.12	14.29	20.68
Dec	12.75	19.11	11.68	17.60	11.65	17.42	11.91	18.51	11.69	18.10

Projected Average monthly average temperature (^{0}C) in Dhunche and Nuwakot Station in mid future under SSP 585										
Model	**EC-Earth3-Veg**		**INM-CM4-8**		**MPI-ESM1-2-LR**		**MRI-ESM2-0**		**NorESM2-MM**	
Month	**Dhunche (Tavg) °C**	**Nuwakot (Tavg) °C**	**Dhunche (Tavg) °C**	**Nuwakot (Tavg) °C**	**Dhunche (Tavg) °C**	**Nuwakot (Tavg) °C**	**Dhunche (Tavg) °C**	**Nuwakot (Tavg) °C**	**Dhunche (Tavg) °C**	**Nuwakot (Tavg) °C**
Jan	11.77	18.10	10.57	17.94	11.23	18.09	11.93	19.04	12.02	18.63
Feb	12.98	20.80	11.65	20.27	12.66	20.73	12.95	21.34	12.76	21.49
Mar	16.32	24.97	15.33	23.65	15.64	24.25	15.87	25.09	16.02	24.87
Apr	19.09	28.46	18.20	26.66	18.44	26.36	19.20	28.73	18.62	26.84
May	20.06	27.37	19.86	27.72	19.83	27.80	20.88	28.55	19.92	27.26
Jun	22.01	29.44	20.98	31.21	20.77	29.38	22.73	30.15	21.87	29.37
Jul	22.46	29.57	22.51	30.70	21.24	29.04	21.44	30.02	21.84	29.57
Aug	22.25	29.35	22.77	30.84	21.13	29.30	21.04	29.75	21.58	29.35
Sep	21.58	28.64	21.35	29.74	20.59	28.87	20.47	28.36	20.81	28.45
Oct	18.28	25.76	18.13	25.09	18.10	25.28	18.05	25.48	18.43	25.48
Nov	15.08	22.67	14.78	21.58	15.37	21.72	15.06	22.10	15.24	21.65
Dec	13.72	20.55	12.62	18.19	12.92	18.98	13.18	19.50	12.81	19.13

Projected Average monthly average temperature (^{0}C) in Dhunche and Nuwakot Station in far future under SSP 245										
Model	**EC-Earth3-Veg**		**INM-CM4-8**		**MPI-ESM1-2-LR**		**MRI-ESM2-0**		**NorESM2-MM**	
Month	**Dhunche (Tavg) °C**	**Nuwakot (Tavg) °C**	**Dhunche (Tavg) °C**	**Nuwakot (Tavg) °C**	**Dhunche (Tavg) °C**	**Nuwakot (Tavg) °C**	**Dhunche (Tavg) °C**	**Nuwakot (Tavg) °C**	**Dhunche (Tavg) °C**	**Nuwakot (Tavg) °C**
Jan	13.16	19.30	9.86	16.64	11.73	18.34	10.83	17.88	11.87	18.66
Feb	13.14	20.30	10.98	19.52	12.37	20.79	12.62	20.60	12.72	21.31
Mar	15.66	24.01	14.60	23.07	15.34	23.72	15.43	24.39	15.18	23.82
Apr	18.63	27.87	17.86	25.92	18.51	26.71	18.92	28.19	18.52	26.55
May	20.58	27.27	19.31	27.17	19.96	27.61	20.55	28.23	19.73	26.81
Jun	22.00	29.56	20.53	30.08	20.90	28.99	22.88	29.86	22.73	28.83
Jul	22.07	29.20	21.92	30.12	21.05	28.60	21.85	29.84	21.81	29.38
Aug	22.22	29.04	21.92	30.22	20.99	28.78	21.08	29.17	21.57	29.27
Sep	21.26	28.24	20.71	28.67	20.45	28.31	20.26	27.76	20.75	28.47
Oct	18.10	25.22	17.56	24.41	17.72	24.86	17.82	25.06	18.34	25.31
Nov	15.29	22.60	14.01	21.13	14.58	20.72	14.63	21.55	14.95	21.37
Dec	14.01	20.16	11.78	17.68	12.91	18.79	12.34	18.68	12.11	18.51

Projected Average monthly average temperature (^{0}C) in Dhunche and Nuwakot Station in far future SSP 585										
Model	**EC-Earth3-Veg**		**INM-CM4-8**		**MPI-ESM1-2-LR**		**MRI-ESM2-0**		**NorESM2-MM**	
Month	**Dhunche (Tavg) °C**	**Nuwakot (Tavg) °C**	**Dhunche (Tavg) °C**	**Nuwakot (Tavg) °C**	**Dhunche (Tavg) °C**	**Nuwakot (Tavg) °C**	**Dhunche (Tavg) °C**	**Nuwakot (Tavg) °C**	**Dhunche (Tavg) °C**	**Nuwakot (Tavg) °C**
Jan	14.81	21.48	12.71	18.98	12.99	19.88	13.60	21.06	13.56	20.60
Feb	15.55	23.76	13.20	21.13	14.53	22.66	14.77	23.58	14.34	23.65
Mar	18.31	27.68	16.82	25.08	16.73	25.70	17.25	26.92	17.45	26.62
Apr	21.17	30.13	19.74	27.99	19.39	27.97	20.65	30.87	20.03	28.81
May	22.45	29.30	22.06	29.32	20.68	29.82	23.08	31.02	21.43	29.24
Jun	23.99	32.75	21.88	32.56	21.07	31.34	24.48	32.27	24.21	32.00
Jul	23.81	31.49	23.34	31.67	21.88	30.97	22.78	31.90	22.75	31.56
Aug	23.74	31.49	23.88	31.85	21.75	31.25	21.70	31.65	22.47	31.49
Sep	23.38	31.09	22.41	31.44	21.33	31.62	21.06	30.32	21.71	31.05
Oct	20.02	28.14	19.07	25.83	19.21	27.53	18.72	26.61	19.28	27.16
Nov	16.99	25.39	15.87	22.80	16.87	23.62	16.06	23.97	16.35	23.59
Dec	16.03	23.57	14.51	19.56	15.07	21.22	14.56	21.53	13.92	20.47

APPENDIX B: Projected Average monthly precipitation (mm) in Thamachit and Pansayakhola station in the near, mid and far future under SSP245 and SSP 585

Average monthly precipitation (mm) in Thamachit and Pansayakhola Station in the near future under SSP245										
Model	**EC-Earth3-Veg**		**INM-CM4-8**		**MPI-ESM1-2-LR**		**MRI-ESM2-0**		**NorESM2-MM**	
Month	**Thamachit (PCP) mm**	**Pansayakhol a (PCP) mm**	**Thamachi t (PCP) mm**	**Pansayakhol a (PCP) mm**	**Thamachi t (PCP) mm**	**Pansayakhol a (PCP) mm**	**Thamachi t (PCP) mm**	**Pansayakhol a (PCP) mm**	**Thamachi t (PCP) mm**	**Pansayakhol a (PCP) mm**
Jan	9.06	15.90	8.71	19.02	2.25	3.64	6.94	10.26	10.01	22.50
Feb	24.96	27.21	21.14	22.95	13.48	14.34	21.15	30.57	26.27	28.62
Mar	7.88	10.36	18.27	38.58	11.94	27.09	13.35	33.17	9.80	13.79
Apr	12.17	13.97	17.06	49.93	10.65	20.88	14.67	44.32	14.00	35.02
May	23.83	72.48	31.30	230.02	17.29	61.34	17.81	64.12	16.04	48.10
Jun	104.55	393.69	151.38	703.27	106.52	412.83	76.18	302.82	85.04	298.71
Jul	238.94	894.90	232.75	870.71	214.87	831.47	288.91	1029.04	231.56	885.31
Aug	242.61	941.25	165.75	561.04	211.23	815.68	218.44	800.51	235.25	874.50
Sep	80.10	339.27	81.89	414.33	95.32	382.77	107.78	426.45	101.73	405.50
Oct	9.06	23.89	40.17	75.07	6.66	23.03	24.54	44.63	13.82	37.03
Nov	0.17	1.01	1.15	3.77	0.63	1.60	0.64	2.94	0.65	2.33
Dec	2.19	5.77	6.89	18.03	4.09	9.44	3.60	12.16	3.41	8.33

Average monthly precipitation (mm) in Thamachit and Pansayakhola Station in the near future under SSP585										
Model	**EC-Earth3-Veg**		**INM-CM4-8**		**MPI-ESM1-2-LR**		**MRI-ESM2-0**		**NorESM2-MM**	
Month	**Thamachit (PCP) mm**	**Pansayakhola (PCP) mm**	**Thamachit (PCP) mm**	**Pansayakhola (PCP) mm**	**Thamachit (PCP) mm**	**Pansayakhola (PCP) mm**	**Thamachit (PCP) mm**	**Pansayakhola (PCP) mm**	**Thamachit (PCP) mm**	**Pansayakhola (PCP) mm**
Jan	12.05	22.09	10.22	21.86	3.12	6.29	5.62	9.76	11.44	23.69
Feb	17.39	19.28	30.37	36.03	17.79	24.44	22.14	33.84	21.93	23.28
Mar	7.02	7.24	25.22	54.66	5.53	12.81	14.94	32.45	14.91	24.14
Apr	5.9	7.08	26.16	85.13	10.61	22.25	15.93	42.63	13.07	26.42
May	32.57	115.1	27.52	203.79	12.19	49.89	18.19	60.06	20.69	70.31
Jun	105.34	401.71	130.29	620.39	114.45	459.53	101.03	405.87	67.17	235
Jul	264.14	969.72	235.47	892.63	209.91	814.23	272.68	979.36	228.17	871.71
Aug	228.65	893.34	188.82	631.93	207.28	787.37	248.12	915.54	234.17	871.18
Sep	80.05	340.8	76.1	383.29	97.93	391.09	80.06	325.97	112.54	450
Oct	11.22	26.16	24.52	41.88	9.81	32.84	12.59	16.97	17.46	52.53
Nov	0.28	1.26	3.11	8.71	1.29	3.28	0.79	3.08	0.21	0.7
Dec	3.17	7.16	6.47	18.49	2.77	8.7	3.02	9.86	4.17	10.79

Average monthly precipitation (mm) in Thamachit and Pansayakhola Station in the mid future under two scenarios SSP 245 Scenario										
Model	**EC-Earth3-Veg**		**INM-CM4-8**		**MPI-ESM1-2-LR**		**MRI-ESM2-0**		**NorESM2-MM**	
Month	**Thamachit (PCP) mm**	**Pansayakhola (PCP) mm**	**Thamachit (PCP) mm**	**Pansayakhola (PCP) mm**	**Thamachit (PCP) mm**	**Pansayakhola (PCP) mm**	**Thamachit (PCP) mm**	**Pansayakhola (PCP) mm**	**Thamachit (PCP) mm**	**Pansayakhola (PCP) mm**
Jan	4.98	9.31	15.57	36.09	3.71	7.03	8.22	11.89	6.99	15.58
Feb	14.60	14.41	21.09	24.78	6.47	8.71	29.82	41.73	15.88	14.44
Mar	8.53	10.37	16.78	39.09	8.53	15.45	9.84	26.00	5.23	6.37
Apr	11.06	9.56	23.31	75.90	10.01	20.83	15.02	41.74	8.85	19.40
May	27.29	74.58	39.28	267.19	13.74	52.14	14.54	55.32	6.18	15.30
Jun	109.39	417.41	175.65	821.44	101.87	388.62	104.75	423.78	81.11	279.31
Jul	289.18	1052.95	229.92	871.72	215.38	825.06	278.86	990.55	258.03	980.22
Aug	268.40	1016.19	209.91	729.00	224.76	880.19	236.65	860.40	251.66	925.82
Sep	95.01	395.46	89.48	445.95	101.23	400.80	95.84	366.85	121.58	476.90
Oct	13.21	37.30	29.14	50.43	2.96	10.64	26.62	41.64	11.72	36.55
Nov	0.28	1.10	2.47	8.38	1.73	3.63	0.61	2.84	0.20	0.70
Dec	2.45	5.90	7.95	22.36	8.18	19.28	3.31	9.64	1.22	1.99

Average monthly precipitation (mm) in Thamachit and Pansayakhola Station in the mid future under SSP 585										
Model	**EC-Earth3-Veg**		**INM-CM4-8**		**MPI-ESM1-2-LR**		**MRI-ESM2-0**		**NorESM2-MM**	
Month	**Thamachit (PCP) mm**	**Pansayakhola (PCP) mm**	**Thamachit (PCP) mm**	**Pansayakhola (PCP) mm**	**Thamachit (PCP) mm**	**Pansayakhola (PCP) mm**	**Thamachit (PCP) mm**	**Pansayakhola (PCP) mm**	**Thamachit (PCP) mm**	**Pansayakhola (PCP) mm**
Jan	5.02	8.61	6.03	13.59	3.89	7.76	7.56	11.92	10.12	20.58
Feb	9.52	8.74	28.93	33.69	5.15	6.79	26.93	39.71	18.29	19.4
Mar	9.51	14.88	20.62	45.73	7.47	14.76	13.04	31.87	9.32	16.08
Apr	26.5	34.4	24.01	81.23	7.12	13.09	15.44	39.27	19.25	48.63
May	60.11	193.97	33.72	248.1	19.6	91.71	23.22	97.69	22.21	71.53
Jun	121.41	454.16	159.54	769.36	122.94	507.01	110.16	455.34	105.32	378.83
Jul	308.26	1110.96	290.63	1122.46	224.8	855.79	308.13	1117.54	250.05	950.08
Aug	314.08	1189.83	253.59	923.21	231.96	889.94	313.6	1147.03	275.48	993.67
Sep	96.77	423.24	96.22	492.45	110.02	415.8	117.64	454.02	133.08	541.19
Oct	12.41	36.52	27.42	50.76	13.53	41.94	29.13	51.79	19.01	56.47
Nov	0.56	2.18	0.95	3.04	1.42	3.3	0.93	3.54	0.33	1.21
Dec	2.88	7.74	7.4	20.36	1.44	3.44	2.43	6.74	0.93	1.42

Average monthly precipitation (mm) in Thamachit and Pansayakhola Station in the far future under SSP 245										
Model	**EC-Earth3-Veg**		**INM-CM4-8**		**MPI-ESM1-2-LR**		**MRI-ESM2-0**		**NorESM2-MM**	
Month	**Thamachit (PCP) mm**	**Pansayakhola (PCP) mm**	**Thamachit (PCP) mm**	**Pansayakhola (PCP) mm**	**Thamachit (PCP) mm**	**Pansayakhola (PCP) mm**	**Thamachit (PCP) mm**	**Pansayakhola (PCP) mm**	**Thamachit (PCP) mm**	**Pansayakhola (PCP) mm**
Jan	6.09	9.56	9.74	21.69	0.97	1.65	6.03	10.04	7.74	18.43
Feb	26.67	27.45	43.74	47.23	18.21	21.97	17.69	26.04	11.39	11.26
Mar	9.40	11.32	26.58	54.93	10.64	20.84	16.09	40.65	11.87	19.74
Apr	26.91	32.95	24.27	83.84	7.00	13.00	13.97	37.67	14.02	34.34
May	35.61	114.55	37.00	266.89	16.01	68.18	19.48	75.25	14.91	33.37
Jun	128.68	449.91	143.92	706.70	101.62	391.15	72.18	284.51	42.97	139.28
Jul	312.87	1128.56	253.27	969.01	230.54	894.56	300.86	1082.33	226.91	863.54
Aug	280.38	1077.83	268.64	951.71	239.69	915.48	272.26	1008.92	255.80	935.68
Sep	104.07	448.24	97.68	494.45	102.81	407.38	109.14	418.38	120.66	474.82
Oct	16.04	44.20	24.12	44.87	10.43	35.30	19.36	31.82	14.89	44.55
Nov	0.10	0.51	2.57	8.74	0.38	0.34	0.49	2.12	0.19	0.75
Dec	1.48	4.49	4.42	13.19	1.84	4.57	4.92	14.02	0.78	1.36

Average monthly precipitation (mm) in Thamachit and Pansayakhola Station in the far future under SSP 585										
Model	**EC-Earth3-Veg**		**INM-CM4-8**		**MPI-ESM1-2-LR**		**MRI-ESM2-0**		**NorESM2-MM**	
Month	**Thamachit (PCP) mm**	**Pansayakhola (PCP) mm**	**Thamachit (PCP) mm**	**Pansayakhola (PCP) mm**	**Thamachit (PCP) mm**	**Pansayakhola (PCP) mm**	**Thamachit (PCP) mm**	**Pansayakhola (PCP) mm**	**Thamachit (PCP) mm**	**Pansayakhola (PCP) mm**
Jan	4.98	6.82	5.27	11.65	5.15	8.04	8.08	15.37	12.79	28.95
Feb	19.46	20.49	31.45	35.45	9.06	9.46	19.82	31.13	12.92	11.46
Mar	11.93	15.47	18.62	36.17	10.93	21.89	11.43	28.9	6.41	11.85
Apr	24.4	29.06	30.71	107.24	6.08	11.62	13.32	32.11	7.38	22.78
May	42.46	154.19	25.52	189.76	8.19	19.04	22.84	93.07	18.5	51.34
Jun	190.51	698.87	171.2	844.55	157.41	651.95	106.43	425.77	68.63	233.06
Jul	404.28	1375.08	394.99	1556.4	231.49	915.74	327.75	1183.2	239.48	902.62
Aug	459.25	1644.72	393.17	1462.38	245.77	967.69	328.97	1233.59	282.7	988.1
Sep	161.5	687.21	119.68	624.09	133.85	531.83	157.13	668.4	143.27	565.38
Oct	20.92	54.02	11.61	20.62	15.32	52.91	36.39	63.91	17.41	53.17
Nov	0.49	1.86	1.51	3.83	0.43	0.95	0.06	1.32	0.62	2.33
Dec	3.26	8.11	1.13	2.95	1.23	2.2	3.04	9.96	3.81	11.63

APPENDIX C: Average energy generation (GWh) in the near, mid and far future under SSP 245 and SSP 585

Average energy generation (GWh) in the near future under SSP 245						
Month	Historical	EC-Earth3-Veg	INM-CM4-8	MPI-ESM1-2-LR	MRI-ESM2-0	NorESM2-MM
Jan	10.65	10.75	9.82	10.64	10.84	10.72
Feb	7.14	9.59	8.81	9.15	9.70	9.59
Mar	7.45	10.20	10.14	10.00	10.60	10.27
Apr	8.71	9.21	10.48	9.28	10.52	8.75
May	10.89	9.59	10.73	9.58	10.18	9.23
Jun	10.54	10.32	10.54	10.31	10.36	9.71
Jul	10.89	10.89	10.89	10.89	10.89	10.89
Aug	10.89	10.89	10.89	10.89	10.89	10.89
Sep	10.54	10.54	10.54	10.54	10.54	10.54
Oct	10.89	10.89	10.89	10.89	10.89	10.89
Nov	10.54	10.54	10.51	10.54	10.54	10.54
Dec	10.89	10.89	10.56	10.89	10.89	10.89

Average energy generation (GWh) in the near future under SSP585						
Month	Historical	EC-Earth3-Veg	INM-CM4-8	MPI-ESM1-2-LR	MRI-ESM2-0	NorESM2-MM
Jan	10.65	10.89	9.85	10.60	10.73	10.82
Feb	7.14	9.63	8.44	9.44	9.32	9.61
Mar	7.45	10.31	9.93	9.91	10.54	10.55
Apr	8.71	8.39	10.44	9.07	10.37	9.11
May	10.89	9.44	10.86	9.05	10.29	9.37
Jun	10.54	10.22	10.54	10.35	10.53	9.46
Jul	10.89	10.89	10.89	10.89	10.89	10.89
Aug	10.89	10.89	10.89	10.89	10.89	10.89
Sep	10.54	10.54	10.54	10.54	10.54	10.54
Oct	10.89	10.89	10.89	10.89	10.89	10.89
Nov	10.54	10.54	10.36	10.54	10.54	10.54
Dec	10.89	10.89	10.48	10.88	10.89	10.89

Average energy generation (GWh) in the mid future under SSP 245						
Month	Historical	EC-Earth3-Veg	INM-CM4-8	MPI-ESM1-2-LR	MRI-ESM2-0	Nor-ESM2-MM
Jan	10.65	10.79	10.74	10.64	10.70	10.89
Feb	7.14	9.53	9.26	9.15	9.69	9.71
Mar	7.45	10.12	10.20	10.04	9.83	10.26
Apr	8.71	8.80	10.41	9.14	9.54	8.81
May	10.89	9.29	10.73	9.01	9.90	8.68
Jun	10.54	9.89	10.54	10.00	10.07	9.99
Jul	10.89	10.89	10.89	10.89	10.89	10.89
Aug	10.89	10.89	10.89	10.89	10.89	10.89
Sep	10.54	10.54	10.54	10.54	10.54	10.54
Oct	10.89	10.89	10.89	10.89	10.89	10.89
Nov	10.54	10.54	10.54	10.54	10.54	10.54
Dec	10.89	10.89	10.76	10.89	10.84	10.89

Average energy generation (GWh) in the mid future under SSP585						
Month	Historical	EC-Earth3-Veg	INM-CM4-8	MPI-ESM1-2-LR	MRI-ESM2-0	NorESM2-MM
Jan	10.65	10.89	10.60	10.78	10.74	10.89
Feb	7.14	9.64	9.45	9.21	9.68	9.77
Mar	7.45	9.78	10.44	9.78	10.75	10.18
Apr	8.71	9.33	10.42	8.90	10.44	9.39
May	10.89	10.82	10.81	8.91	10.01	9.24
Jun	10.54	10.43	10.54	10.31	10.14	9.69
Jul	10.89	10.89	10.89	10.89	10.89	10.89
Aug	10.89	10.89	10.89	10.89	10.89	10.89
Sep	10.54	10.54	10.54	10.54	10.54	10.54
Oct	10.89	10.89	10.89	10.89	10.89	10.89
Nov	10.54	10.54	10.48	10.54	10.54	10.54
Dec	10.89	10.89	10.69	10.89	10.83	10.89

Average energy generation (GWh) in the far future under SSP 245						
Month	Historical	EC-Earth3-Veg	INM-CM4-8	MPI-ESM1-2-LR	MRI-ESM2-0	NorESM2-MM
Jan	10.65	10.89	10.83	10.74	10.60	10.84
Feb	7.14	9.71	9.54	9.50	9.21	9.43
Mar	7.45	10.36	10.58	10.28	10.43	9.67
Apr	8.71	9.82	10.53	8.90	10.04	8.41
May	10.89	10.53	10.71	8.80	10.07	8.99
Jun	10.54	10.42	10.54	9.98	10.22	9.50
Jul	10.89	10.89	10.89	10.89	10.89	10.89
Aug	10.89	10.89	10.89	10.89	10.89	10.89
Sep	10.54	10.54	10.54	10.54	10.54	10.54
Oct	10.89	10.89	10.89	10.89	10.89	10.89
Nov	10.54	10.54	10.54	10.54	10.54	10.54
Dec	10.89	10.89	10.89	10.89	10.89	10.88

Average energy generation (GWh) in the far future under SSP585						
Month	Historical	EC-Earth3-Veg	INM-CM4-8	MPI-ESM1-2-LR	MRI-ESM2-0	NorESM2-MM
Jan	10.65	10.89	10.89	10.85	10.85	10.77
Feb	7.14	9.81	9.84	9.67	9.72	9.57
Mar	7.45	10.38	10.72	10.46	10.29	9.47
Apr	8.71	9.32	10.54	9.43	9.48	8.10
May	10.89	10.39	10.89	9.17	10.41	8.67
Jun	10.54	10.54	10.54	10.42	9.89	9.79
Jul	10.89	10.89	10.89	10.89	10.89	10.89
Aug	10.89	10.89	10.89	10.89	10.89	10.89
Sep	10.54	10.54	10.54	10.54	10.54	10.54
Oct	10.89	10.89	10.89	10.89	10.89	10.89
Nov	10.54	10.54	10.54	10.54	10.54	10.54
Dec	10.89	10.89	10.89	10.89	10.89	10.89

APPENDIX D: Relative change % Of precipitation and temperature near, mid and far future under SSP 245 and SSP 585

Relative change % Of pcp and temp. near future SSP 245 and SSP 585					
SSP 245			**SSP 585**		
Precipitation (mm)					
Thamachit					
Jan	MPI-ESM1-2-LR	-79.23	Mar	MPI-ESM1-2-LR	-79.63
Sep	INM-CM4-8	152.47	Nov	INM-CM4-8	321.19
Pansayakhola					
Apr	EC-Earth3-Veg	-84.3	Apr	EC-Earth3-Veg	-92.05
Jun	INM-CM4-8	60.45	Dec	INM-CM4-8	54.11
Temperature (°C)					
Maximum Temperature					
Dhunche Max.					
Jun	INM-CM4-8	-0.51	Jun	MPI-ESM1-2-LR	0.33
Dec	EC-Earth3-Veg	13.78	Dec	MRI-ESM2-0	15.70
Nuwakot Max					
May	MPI-ESM1-2-LR	0.9	May	MPI-ESM1-2-LR	0.71
Mar	MRI-ESM2-0	8.72	Jan	MRI-ESM2-0	11.62
Minimun Temperature					
Dhunche Min					
Mar	INM-CM4-8	-4.24	Jun	INM-CM4-8	-2.01
Dec	MPI-ESM1-2-LR	41.71	Jan	MRI-ESM2-0	59.15
Nuwakot Min					
May	MPI-ESM1-2-LR	0.95	May	MPI-ESM1-2-LR	0.41
Jan	MPI-ESM1-2-LR	18.1	Jan	MRI-ESM2-0	23.71
Dhunche Avg					
Jun	INM-CM4-8	-1.94	Jun	MPI-ESM1-2-LR	-0.45
Dec	MPI-ESM1-2-LR	19.25	Jan	MRI-ESM2-0	22.76
Nuwakot Avg					
May	MPI-ESM1-2-LR	0.92	May	MPI-ESM1-2-LR	0.59
Dec	EC-Earth3-Veg	11.32	Jan	MRI-ESM2-0	15.08

Relative change % Of pcp and temp. mid future SSP 245 and SSP 585					
SSP 245			SSP 585		
Precipitation (mm)					
Thamachit					
Sep	MPI-ESM1-2-LR	-81.4	Dec	NorESM2-MM	-80.01
Nov	INM-CM4-8	233.56	May	EC-Earth3-Veg	111.98
Pansayakhola					
May	NorESM2-MM	-92.04	Dec	NorESM2-MM	-88.16
Jun	INM-CM4-8	87.42	Jun	INM-CM4-8	75.53
Temperature (°C)					
Maximum Temperature					
Dhunche Max.					
Jun	INM-CM4-8	1.73	Jun	MPI-ESM1-2-LR	4.40
Dec	EC-Earth3-Veg	24.49	Dec	EC-Earth3-Veg	30.81
Nuwakot Max					
May	EC-Earth3-Veg	3.05	May	NorESM2-MM	5.65
Dec	EC-Earth3-Veg	16.66	Dec	EC-Earth3-Veg	23.17
Minimun Temperature					
Dhunche Min					
Jun	INM-CM4-8	-1.56	Aug	MRI-ESM2-0	4.58
Jan	NorESM2-MM	104.29	Jan	NorESM2-MM	127.22
Nuwakot Min					
May	EC-Earth3-Veg	3.61	May	EC-Earth3-Veg	7.68
Jan	NorESM2-MM	36.27	Dec	EC-Earth3-Veg	48.94
Dhunche Avg					
Jun	INM-CM4-8	0.47	Jun	MPI-ESM1-2-LR	4.75
Jan	NorESM2-MM	36.25	Dec	EC-Earth3-Veg	46.16
Nuwakot avg					
May	EC-Earth3-Veg	3.26	May	NorESM2-MM	6.68
Dec	EC-Earth3-Veg	21.74	Dec	EC-Earth3-Veg	30.96

Relative Change % Of pcp and temp. far future SSP 245 and SSP 585					
SSP 245			**SSP 585**		
Precipitation (mm)					
Thamachit					
Jan	MPI-ESM1-2-LR	-91.04	Nov	MRI-ESM2-0	-91.34
Nov	INM-CM4-8	248.37	Sep	MRI-ESM2-0	128.73
Pansayakhola					
Nov	MPI-ESM1-2-LR	-94.52	May	MPI-ESM1-2-LR	-90.10
Jun	INM-CM4-8	61.24	Aug	EC-Earth3-Veg	101.75
Temperature (°C)					
Maximum Temperature					
Dhunche Max.					
Jul	MPI-ESM1-2-LR	4.06	Jun	MPI-ESM1-2-LR	5.64
Jan	EC-Earth3-Veg	36.94	Jan	EC-Earth3-Veg	48.21
Nuwakot Max					
May	NorESM2-MM	4.24	Sep	INM-CM4-8	10.10
Jan	EC-Earth3-Veg	22.31	Dec	EC-Earth3-Veg	38.24
Minimun Temperature					
Dhunche Min					
Jun	INM-CM4-8	2.17	Jun	MPI-ESM1-2-LR	7.29
Jan	EC-Earth3-Veg	160.57	Jan	EC-Earth3-Veg	223.57
Nuwakot Min					
May	NorESM2-MM	5.94	Sep	INM-CM4-8	13.89
Jan	EC-Earth3-Veg	50.9	Dec	EC-Earth3-Veg	77.80
Dhunche Avg					
Jun	INM-CM4-8	3.57	Jun	MPI-ESM1-2-LR	6.27
Jan	EC-Earth3-Veg	57.35	Jan	EC-Earth3-Veg	77.16
Nuwakot avg					
May	NorESM2-MM	4.89	Sep	INM-CM4-8	11.55
Jan	EC-Earth3-Veg	30.5	Dec	EC-Earth3-Veg	50.20

APPENDIX E: Annual average value based on ensemble average near, mid and far future under SSP245 and SSP 585

Annual Average Value based on Ensemble Average Near Future SSP245				
Month	**Relative Change in Discharge**	**Relative Change in Energy**	**Discharge (m3/s)**	**Energy (GWh)**
Jan	-4.79	-5.96	46.87	9.72
Feb	43.61	10.67	65.23	10.54
Mar	36.84	11.68	61.35	10.50
Apr	0.04	-3.31	61.35	10.19
May	-36.74	0.00	71.20	10.54
Jun	-31.72	0.00	201.51	10.54
Jul	0.49	0.00	592.58	10.54
Aug	0.71	0.00	696.20	10.54
Sep	9.48	0.00	472.31	10.54
Oct	-21.07	0.00	172.33	10.54
Nov	-37.15	0.00	73.06	10.54
Dec	-20.34	-0.93	55.20	10.44
Annual	-5.05	1.01	214.10	125.16
Historical Baseline			217.09	120.03
Difference			-2.99	5.13
Relative Change %			**-1.4**	**4.3**

Annual Average Value based on Ensemble Average Near Future SSP585				
Month	**Relative Change in Discharge**	**Relative Change in Energy**	**Discharge (m3/s)**	**Energy (GWh)**
Jan	3.10	-1.82	50.76	10.14
Feb	48.10	10.67	67.26	10.54
Mar	47.46	9.63	66.11	10.30
Apr	2.34	-7.10	62.76	9.79
May	-34.86	-0.88	73.31	10.45
Jun	-33.63	0.00	195.86	10.54
Jul	2.57	0.00	604.81	10.54
Aug	1.96	0.00	704.84	10.54
Sep	6.88	0.00	461.09	10.54
Oct	-25.94	0.00	161.70	10.54
Nov	-38.95	0.00	70.97	10.54
Dec	-18.21	0.00	56.68	10.54
Annual	-3.27	0.88	214.68	125.01
Historical Baseline			217.09	120.03
Difference			-2.41	4.97
Relative Change %			**-1.1**	**4.1**

Annual Average Value based on Ensemble Average Mid Future SSP245				
Month	**Relative Change in Discharge**	**Relative Change in Energy**	**Discharge (m3/s)**	**Energy (GWh)**
Jan	6.80	-1.82	52.58	10.14
Feb	50.68	6.93	68.44	10.18
Mar	24.89	9.94	55.99	10.33
Apr	-3.26	-5.69	59.32	9.94
May	-35.11	-4.81	73.03	10.03
Jun	-27.43	0.00	214.18	10.54
Jul	7.05	0.00	631.26	10.54
Aug	8.37	0.00	749.17	10.54
Sep	16.23	0.00	501.45	10.54
Oct	-21.51	0.00	171.35	10.54
Nov	-35.71	0.00	74.74	10.54
Dec	-14.80	0.00	59.04	10.54
Annual	-1.98	0.38	225.88	124.41
Historical Baseline			217.09	120.03
Difference			8.79	4.38
Relative Change %			**4.0**	**3.6**

Annual Average Value based on Ensemble Average Mid Future SSP585				
Month	**Relative Change in Discharge**	**Relative Change in Energy**	**Discharge (m3/s)**	**Energy (GWh)**
Jan	7.88	-2.17	53.11	10.11
Feb	54.76	8.75	70.29	10.36
Mar	42.18	8.68	63.75	10.21
Apr	9.45	-0.23	67.12	10.52
May	-18.13	0.00	92.14	10.54
Jun	-14.57	0.00	252.11	10.54
Jul	14.76	0.00	676.70	10.54
Aug	20.69	0.00	834.32	10.54
Sep	25.56	0.00	541.69	10.54
Oct	-12.12	0.00	191.86	10.54
Nov	-32.25	0.00	78.75	10.54
Dec	-12.37	0.00	60.73	10.54
Annual	7.15	1.25	248.55	125.51
Historical Baseline			217.09	120.03
Difference			31.46	5.48
Relative Change %			**14.5**	**4.6**

Annual Average Value based on Ensemble Average Far Future SSP245				
Month	**Relative Change in Discharge**	**Relative Change in Energy**	**Discharge (m3/s)**	**Energy (GWh)**
Jan	1.30	-1.02	49.87	10.23
Feb	60.42	10.67	72.86	10.54
Mar	57.86	12.15	70.77	10.54
Apr	7.44	-2.74	65.89	10.25
May	-25.60	0.00	83.73	10.54
Jun	-35.93	0.00	189.07	10.54
Jul	7.12	0.00	631.67	10.54
Aug	15.22	0.00	796.54	10.54
Sep	21.97	0.00	526.22	10.54
Oct	-18.93	0.00	176.99	10.54
Nov	-33.92	0.00	76.81	10.54
Dec	-16.44	0.00	57.91	10.54
Annual	3.38	1.59	233.19	125.88
Historical Baseline			217.09	120.03
Difference			16.11	5.84
Relative Change %			**7.4**	**4.9**

Annual Average Value based on Ensemble Average Far Future SSP585				
Month	**Relative Change in Discharge**	**Relative Change in Energy**	**Discharge (m3/s)**	**Energy (GWh)**
Jan	14.02	2.03	56.13	10.54
Feb	75.28	10.67	79.61	10.54
Mar	34.83	11.59	60.45	10.49
Apr	7.24	-2.79	65.77	10.25
May	-31.32	-4.64	77.29	10.05
Jun	-10.62	0.00	263.78	10.54
Jul	28.88	0.00	760.00	10.54
Aug	38.37	0.00	956.55	10.54
Sep	44.47	0.00	623.27	10.54
Oct	-5.23	0.00	206.90	10.54
Nov	-28.60	0.00	83.00	10.54
Dec	-10.01	0.00	62.37	10.54
Annual	13.11	1.41	274.59	125.64
Historical Baseline			217.09	120.03
Difference			57.50	5.61
Relative Change %			**26.5**	**4.7**

Impact of Climate Change on Hydropower Generation: A Case Study of Devighat Hydropower Station

ORIGINALITY REPORT

12%
SIMILARITY INDEX

PRIMARY SOURCES

1	conference.ioe.edu.np Internet	206 words — 1%
2	"Development of Water Resources in India", Springer Science and Business Media LLC, 2017 Crossref	175 words — 1%
3	www.researchgate.net Internet	146 words — 1%
4	swat.tamu.edu Internet	84 words — < 1%
5	Raj Singh, Nawraj Bhattarai, Anita Prajapati, Shree Raj Shakya. "Impact of variation in climatic parameters on hydropower generation: A case of hydropower project in Nepal", Heliyon, 2022 Crossref	80 words — < 1%
6	www.mdpi.com Internet	78 words — < 1%
7	link.springer.com Internet	60 words — < 1%
8	Springer Geography, 2016. Crossref	58 words — < 1%

9	Kashish Sadhwani, T. I. Eldho. "Assessing the Vulnerability of Water Balance to Climate Change at River Basin Scale in Humid Tropics: Implications for a Sustainable Water Future", Sustainability, 2023 Crossref	54 words — < 1%
10	"Pre-eminent Strategy for Effective Utilization of Power in Data Center", International Journal of Recent Technology and Engineering, 2020 Crossref	47 words — < 1%
11	Zulfiqar Ahmad, Arshad Ashraf, Muhammad Zaheer, Humaira Bashir. "Hydrological response to environment change in Himalayan watersheds: Assessment from integrated modeling approach", Journal of Mountain Science, 2015 Crossref	45 words — < 1%
12	www.imnepal.com Internet	45 words — < 1%
13	worldwidescience.org Internet	40 words — < 1%
14	Veysel Gumus, Nabil El Moçayd, Mehmet Seker, Mohammed Seaid. "Evaluation of future temperature and precipitation projections in Morocco using the ANN-based multi-model ensemble from CMIP6", Atmospheric Research, 2023 Crossref	37 words — < 1%
15	eprints.nottingham.ac.uk Internet	37 words — < 1%
16	etd.aau.edu.et Internet	37 words — < 1%